AD NUMBER

ADB002067

NEW LIMITATION CHANGE

TO

Approved for public release, distribution unlimited

FROM

Distribution authorized to U.S. Gov't. agencies only; Test and Evaluation; Jan 1975. Other requests shall be referred to Eustis Directorate, US Army Air Mobility Research and Development Lab., Fort Eustis, VA 23604.

AUTHORITY

US Army Air Mobility R&D Lab ltr dtd 30 Mar 1976

DISCLAIMER NOTICE

THIS DOCUMENT IS BEST QUALITY PRACTICABLE. THE COPY FURNISHED TO DTIC CONTAINED A SIGNIFICANT NUMBER OF PAGES WHICH DO NOT REPRODUCE LEGIBLY.

USAAMRDL-TR-74-102A

AD B002067

CORRELATION OF ACTUAL AND ANALYTICAL HELICOPTER AURAL DETECTION CRITERIA
VOLUME I

Wyle Laboratories
3200 Magruder Boulevard
Hampton, Va. 23666

January 1975

Final Report for Period March 1973 - December 1974

Prepared for

EUSTIS DIRECTORATE
U. S. ARMY AIR MOBILITY RESEARCH AND DEVELOPMENT LABORATORY
Fort Eustis, Va. 23604

EUSTIS DIRECTORATE POSITION STATEMENT

This report has been reviewed by this Directorate and is considered to be technically sound. The technical monitor for this effort was Mr. B. W. Scruggs, Safety and Survivability Technical Area, Military Operations Division.

Unclassified
SECURITY CLASSIFICATION OF THIS PAGE (When Data Entered)

REPORT DOCUMENTATION PAGE		READ INSTRUCTIONS BEFORE COMPLETING FORM
1. REPORT NUMBER USAAMRDL-TR-74-102A	2. GOVT ACCESSION NO.	3. RECIPIENT'S CATALOG NUMBER
4. TITLE (and Subtitle) Correlation of Actual and Analytical Helicopter Aural Detection Criteria Volume I		5. TYPE OF REPORT & PERIOD COVERED Final Contractor Report March 1973-December 1974 6. PERFORMING ORG. REPORT NUMBER Not Applicable
7. AUTHOR(s) A. Louis Abrahamson		8. CONTRACT OR GRANT NUMBER(s) DAAJ02-73-C-0057
9. PERFORMING ORGANIZATION NAME AND ADDRESS Wyle Laboratories 3200 Magruder Boulevard Hampton, Virginia 23666		10. PROGRAM ELEMENT, PROJECT, TASK AREA & WORK UNIT NUMBERS Task 1F126205AH8801
11. CONTROLLING OFFICE NAME AND ADDRESS Eustis Directorate U.S. Army Air Mobility R&D Laboratory Fort Eustis, Virginia 23604		12. REPORT DATE January 1975 13. NUMBER OF PAGES 131
14. MONITORING AGENCY NAME & ADDRESS(if different from Controlling Office)		15. SECURITY CLASS. (of this report) Unclassified 15a. DECLASSIFICATION/DOWNGRADING SCHEDULE None

16. DISTRIBUTION STATEMENT (of this Report)

Distribution limited to U.S. Government agencies only; test and evaluation; January 1975. Other requests for this document must be referred to the Eustis Directorate, U.S. Army Air Mobility Research and Development Laboratory, Fort Eustis, Virginia 23604.

17. DISTRIBUTION STATEMENT (of the abstract entered in Block 20, if different from Report)

18. SUPPLEMENTARY NOTES

This study was supported by the Langley Research Center and Wallops Flight Station of the National Aeronautics and Space Administration, the National Oceanographic and Atmospheric Administration, and the Space Radiation Effects Laboratory.

19. KEY WORDS (Continue on reverse side if necessary and identify by block number)

Helicopter
Aural
Detection
Hearing
Atmosphere
Sound
Propagation
Spectrum analysis
Acoustic masking

20. ABSTRACT (Continue on reverse side if necessary and identify by block number)

This study was conceived as a basic experiment for measurement of helicopter aural detectability, and for assessment of the accuracy of a model developed by Ollerhead for computing aural detection distances.

The experiment was conducted over a period of two weeks at NASA Wallops Station utilizing 25 Army personnel as listening subjects, and three different types of helicopters

DD FORM 1 JAN 73 1473 EDITION OF 1 NOV 65 IS OBSOLETE

Unclassified
SECURITY CLASSIFICATION OF THIS PAGE (When Data Entered)

20. Continued.

currently in Army service. The effect of the following parameters was investigated: ambient noise level, flight profile, listener attentiveness, atmospheric conditions.

Reduction of data was executed using a new procedure for simulating aural frequency decomposition of sound. Correlation with Ollerhead's model confirmed his laboratory-derived detectability criterion as a median case for individual response and allowed extension of the criterion in the context of a measured statistical distribution.

Published data included in Ollerhead's model for sound attenuation, other than for atmospheric absorption, was found to be inapplicable and a new comprehensive attenuation model based on measured results was formulated.

Comparison of theoretical results, derived using the improved model for predicting helicopter aural detection distances, with measured values provided satisfactory correlation.

PREFACE

The work reported herein was performed by Wyle Laboratories' Hampton Facility Research Staff, under Contract DAAJ02-73-C-0057 for the Eustis Directorate, U. S. Army Air Mobility Research and Development Laboratory, Fort Eustis, Virginia, and was carried out under the technical cognizance of Mr. Bill W. Scruggs, Jr., of the USAAMRDL staff.

The study was supported by the Langley Research Center and Wallops Flight Station of the National Aeronautics and Space Administration. Mr. David A. Hilton, of the Acoustics and Noise Reduction Division, NASA-Langley, coordinated the NASA support and assisted in the technical planning of the field test. In addition, Wyle Laboratories acknowledges the assistance of the following NASA personnel for their efforts in this program: Mr. Domenic J. Maglieri for his support throughout the project and for providing computation and data reduction facilities; Mr. Gene Godwin, who directed the flight operations, coordinated radar and meteorological measurements, and provided digital processing of the radar data; Mr. Ralph B. Lewis for providing many of the measuring instruments; and Dr. Walter J. Gunn for psychological consultation related to the tests.

Wyle Laboratories also acknowledges the support of the National Oceanographic and Atmospheric Administration for acquiring the meteorological data, and the Space Radiation Effects Laboratory for use of their computer to reformat digital data.

This report describes the efforts of many of the Wyle Laboratories' staff. The author especially thanks: Mr. John Wood and Mr. Lou Sutherland for their assistance and helpful advice throughout the project; Mr. Ed Braganza for planning and supervising the acoustic measurements; Mr. Monte Haun for programming the computer model and data reduction procedures; Mr. John Ollerhead and Mr. David Brown for program planning assistance; Mrs. Brenda White, Mrs. Mary Massarotti and Mr. Malcolm Anderson for the many tedious hours spent in reducing the data; and Mrs. Karen Beissner and Mr. C. D. Sherman for illustrating and editing the report.

TABLE OF CONTENTS

LIST OF ILLUSTRATIONS

Figure		Page
31	Effect of Wind Velocity on Excess Atmospheric Attenuation From Measured 1/3-Octave Data (250 Hz, Downwind Propagation)	70
32	Effect of Wind Velocity on Excess Atmospheric Attenuation from Measured 1/3-Octave Data (500 Hz, Downwind Propagation)	71
33	Results of Regression Analysis on Excess Atmospheric Absorption for Sound Propagation Upwind	72
34	Results of Regression Analysis on Excess Atmospheric Absorption for Sound Propagation Downwind	73
35	Combinations of Distance and Elevation Angle Between 2 and 10°	76
36	Plot of Weighting Factor to be Applied to Linearized Values of Excess Atmospheric Attenuation for $2^\circ < \theta < 10^\circ$	78
37	Pure Tone Threshold (From References 3 and 38)	82
38	Summary of Measured Detection Data for Run 7 (4-Second Average)	83
39	Summary of Measured Detection Data for Run 19 (4-Second Average)	84
40	Summary of Measured Detection Data for Run 23 (4-Second Average)	85
41	Summary of Measured Detection Data for Run 24 (4-Second Average)	86
42	Summary of Measured Detection Data for Run 37 (2-Second Average)	87
43	Summary of Measured Detection Data for Run 38 (2-Second Average)	88

LIST OF TABLES

INTRODUCTION

HELICOPTER AURAL DETECTABILITY: SIGNIFICANCE

Detectability of any military vehicle by enemy forces profoundly affects the potential usefulness of that vehicle and the degree of utilization and survivability which can be achieved in combat situations.

In the case of military helicopters, whether operating in surveillance, close air support, or transport roles, it is usual for aural detectability to assume significant importance relative to visual and infrared detection modes.

Particularly, in the case of an armed helicopter operating in the close air support role at very low altitudes using terrain for concealment and protection in nap-of-the-earth flight, aural detection distances are typically greater than distances derived from other detection modes by a wide margin.

OUTLINE OF THE PROBLEM

This study concerns itself with helicopter aural detectability. There are three broad categories of effects which need to be quantified and modeled:

1. Helicopter noise generating and radiating characteristics.

2. Propagation of sound over long distances near grazing angles through the atmosphere.

3. Reception and recognition of complex noise signatures (i.e., helicopter noise) by listeners.

All these topics have been studied separately in several instances. There have been relatively few attempts to present a unified approach to helicopter aural detectability per se. The first reported measurements of aircraft aural detectability were carried out by Hubbard and Maglieri[1] in 1958, but these were related to a noise reduction program on a particular aircraft. Loewy[2] presented a comprehensive analysis of the problem, and using data gathered from a variety of sources was able to formulate a model for helicopter aural detectability. Ollerhead[3] carried out a laboratory study of the particular characteristics of helicopter noise influencing aural detectability, and used further published data on atmospheric sound propagation to advance Loewy's model. Ungar[4] also outlined a method for prediction of aural detection distances but this was oriented toward light aircraft, and Fidell et al[5] carried out laboratory experiments in the aural detectability of aircraft in noise backgrounds.

Only one previous attempt has been made to check any of these models in a field experiment. Hartman and Sternfeld[6] specifically set out to assess the aural detectability portion of Ollerhead's model but were unable to obtain satisfactory agreement. This was perhaps due to the difficulty of measuring an extremely sensitive parameter in field conditions.

The problem of quantifying helicopter aural detectability is not as simple as it might first appear. Helicopter noise generating mechanisms are many and complex, and all are still not entirely understood. In addition, the radiated noise is highly directive, and due to the unstable character of helicopter flight, its average parameters are not stationary with time. Then, too, propagation of sound through the lower atmosphere is one of the least easily quantifiable effects in acoustics today. This is due to the inhomogeneous nature of the layer of air close to the earth's surface which varies with terrain and weather conditions, and also due to the terrain itself.

Due to the physical variability found among human beings, their ability to improve their perception and recognition by learning, and the effects of other subjective parameters such as concentration and motivation which are almost unquantifiable, the topic of aural detection itself is perhaps the one least easy to model.

BRIEF DESCRIPTION OF THIS STUDY

It was not the purpose of this study to evaluate helicopter noise prediction models, since that is properly the subject of separate studies. The problem is thus divided naturally into the latter two independent segments of sound propagation and listener reception listed above, with a typical noise source assumed. This approach was adopted by Ollerhead,[3] and it is followed here.

This study was conceived as a basic experiment for measurement of helicopter aural detectability, and for assessment of the accuracy of different aspects of models - particularly Ollerhead's - for computing aural detection distances.

In the current study, three Army helicopters and a group of 25 Army personnel participated in an exercise spread over two weeks at the

NASA Flight Test Facility at Wallops Station, Virginia. Noise recordings were made at five separate stations along two 12-mile test courses to measure sound propagation decrements, while the response from 20 subjects, who were visually screened from approaching helicopters, was monitored.

BACKGROUND TO HELICOPTER AURAL DETECTABILITY

HELICOPTER NOISE CHARACTERISTICS

Clearly, the main sources of helicopter noise are its rotors and engines, usually in that order. Noise sources and mechanisms are generally broken up into many different categories, and since they are usually linear phenomena, the resultant field is simply the addition of the fields due to all the separate components. The main and tail rotors generate several different types of noise, and each type can be represented by an equivalent acoustic source:

1. Rotational Noise - Consider the disc of air through which the rotor blades pass. Immediately under the blades, a section of air is being accelerated away from the blade while the reverse effect is evidenced on top of the blade. Any acceleration of a gas produces a radiated acoustic field. This same section of air, a short time after the blade has passed, will return to a semiequilibrium state, only to be disturbed again by the following blade. This successive thumping of air within the disc gives helicopter noise its characteristic pulsatile sound (References 7-9).

2. Aerodynamic Noise - Even an aerodynamically streamlined object moving through air leaves a turbulent wake behind it, composed of relatively unorderly motion of air returning to equilibrium after the recent disturbance. This mechanism generates a swishing noise (References 9-12), which is characteristically broadband. In the case of rotors, it is modulated at the blade passage frequency and its harmonics.

3. Blade Slap - The most common mechanism for this intense periodic banging noise, which is occasionally emitted by helicopters during high-speed flight or maneuvers, occurs when a blade passes through the vortex shed by the tip of the previous blade causing transient loadings and velocities approaching sonic speeds. This phenomenon has been observed only for main rotors (References 13 and 14).

Noise sources attributable to jet engines and drive mechanism may be delineated as follows:

1. Jet Noise - Broad frequency band aerodynamic noise originating in the jet efflux from turbulence generated by the shearing

motion of the jet stream relative to the ambient flow (References 10-12, 15).

2. Compressor and Fan Noise - Noise from primary stages within the engine which is qualitatively similar to rotational and aerodynamic noise sources discussed in the case of helicopter rotors above (References 6-17).

3. Gear Noise - Noise originating from the meshing of gears and dynamic oscillation of drive shafts. This is usually the principal noise source within the cabin environment (Reference 18).

At distances where detection first occurs, these latter three noise sources rarely contribute significantly to the detectable sound field.

PROPAGATION OF SOUND THROUGH THE LOWER ATMOSPHERE

Individual Effects on Sound Propagation in the Lower Atmosphere

Propagation of sound through the lower atmosphere is influenced by numerous factors which are difficult to measure and more difficult to predict. This section will outline the nature of these factors and explain some of the anomalies which have been evidenced in previous experiments.

First, consider the well-known effects, which may be observed in a laboratory:

1. Spherical Spreading Losses - A point source in an ideal medium radiates a spherical wave front which expands uniformly. Accordingly, the sound energy incident on unit surface area of the sphere decreases with increasing distance from the source by an inverse square relation. Thus,

$$P_1^2 \propto \frac{1}{r_1^2} \quad , \quad P_2^2 \propto \frac{1}{r_2^2}$$

where P_1 and P_2 = sound pressure amplitudes at r_1 and r_2 respectively; i. e.,

$$P_2 = P_1 \frac{r_1}{r_2} \quad \text{or} \quad SPL_2 = SPL_1 + 20 \log \frac{r_1}{r_2}$$

where SPL_1 and SPL_2 = sound pressure levels in dB at distances r_1 and r_2 from the source respectively.

2. Absorption by the Atmosphere - Atmospheric absorption losses have two forms:

   a. Losses associated with the change of acoustical energy or ordered energy of air molecules into heat or disordered energy of air molecules. In a given volume of a gas, the molecules within will be in random motion so that at any instant the total vector sum of all their velocities will be zero. When a sound wave passes through this volume, the random motion of the molecules will have superimposed upon it a net resultant velocity. Transport losses in a gas represent the gradual decomposition from relatively ordered motion of the molecules to random motion or heat (References 19 and 20), through the dual mechanisms of conduction and viscosity.

   b. Air is composed of several different gases whose molecular constituency is polyatomic. Polyatomic molecules may exist in several internal configurations, each with an associated energy state. It is possible for this type of molecule under the right conditions to commute its energy between internal and external states and vice versa. Molecular relaxation losses are associated with the change of translational kinetic energy of the molecules into internal vibrational or rotational energy within the molecules themselves (References 20-22).

Secondly, consider propagation of sound in the outside atmosphere.

3. Wind Velocity Gradients - When air flows uniformly at a constant velocity over a large solid flat surface, there is a transition from zero velocity at the surface of the solid to the uniform free-stream flow at velocity "U" some distance away. Although the definition of the thickness of this boundary layer thickness is, to a certain extent, arbitrary because transition from the velocity in the boundary to that outside it takes place asymptotically, it is customarily defined as that distance away from the surface of the solid where the velocity differs by 1%

from the free-stream velocity. Instead of the boundary layer thickness, another quantity, the displacement thickness δ^*, is often used. It can be considered as the thickness of a layer with uniform velocity having the same mass flow as actually occurs in the boundary layer. It is defined by the relation:

$$\delta^* = \frac{1}{U} \int_{h=0}^{\infty} \left(U - u(h)\right) dh$$

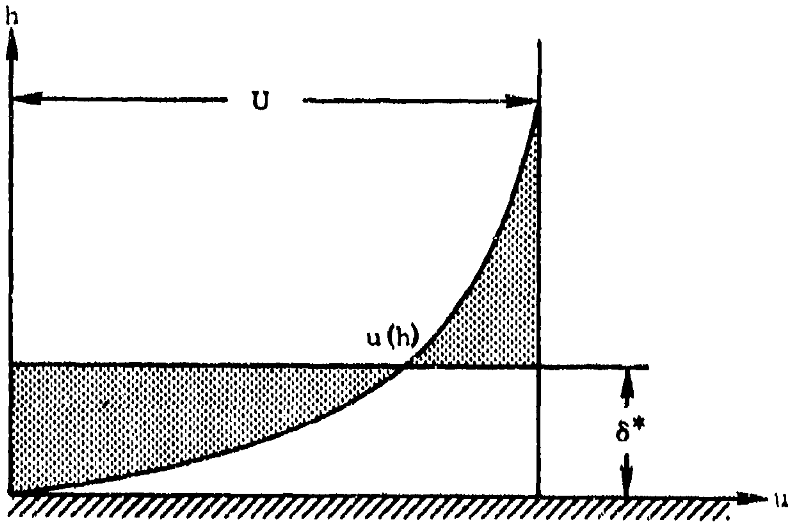

When a sound wave propagates through such a boundary layer, its rays follow curved, instead of straight, paths. Suppose a helicopter is approaching an observer station from downwind at a low altitude. Since, for detectability, we are concerned with propagation over many thousands of feet, the presence of even a small wind gradient is sufficient to bend the sound rays a significant amount. In this case (Figure 1) the sound is bent upward, giving rise to a "shadow zone" some distance away. It is important now to remember that sound is a wave motion and Huygens' principle that all points on a wave front act as secondary sources applies. Thus, diffraction, or the ability of waves to bend around corners, occurs into the shadow zone and instead of a sharp complete cutoff, the sound intensity decays exponentially with distance into the shadow (Reference 23).

Consider now a helicopter approaching from upwind. Radiated sound will now bend downward (Figure 2), and apart from following a marginally longer path, the effect on the intensity of sound reaching the observer will be slight. In the presence of a nonuniform gradient, focusing may occur and sound intensity downwind from the source may be substantially amplified.

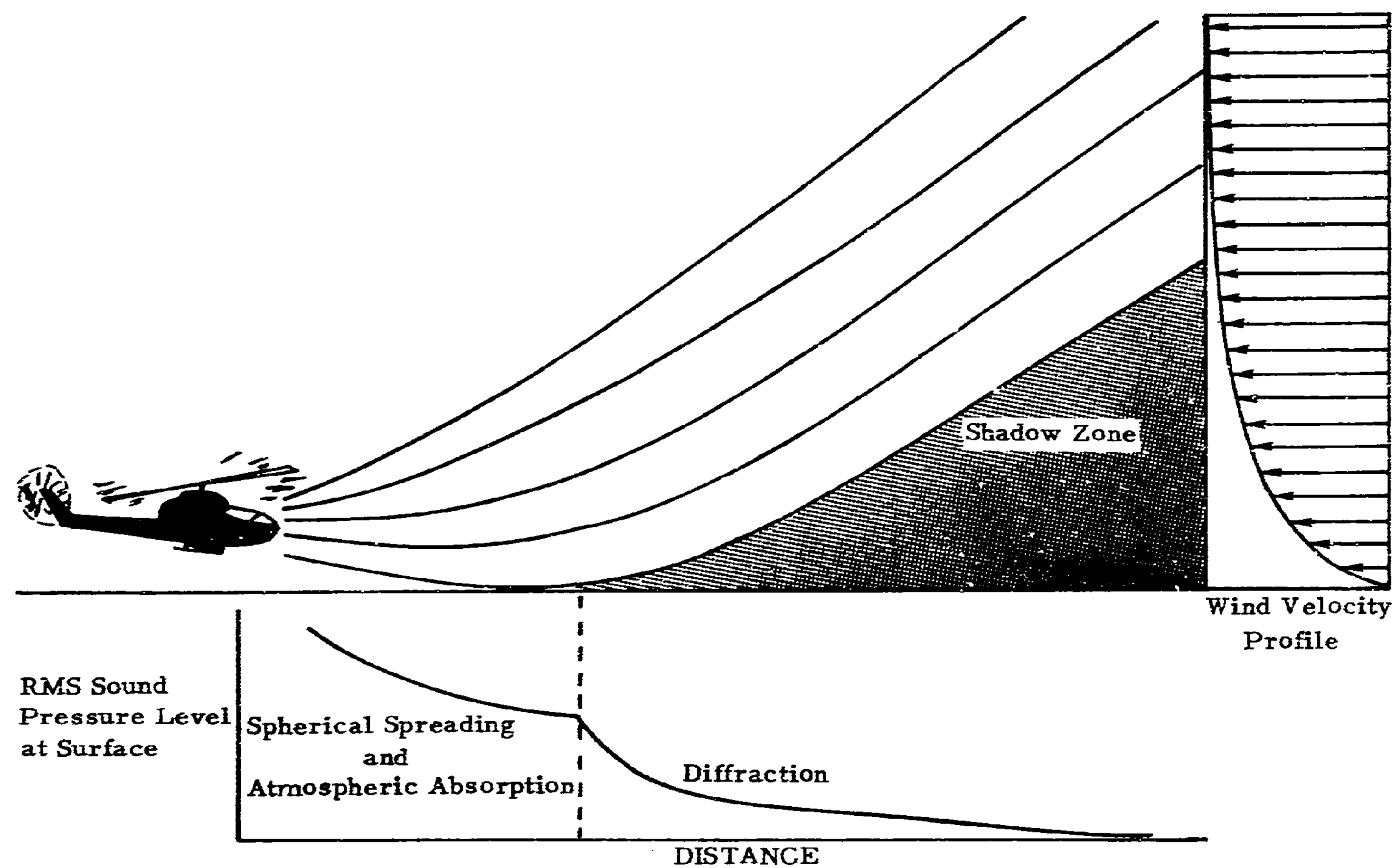

Figure 1. Effect of Wind Gradient on Low Altitude Sound Propagation - Upwind.

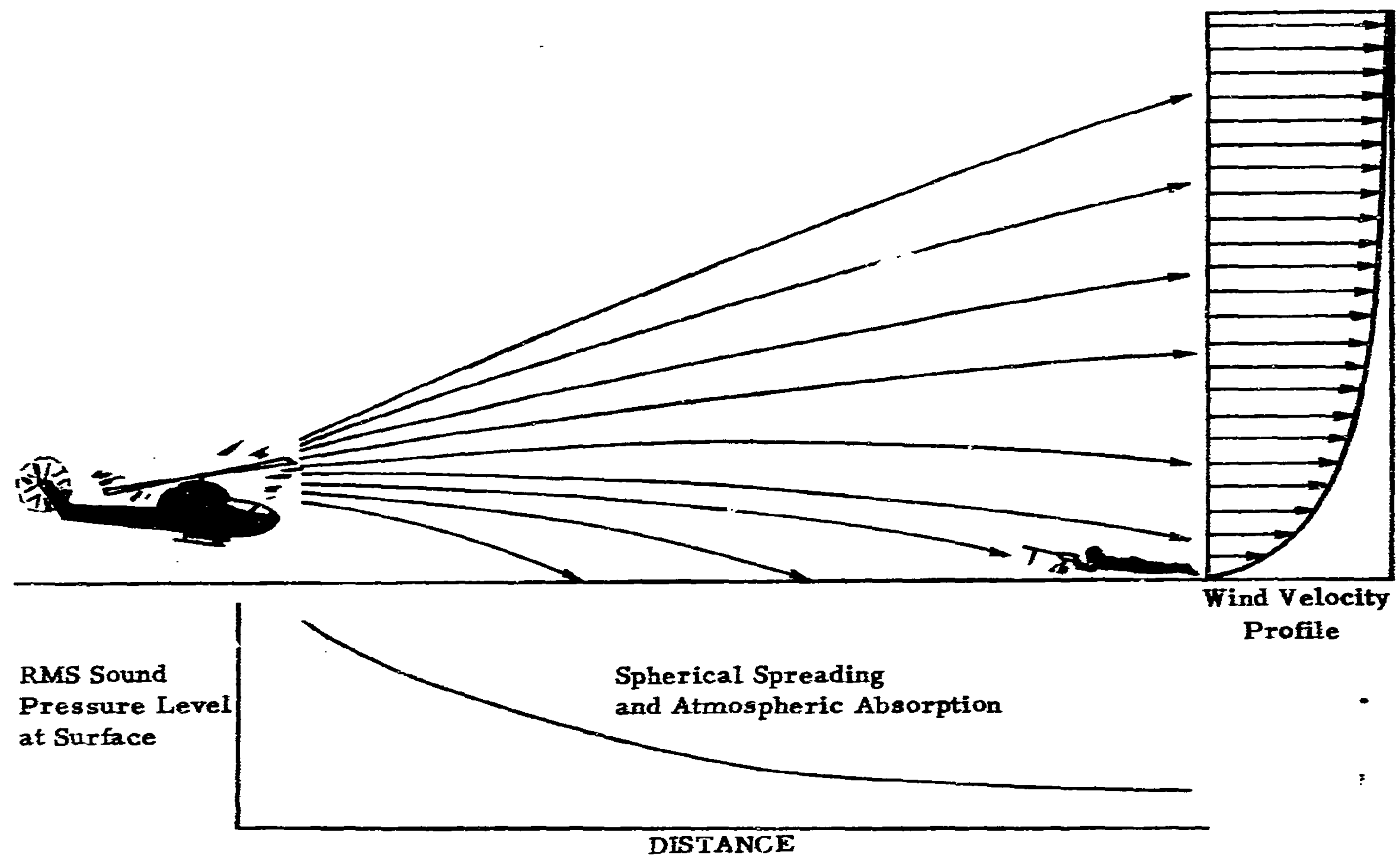

Figure 2. Effect of Wind Gradient on Low Altitude Sound Propagation - Downwind.

4. Temperature Gradients - The temperature of the surface of the earth undergoes cyclic heating and cooling due to direct radiation from the sun and other climatic effects. Thus, a differential generally exists between measurements of air temperature at different altitudes. Since the speed of sound increases with temperature, temperature gradients cause refraction of sound rays similar to wind velocity gradients. A negative temperature gradient (temperature decreasing with altitude) will result in sound waves being bent upward (Figure 1), while a positive temperature gradient will result in sound waves being bent downward (Figure 2).

5. Turbulence - Until now in the discussion, we have considered uniform laminar flow and a stationary temperature gradient. Generally, however, this is not the case since the mere presence of a temperature gradient in air results in convection currents, while flow over a realistically rough terrain with vegetation and topographic irregularities results naturally in turbulent flow. The distinguishing feature of turbulence in a flow is that the velocity at any given time and position is not found to be the same when it is measured several times under seemingly identical conditions. Turbulence is often described as a hierarchy of irregular vortex motions, or eddies, with a continuous transfer of kinetic energy down the scales from larger to smaller where it is eventually dissipated into heat by the action of viscosity. When a sound wave encounters turbulence, it undergoes a process known as scattering. This is a rather loose term for a combination of reflection, refraction, and diffraction. Thus, if an eddy were well-defined and large compared with the wavelength of the sound under consideration, the principal effects would be reflection and refraction; if the eddy were small compared to the wavelength, diffraction would predominate.

   Consider a thin sheet of turbulence covering the earth's surface and evaluate its effect on the propagation of helicopter noise. Usually the helicopter will itself be imbedded in the turbulence, and three effects will be evidenced as illustrated in Figure 3:

   a. A general broadening of the highly directive noise radiation pattern so that some distance away noise measurements are relatively independent of azimuth and elevation.

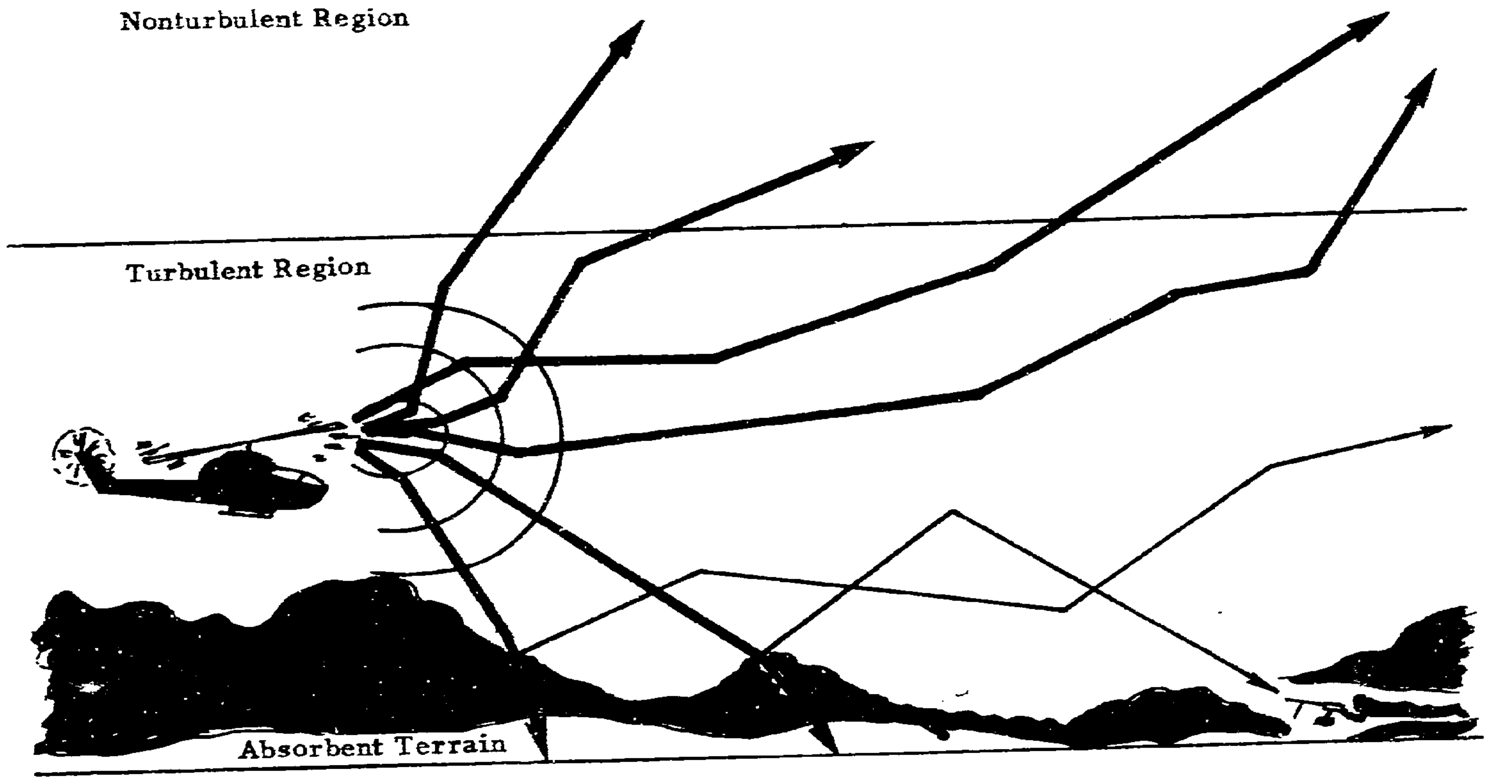

Figure 3. Effect of Atmospheric Turbulence on Low-Level Sound Propagation.

b. Redirection of sound energy, initially traveling parallel to the earth's surface, out of the upper boundary of the sheet of turbulence. Such sound energy will be scattered no more, and is effectively lost to a ground based observer.

c. Redirection of sound energy, initially traveling parallel to the earth's surface, toward the earth's surface where it is partially reflected and partially absorbed. This process may take place many times over long transmission paths.

The first effect may result in relative amplification or attenuation of the sound, while the second effect always results in excess attenuation. The third effect may result in amplification or attenuation, depending on the reflectivity of the earth's surface.

Superimposed on the above effects will be "twinkle" or "flicker" in sound monitored along the propagation path. In terms of a human receiver, it occurs as hearing, then losing, then again hearing the sound. This is due to the random nature of turbulence and the widely different paths which arriving sound may have traveled.

6. Edge Effects and Ground Absorption - Consider a plane wave traveling parallel to a large flat surface. Due to boundary conditions at the surface, the wave will undergo some residual attenuation; however, this is usually a small effect since a sound wave seldom in practice travels parallel to the ground, especially in the presence of refraction and scattering. Thus, the predominant effect is the absorption and partial reflection of a sound wave incident on the surface at an angle other than zero. Clearly, the degree of reflectivity of the surface is dependent upon surface hardness and density of vegetation.

Combined Effects on Sound Propagation in the Lower Atmosphere

All the effects described hitherto are relatively straightforward in concept. When they are combined, however, it is difficult to conceive of their resultant effect. Consider, for example, propagation of sound from a helicopter approaching at low altitude from downwind of an observer station, and allow for the effects of wind refraction, scattering, and ground absorption in addition to spherical spreading and atmospheric absorption (Figure 4). As illustrated in Figure 1, sound rays tend to bend upward, giving rise to an exponentially decaying shadow zone. The effect of scattering, however, is to increase the intensity of sound in the shadow zone since sound is no longer able to

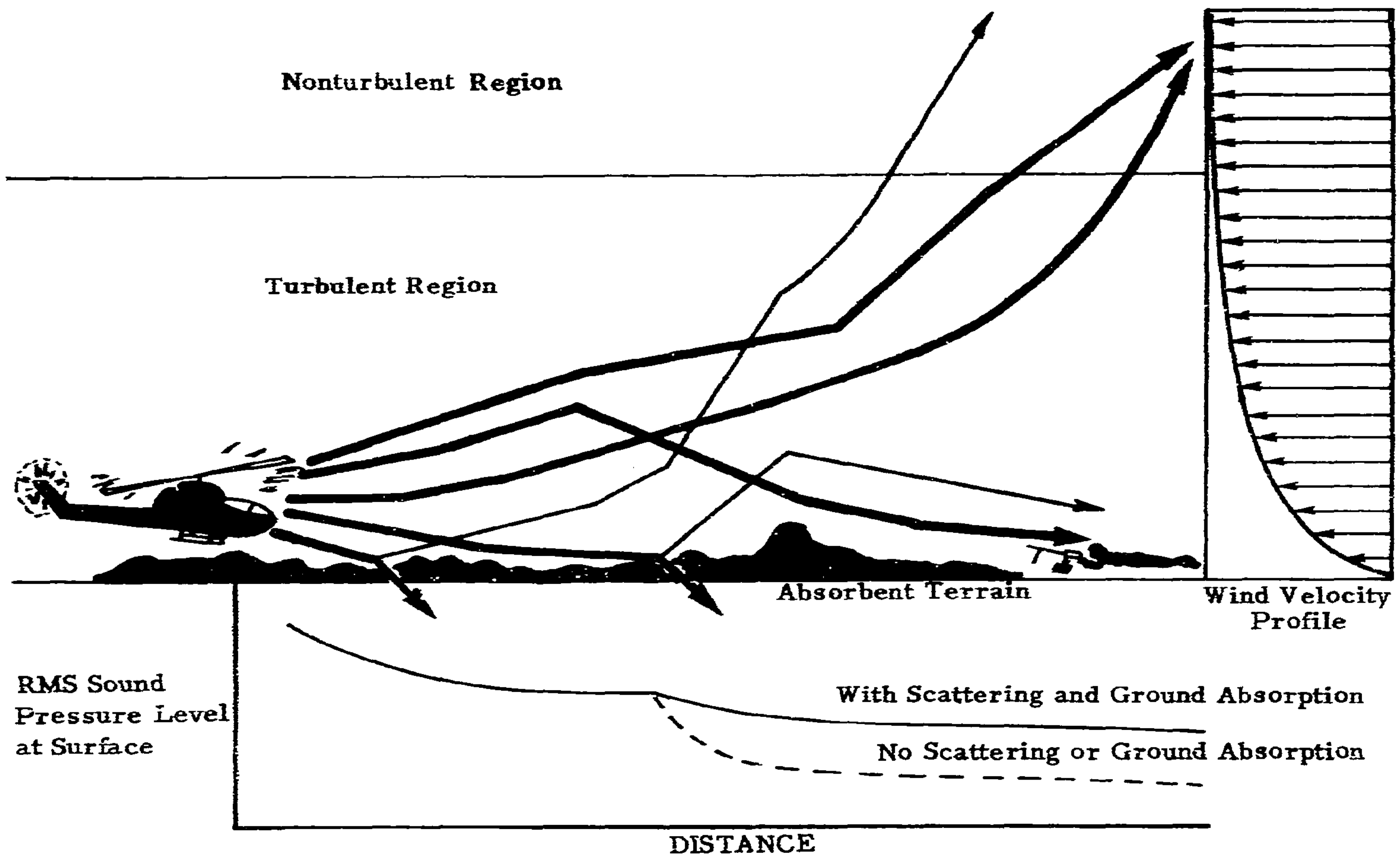

Figure 4. Effects of Wind Refraction, Scattering and Ground Absorption on Sound Propagation, Downwind Approach.

follow the smooth curved path as shown in Figure 1. Indeed, if the turbulence is sufficiently intense and the source is a significant distance above the ground, no shadow zone may even exist.

Under circumstances of severe scattering, ground reflectivity assumes increased importance since a large proportion of the sound eventually reaching the observer will be reflected from the ground at least once. Thus, over dense vegetation, sound attenuation will be significantly increased.

Take now the case of propagation of sound from a helicopter approaching at low altitude from upwind of an observer station (Figure 5) and consider the previously listed effects. Sound rays will tend to bend downward as in Figure 2, but scattering will tend to decrease this refraction, allowing relatively more sound energy to escape from the turbulent layer, and thus effectively increase attenuation over the case of refraction alone. This is contradicted by another effect since sound waves that would have been refracted to the ground will now travel farther without this occurring. Thus, in this case, the net effect of turbulence is probably small.

The above two examples serve merely to illustrate the complex and contradictory results which may be seen when several effects on sound propagation through a real atmosphere are combined.

Since wind velocity gradients are not solely functions of wind velocity measured at a point but are also dependent upon temperature gradient, terrain roughness and large-scale meteorological events, it is extremely difficult to make any quantitative assessment in the absence of continuous data concerning all necessary parameters at all distances and altitudes along the propagation path. However, even if such data were available, a mathematical model has not yet been developed for utilizing it.

The detailed atmospheric and ground surface measurements, coupled with the development of a computer-based solution scheme, were not considered in the scope of this study for several reasons:

1. The atmospheric parameters would be essentially nonstationary.

2. They would not be readily obtainable to anybody wishing to estimate helicopter detection distances for specific cases.

3. The combined nature of the propagation effects described, is that sound intensity as measured over a given distance from a constant source undergoes significant modulation. The

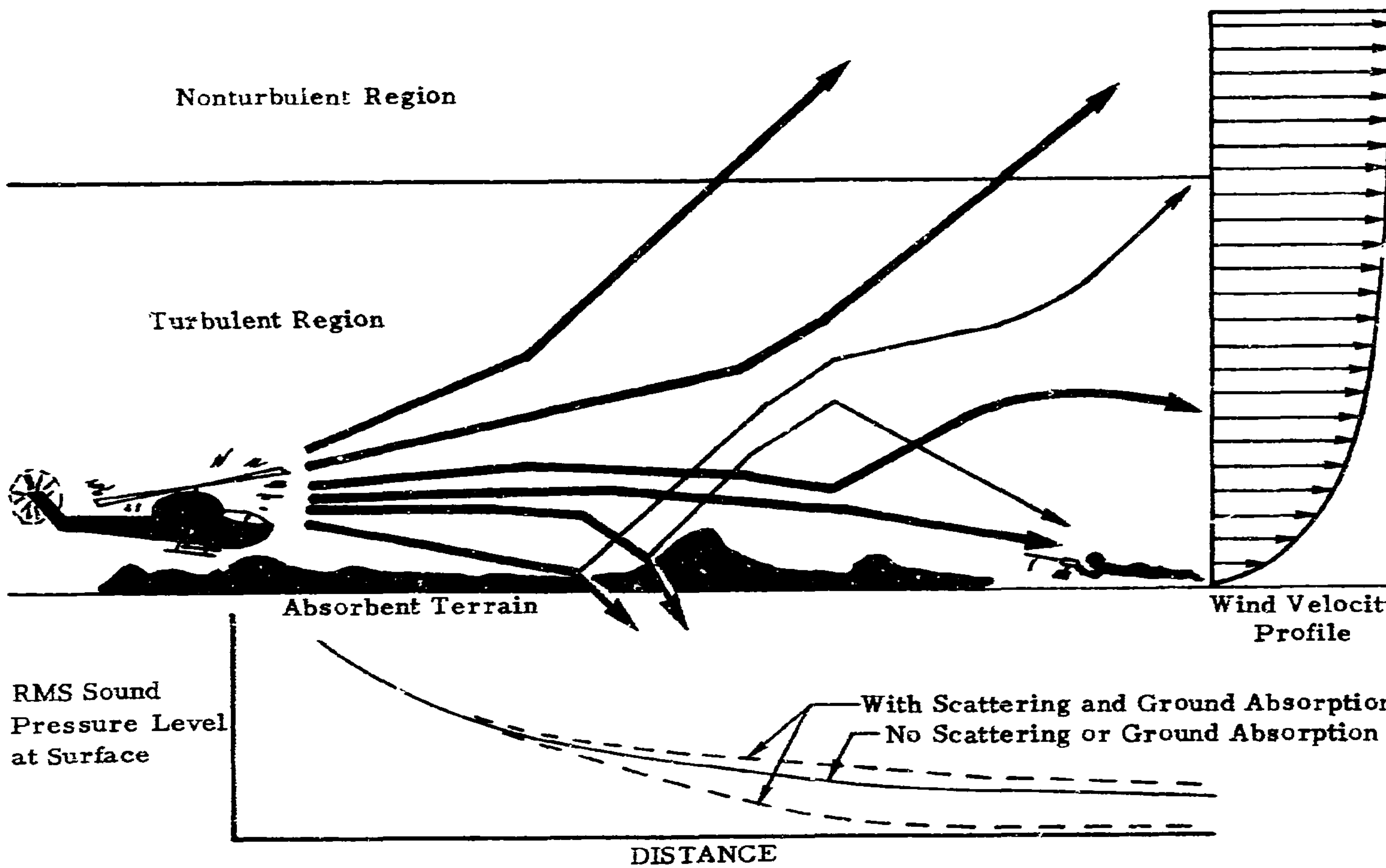

Figure 5. Effects of Wind Refraction, Scattering and Ground Absorption on Sound Propagation, Upwind Approach.

magnitude of these fluctuations is sufficiently great that an exhaustive study would, at best, yield only a probability distribution for atmospheric attenuation.

AURAL DETECTABILITY OF COMPLEX SOUNDS

The Critical Band

Human hearing and our perception of sounds are two of the most fascinating examples of nature's artistry. The ear itself is a brilliantly designed transducer which, when coupled with the topological capabilities of the human brain, allows us not only to interpret rapidly changing information but also to perceive intricate subtleties in the character of the information.

The physical structure of the ear is relatively well-known, as are the mechanisms of the ear cavity, the eardrum, the ossicles, and the fluid dynamics of the perilymph exciting the basilar membrane in the cochlear duct (References 24 and 25).

Any sound will excite the whole length of the basilar membrane, but because of its shape, different areas are much more readily excited by certain frequencies than others. This is because the basilar membrane is long and narrow (about 35 mm in length with a tapering width approximately 0.2 mm at the center). Thus, it is here that frequency decomposition of acoustic signals first takes place, with lower frequencies exciting the wider end preferentially and higher frequencies exciting the narrower end.

Attached between the basilar and relatively rigid tectorial membrane are thousands of tiny hair cell sensing elements. When the basilar membrane distorts, these hair cells generate signals which are transmitted through the auditory nerve to the brain.

The concept of a critical band is simply an analogy which has been used to represent the ear by a series of filters. Such a filter characteristic or aural discriminatory function is defined as being one critical band wide.

This function is known to vary with frequency and sound intensity, and its measurement has been the subject of several contradictory experiments. A contributory reason for this is evident when one considers the subjective nature of decisions which psychoacoustic subjects are required to make, coupled with real physical variation from one person to another and different experimental procedures.

The principal reason for discrepancies between reported results, however, seems to have been that investigators have attempted to measure a critical frequency bandwidth rather than the shape or frequency response of the critical band itself. This approach seems to have been supported by the usual assumption that the critical band function is equivalent to a perfect rectangular filter, while elementary considerations or cochlear dynamics show that it is not.

Major studies on the width of the critical band were performed by Zwicker[26] in the 1950's and Greenwood[27] in the early 1960's. Zwicker used a variety of psychophysical experiments including masking by tones or noise, loudness summation, phase sensitivity, and detection of multiple tones. Greenwood's measurements were made using several experimental masking procedures involving either tones or noise as signal or masker. He subsequently compared critical bandwidth measurements with measurements of position along the basilar membrane.[28]

Greenwood's and Zwicker's measurements agree reasonably well above about 600 Hz (Figure 6) but diverge widely at lower frequencies. Both linearize their measurements with distance of peak response along the basilar membrane, but use different data for frequency response of the basilar membrane. No definitive measurement resolving these discrepancies has yet been published.

References to measurements of the critical band above are distinguished from measurements of another parameter, the "Critical Ratio". Fletcher,[29] in his classic masking experiment, was the first to show existence of an aural discriminatory mechanism in the inner ear. In analyses of his results, Fletcher made two simplifying assumptions:

a. The power in a critical band of random noise is just sufficient to mask a tone of equal power centered on that band.

b. The shape of the critical band is analogous to a rectangular filter.

Both of these assumptions have since been shown in References 30 and 31 to be unjustified.

In their recent book, Zwicker and Feldtkeller[32] give the most orderly presentation to date on the aural mechanism. They present several sets of curves of the critical band function and illustrate how it varies with frequency and amplitude. A typical plot of the aural discriminatory characteristic extracted from this publication is given in Figure 7. The frequency scale is expressed in Bark or critical bandwidths (where

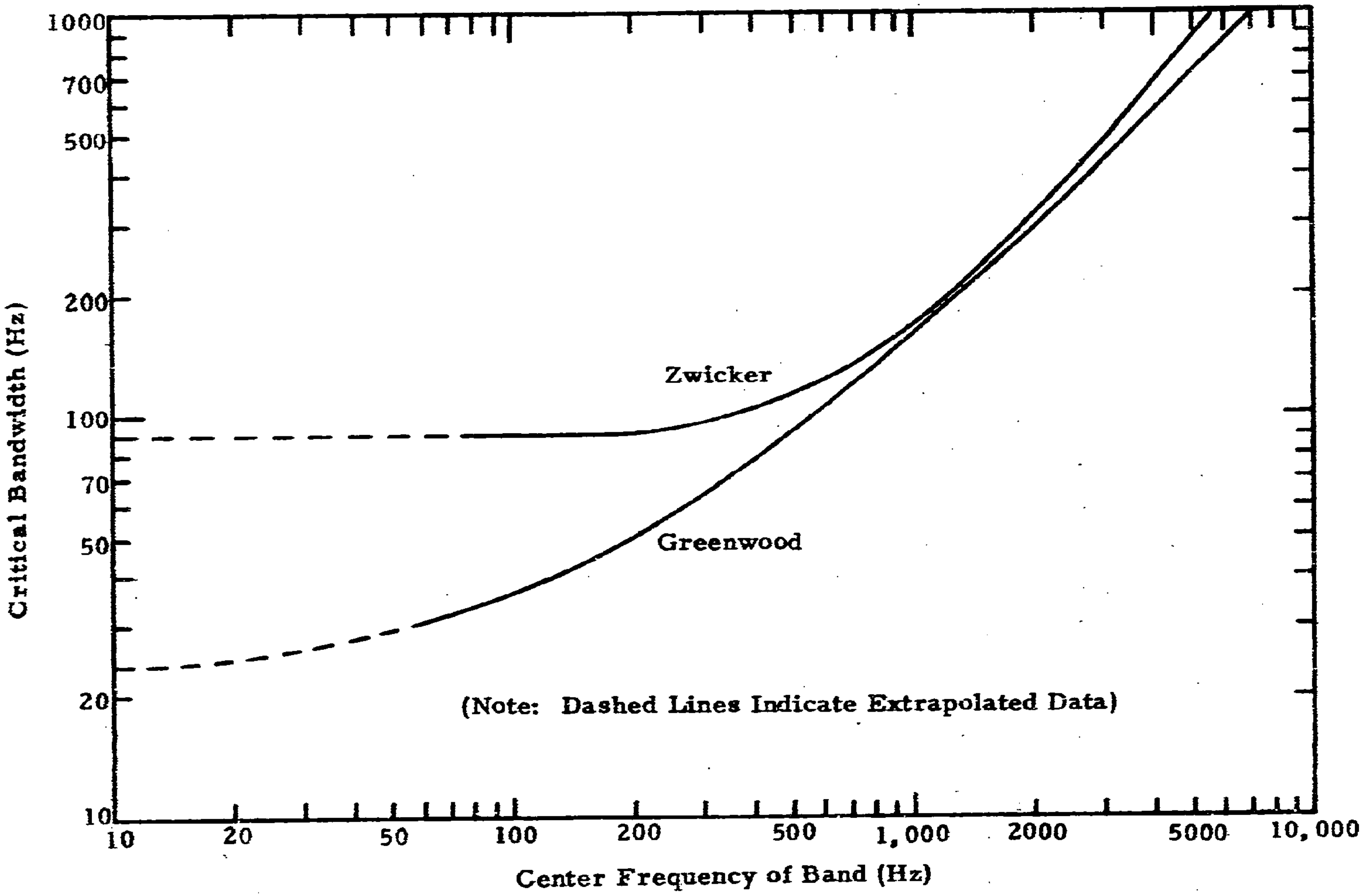

Figure 6. Variations Between Greenwood's and Zwicker's Measurements of Critical Bandwidth.

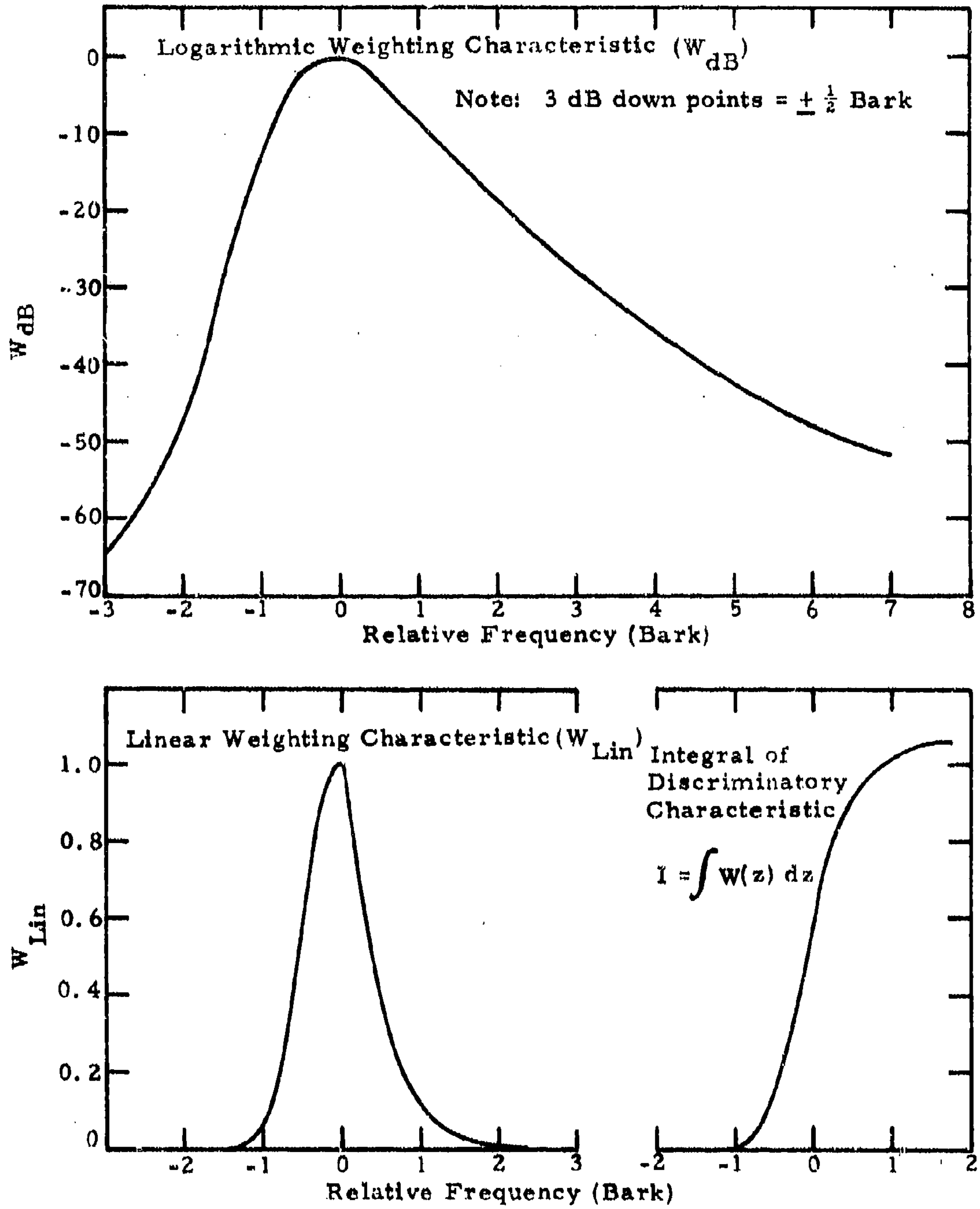

Figure 7. Aural Discriminatory Characteristics in 60-70-dB Range - Zwicker[32].

1 Bark = 1 crit. bw), and plotted relative to the center of the band. The shape of the aural discriminatory characteristic is not constant with frequency expressed in Hertz, but if frequency is expressed in Bark (e.g., as in Figure 8), then the characteristic may be translated without changing shape along the frequency scale. This convenient linearization has been proposed by Zwicker[32, 13] and has been used for conversion of measured to perceived acoustic signals in this study for both the field test data and the computer model.

One further simplification has been used in this study, namely, that the aural discriminatory characteristic is independent of sound intensity. Zwicker[32] shows significant broadening of the characteristic at high noise levels (above 85 dB). Inclusion of this effect increases computer time by about an order of magnitude and was considered to be unjustified since high noise levels are rarely important in detectability. The characteristic shown in Figure 7 was selected from subjective response in the 60-70 dB range.

Perception and Recognition of Complex Sounds

The importance of the ear itself in sensing and decomposing our acoustic environment is complemented by the ability of the human brain in learning, perturbing, and comparing complicated patterns. When viewed in terms of signal processing, the "cocktail party" effect, or the ease with which one can discern the information carried in a single voice at or below the ambient level in a crowded room, is remarkable.

This effect is of prime importance in the detectability of complex sounds, particularly those as distinctive as helicopter noise. Let us dwell on the actual processes to which an acoustic signal is subjected.

First, there is frequency decomposition by the ear. Even the most advanced Fourier analyzers currently in existence do not possess the ear's capacity for processing rapidly changing information. The ear's capability is equivalent to having several thousand matched parallel filters, each terminated by its own perfectly attuned integration network. Few informed measurements have been made of the auditory integration network, but it would seem reasonable to suppose that evolutionary processes would long ago have selectively developed the fundamentals of signal processing theory. Thus, to obtain sensible spectral information from the critical band filter lattice equivalent to the ear, we require a frequency-dependent time constant. The ideal time constants for both Zwicker's and Greenwood's determinations are contained in Figure 9. This has been obtained from the criterion

$$2 \times T \times \Delta f \geqq n \quad (n = 40)$$

where T is the integration time and Δf is the filter bandwidth. The quantity "n" on the right side represents the minimum number of degrees of freedom generally considered adequate for spectral analysis. Percentage error versus degrees of freedom for the 90% confidence level is plotted in Figure 10.

Figure 9 shows that higher frequencies require a very short time constant whereas low frequencies require a long time constant.

Our brain senses the multitude of time varying signals and fits known patterns of them, rejecting rapidly those that do not match. This mechanism may be active or passive; that is, we may obtain cues perhaps in the form of the movement of a persons lips in a noisy environment or we may strain to hear a helicopter that someone else has already heard. Generally, however, our senses or data acquisition facilities are free-running; that is, we do not have to turn them on or reset them as we do when we wish to communicate, and the most sophisticated interpretations are made without any conscious effort on our behalf.

This field appears to be relatively unexplored. Even if a suitable frequency analyzer were available, it would not readily be possible to apply a realistic analysis procedure to the perception and recognition of complex sounds for general computer processing. Programs to perform even simple topology in a reasonable time frame do not exist.

For specific cases, however, an analog may be used for this sophisticated procedure. The approach that is usually adopted is to apply empirical adjustments, for specific nonrandom sounds, to an energy detection model which uses the ratio of signal power to ambient noise power as an indicator of detectability,[34, 35] within each critical band with a frequency-dependent sensitivity term. The experiment performed by Ollerhead[3] represented just such an evaluation for helicopter noise signals.

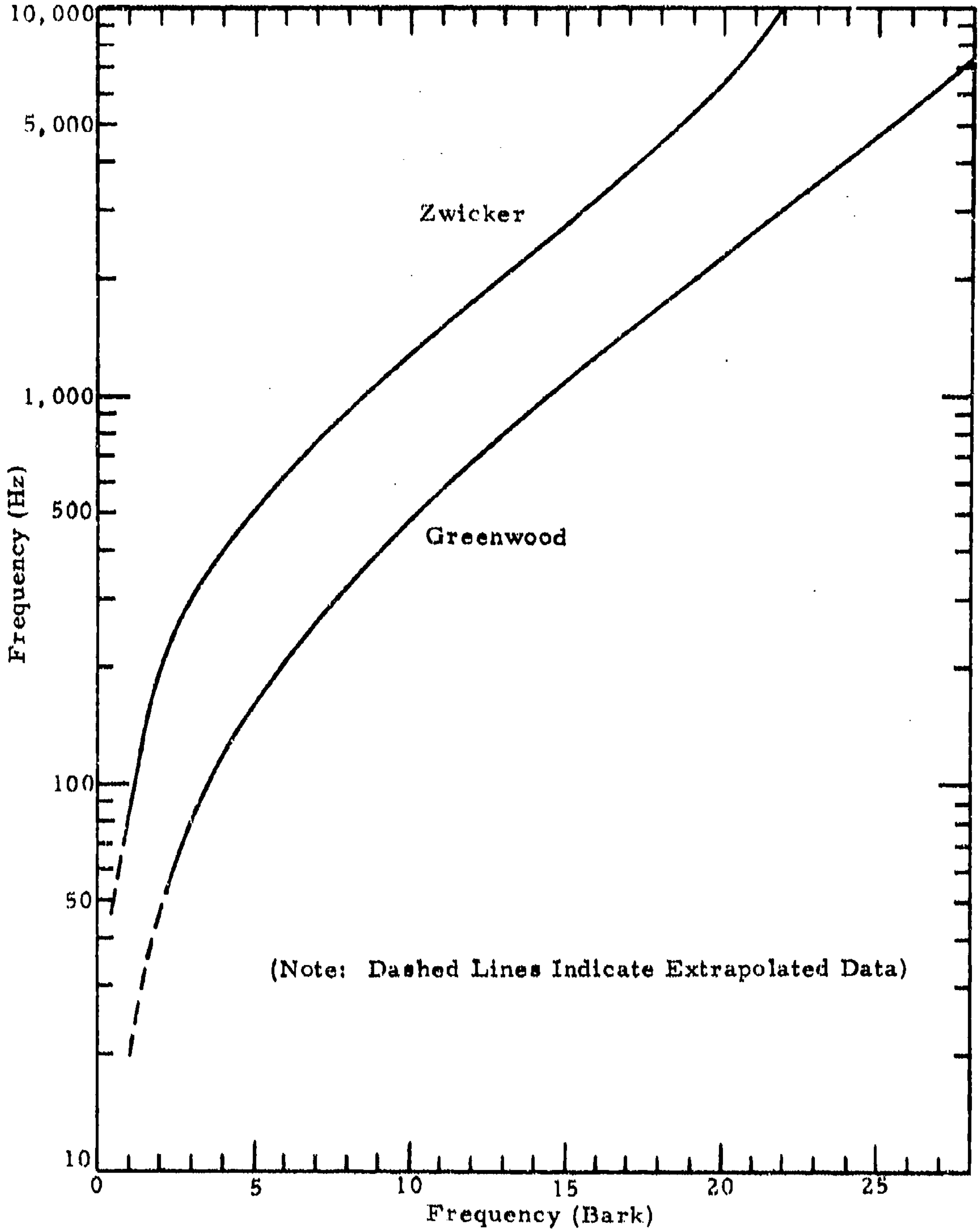

Figure 8. Relationship Between Hertz and Bark.

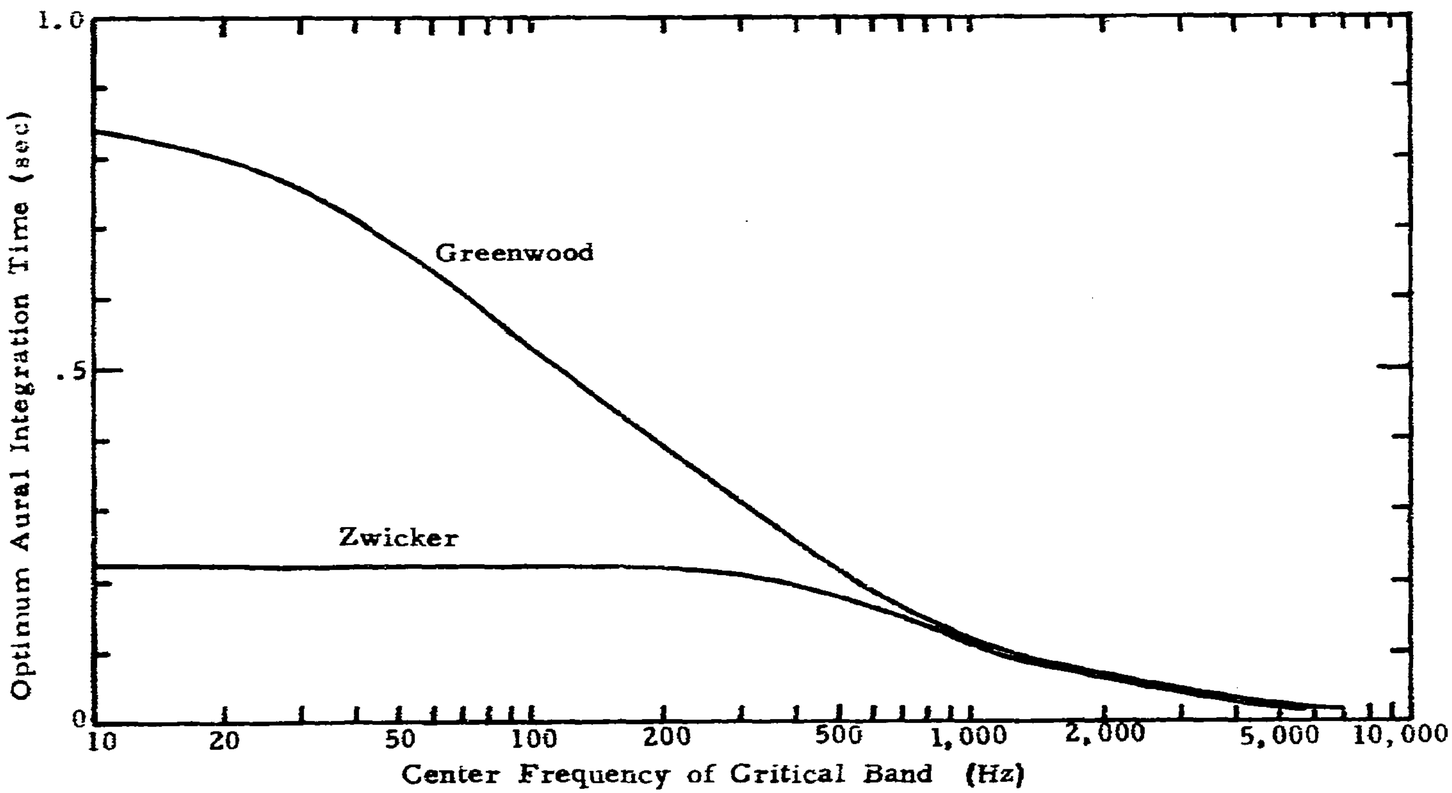

Figure 9. Time Constants for Greenwood's and Zwicker's Determinations of Critical Bandwidth, for 40 Degrees of Freedom ($2T\Delta f = 40$).

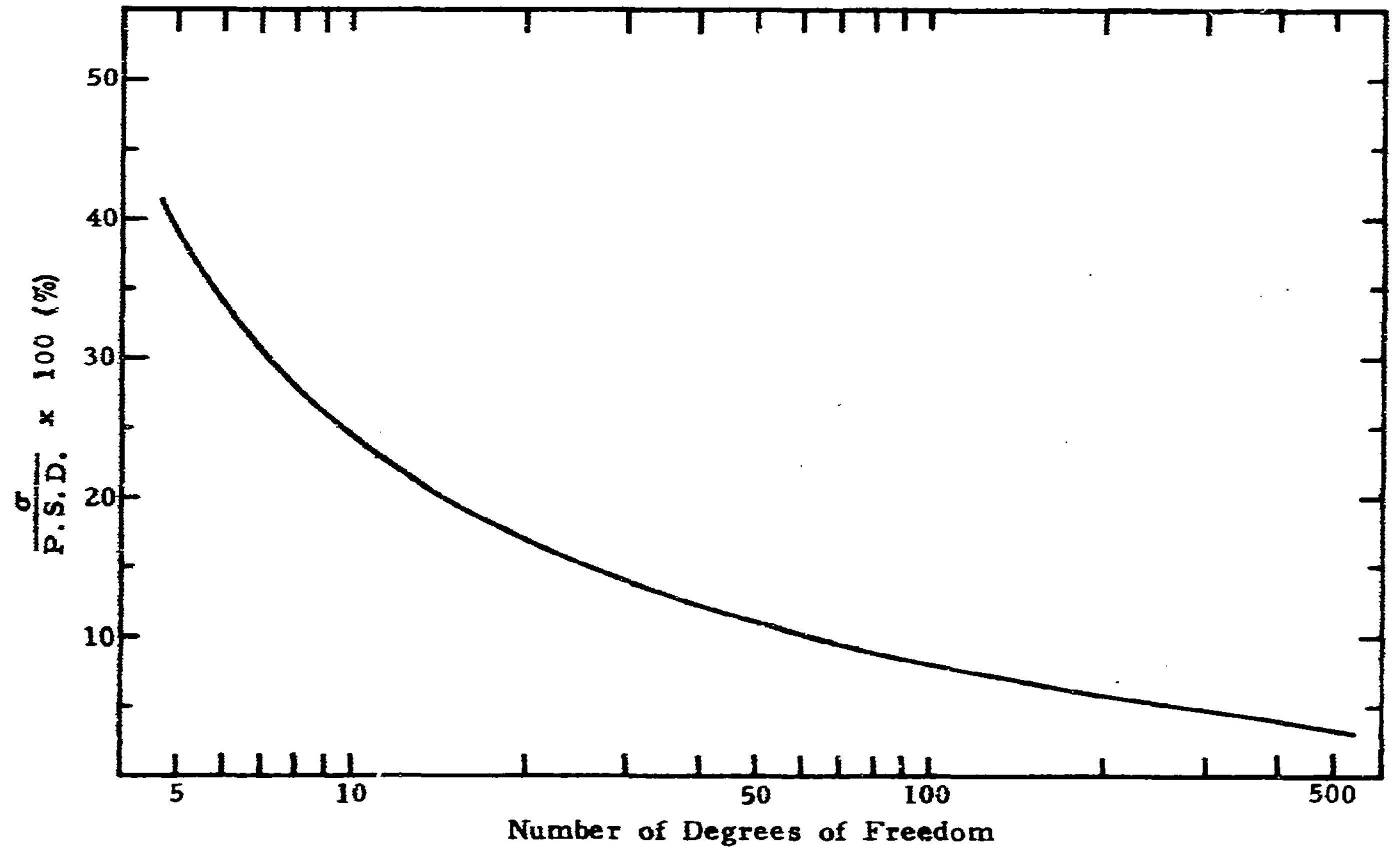

Figure 10. "Percentage of Standard Deviation of Power Spectral Density Estimate" Versus "Degrees of Freedom" for the 90% Confidence Limit.

FIELD MEASUREMENT PROGRAM

INTRODUCTION

The measurement program was designed so that two primary correlations could be performed under a variety of operational and environmental configurations:

1. Field measurements of detection threshold criteria with Ollerhead's[3] laboratory-derived detection threshold criteria.

2. Field measurements of aural detection distances with estimated aural detection distances.

PROGRAM OUTLINE

General

The measurement program was conducted at the NASA Flight Test Facility at Wallops Station over a period of two weeks in May 1973. Tests were conducted in the early morning and late afternoon to minimize interruptions and errors caused by uncontrolled noise in the area.

A geographical outline of NASA's Wallops Station facility and vicinity is given in Figure 11. The main runway is oriented in an east-west direction, with tidal mud flats in a line eastward and partially wooded farmland to the west. Two approach paths for helicopter flights were used, from due east and due west, toward the subject site near the west end of the main runway.

The three helicopters used in the program were selected so that they represented a cross section of types currently in Army service, namely:

1. UH-1B - Iroquois - Utility, seven passenger

2. AH-1G - Cobra - Attack, two seat

3. OH-6A - Cayuse - Light reconnaissance

During test periods, two aircraft were airborne at a time, each carrying a radar transponder for accurate low-level tracking by the field radar installation. The aircraft not engaged in a test run was kept in a loiter area acoustically remote from the test area. With the exception of the final five flights, the helicopters made their approaches singly in

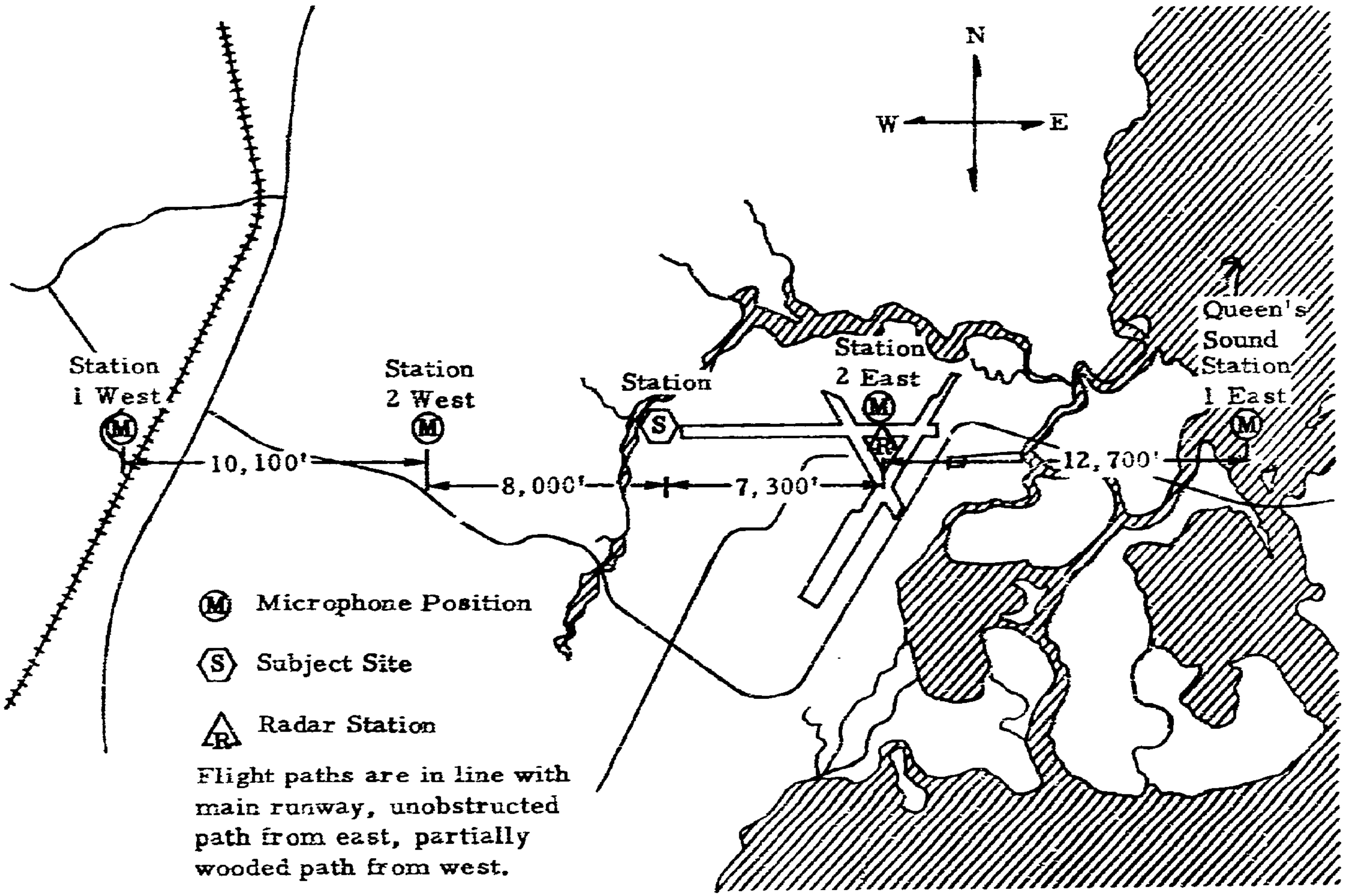

Figure 11. NASA's Wallops Station Geographical Outline.

a randomized order, each helicopter repeating a particular flight path over a given terrain at specific altitude and velocity six times to allow conditions at the listening subject's site to be varied.

Subjective Aspects

The listening subjects consisted of two groups of ten soldiers in the early and mid-twenty age group. They represented a random selection from a group of volunteers. Only those whose audiograms showed unusual hearing losses (greater than 10 dB from normal) were rejected. The configuration of the subject site is illustrated in Figure 12. The two groups represented different conditions of attentiveness and were separated from each other by a distance of about 30 feet. An acoustically transparent, visual screen (constructed from burlap) surrounded each group, visually screening them from each other and from the approaching aircraft. Each subject was visually screened from the other members of his group so that he could not obtain visual cues from his neighbors (Figure 13).

All equipment for communications with the aircraft and the control tower, as well as equipment for monitoring and recording acoustic and subject response data, was located in a trailer approximately 500 feet from the subject site (Figure 12).

Communication with the subjects was achieved via two illuminated display panels, one for each group (Figures 13 and 14).

Activity at the observer site was closely supervised by research staff personnel who were able to communicate with the trailer via a field telephone.

The subjects were given switches by which they were expected to record

1. when they thought they heard an approaching helicopter, and

2. when they could positively confirm that a helicopter was approaching.

To assist in informing and motivating them, they were provided with the following instruction sheet on the day prior to commencement of tests during an introductory meeting. This was followed by a series of practice runs so that they could familiarize themselves with the procedure.

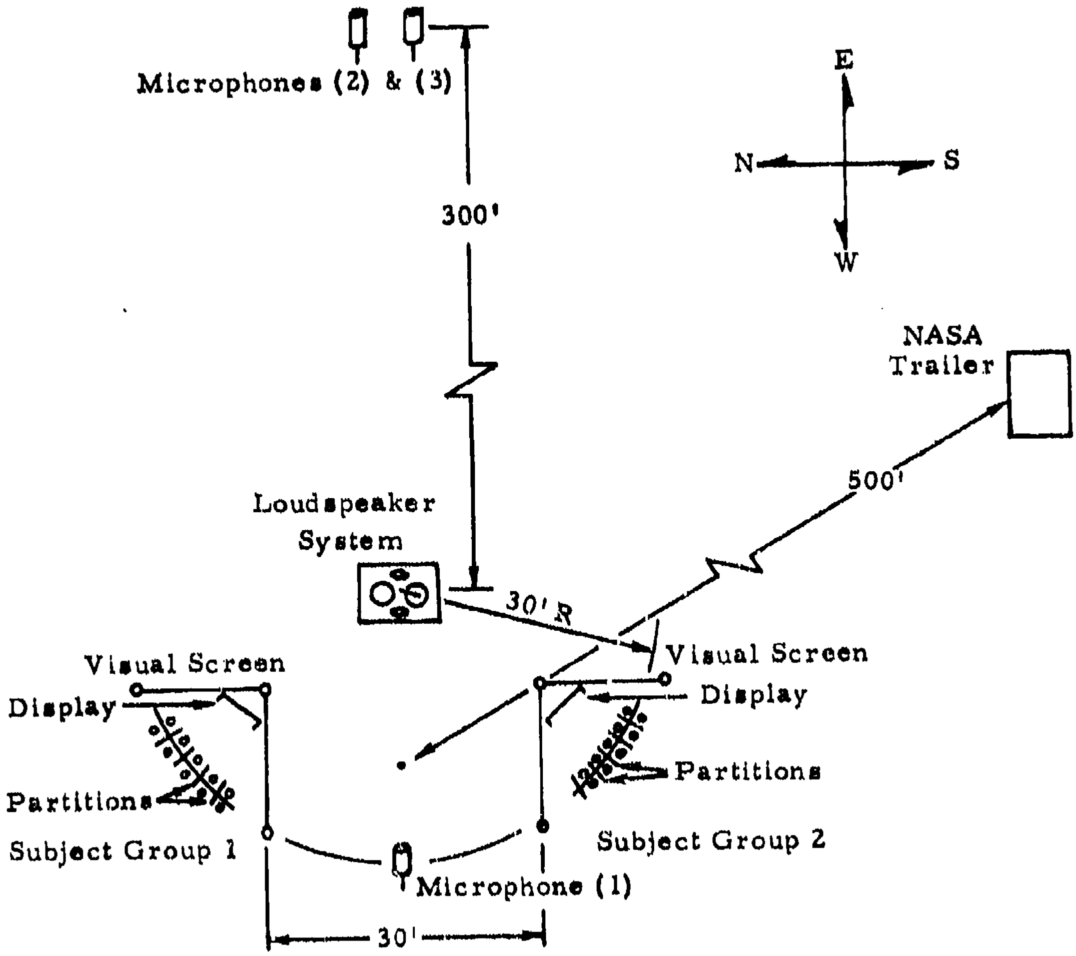

Figure 12. Configuration of Subject Site.

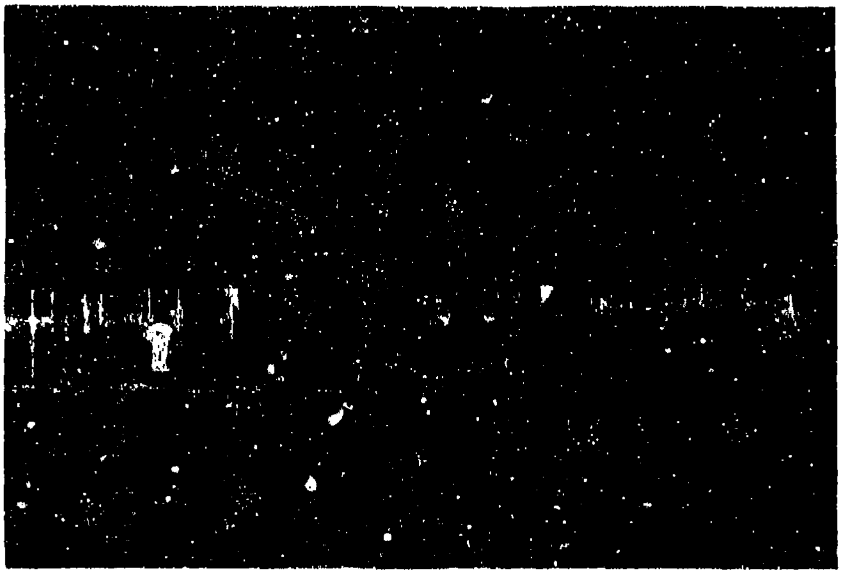

A

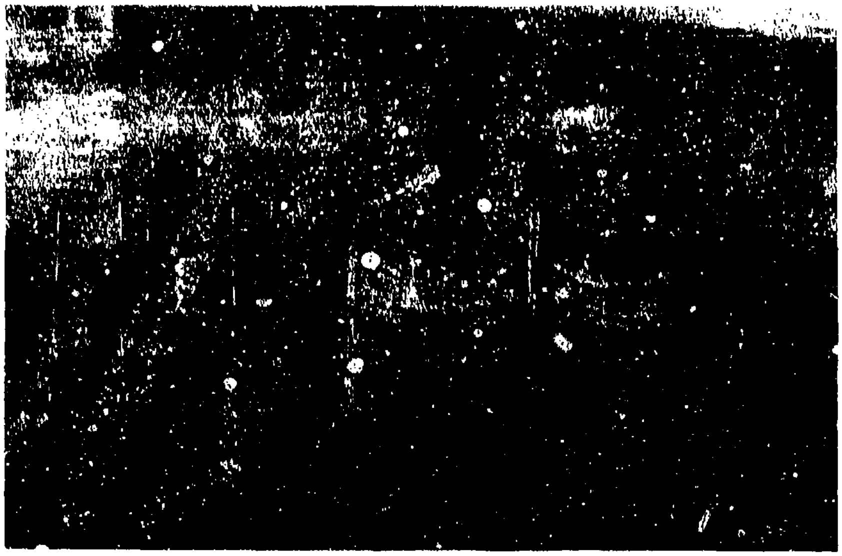

B

Figure 13. Subject Screening and Communications Display Panels

A

B

Figure 14. Communications Display Panel

Instructions Given to Subjects

1. You are here to participate in an experiment in the aural detection of helicopters. This experiment is of great importance to the U. S. Army since it is quite usual to hear an approaching helicopter before it can be seen. The purpose of this experiment is to evaluate existing analytical prediction methods of detection. The results will be used in tactical planning.

2. You will be detecting the aircraft under various ambient conditions, which will be heard over the loudspeaker system located in the direction of the approaching helicopters on the other side of a screen.

3. This screen is here to visually screen you from the helicopter and the other subject group who will be at a condition of alertness different from yourselves. It is most important that you do not communicate with the other group while a test is in progress.

4. Each of you has been given a switch. It has two levels. When you think you hear a helicopter, but are not absolutely sure, you should depress the switch to LEVEL ONE, identified by a weak spring. When you are absolutely sure that you hear a helicopter, depress the switch all the way to LEVEL TWO, identified by a strong spring. This level should be selected only when, in an actual combat situation, you would notify others of a helicopter approach.

   Under some conditions you may think (or be sure) that you hear a helicopter and change your mind. You are quite free to do this and may release your switch to the appropriate level.

   The switch is quite easy to operate; however, because of the spring action, it must be held at the level you select all the time you hear, or think you hear, a helicopter.

5. In order to inform you at all times what the test controller requires you to do, illuminated displays have been provided.

   a. Test Off: (Green) — When the "Test Off" light only is on, you may leave your seats and talk if you wish.

b.	Standby: (Yellow)	When the "Standby" light is on, you should remain seated, but you may talk if you wish.
c.	Quiet (Blue)	Remain seated and maintain complete silence.
d.	Listen: (Red)	Hold your switch in your hand and respond if you hear a helicopter.
e.	Diversions: (Yellow)	In order to simulate a real-life situation, you will sometimes be requested to perform certain tasks, participate in organized activity, or perhaps just read the literature of your choice. You will not be warned of a helicopter approach, but you will be expected to keep the switch in your hand and respond immediately if you hear a helicopter.
f.	Helicopter Approaching: (Red Flashing)	On about half the occasions, you will be warned that a helicopter has begun its approach toward you; refrain from all other activity, hold your switch in your hand, and concentrate on listening for a helicopter.

6. Your Group Supervisor will provide you with an observation sheet on which you should record the run number. He will call out this number before the start of each run.

   If there are any comments that you would like to make about a particular run--for example, you heard a jet aircraft fly overhead during the run, or you were disturbed by an insect, or any situation that may have occurred--please write them next to run number on the observation sheets.

7. Please base your decision according to when <u>you</u> detect the helicopter--there are no right or wrong answers, and it is important that you do not watch the person next to you during a run and allow him to influence your decision.

Subject Group Diversions

The inattentive subject group was given a series of tasks to perform. These were intended as diversions and consisted of the following:

1.	Completing Standard Psychological Questionnaires	"The Adjective Check List" and "The Strong Vocational Interest Blank" were used under this activity category.
2.	Performing Tests	College entrance type "Scholastic Aptitude Tests" were distributed to the subjects. Since some were considering entering college themselves, this proved to be a relevant activity. When they had completed them, they were given answer sheets and allowed to correct their own work.
3.	Reading Literature of Choice	Periodicals and books were provided and subjects were encouraged to bring their own reading material.

In order to avoid boredom, the conditions of attentiveness were interchanged at convenient intervals. To account for intergroup variations and to improve confidence levels in the data, each flight was repeated with only the relative attentiveness of the subject groups interchanged.

Controlled background noise conditions were created on two-thirds of the runs using artificially generated noise from a loudspeaker system. This consisted of four 30-inch woofers and a mid-to-high frequency unit located 30 feet from the subject groups. To ensure uniform directivity for the speakers, they were mounted on 1-inch plywood boards placed flush with the ground. Holes dug in the ground provided natural enclosures.

The artificial ambient masking noise was a constant (stationary) random noise whose spectrum was shaped to simulate typical community and transportation noise (Figure 15). Three different subject site background noise levels were used: quiet ambient, and two levels of masking noise. In Figure 15, a comparison is made of the three ambient noise levels at the subject site and surf noise, trash pickup and street cleaning.[36] It should be noted that the noise levels at the subject site were controlled and, therefore, relatively constant, whereas noise from many community and transportation activities is nonstationary. These latter levels as shown in Figure 15 are averages over times, generally long compared with a typical aural integration time, thus in terms of

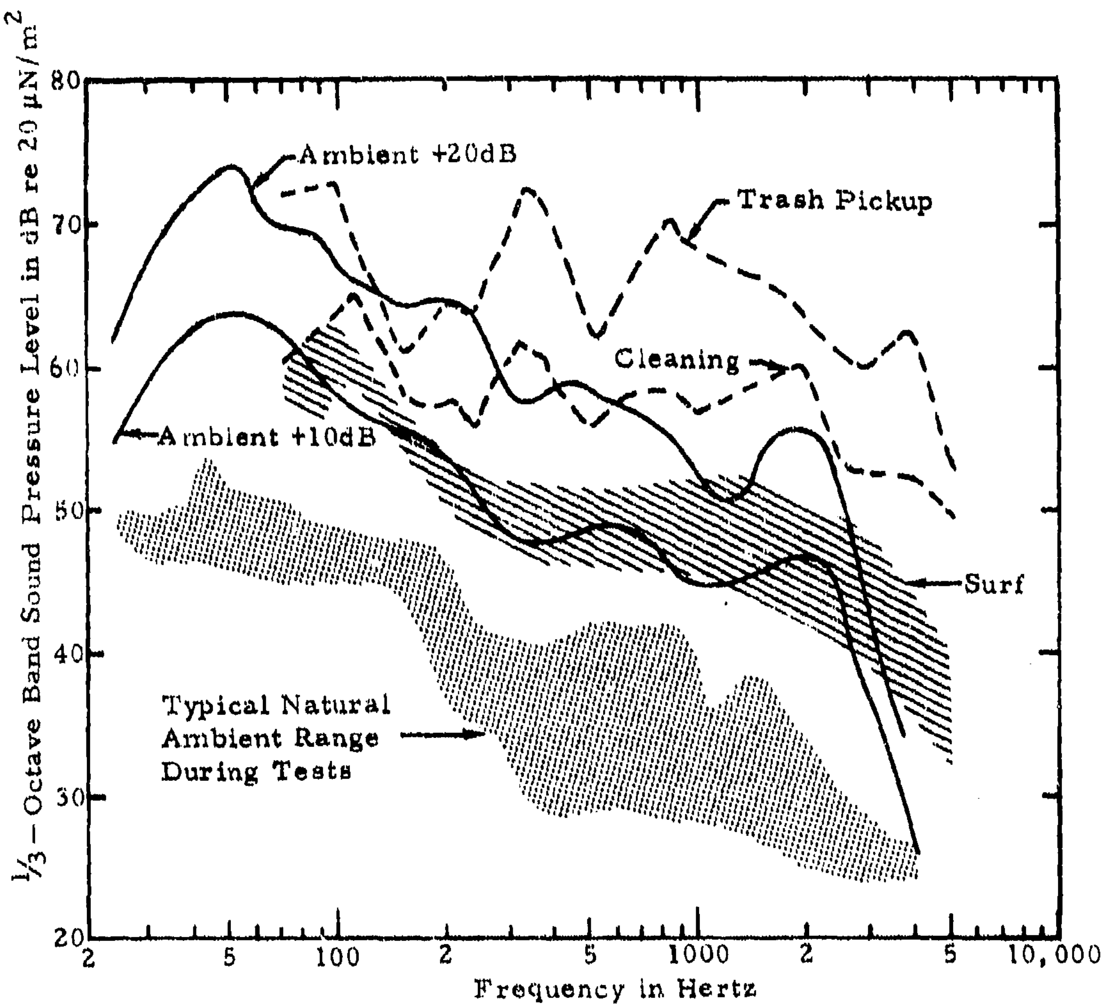

Figure 15. Typical Background Noise Spectra.

aural detectability, it may be inferred that, especially for higher levels of artificially generated masking noise, equivalency with a noisier environment than first apparent may be appropriate. That is, detection might occur in practice during a quiet lull in a noisy background.

Atmospheric Propagation

During each test run, tape recordings were made of the noise at the microphone positions and subject site shown in Figure 11. Since the noise emitted by a helicopter is not stationary with time, even under flight at relatively uniform speed and altitude, it was necessary to locate several acoustic measurement systems in line under the flight path. These systems each incorporated IRIG B time code generators which were synchronized at the start of each day with the computer clock in the radar installation, thus making it possible to relate all noise recordings and radar positioning data back to the instant of emission at the aircraft.

It was not thought possible within the scope of this investigation to make a sufficient number of measurements of atmospheric variables to yield truly detailed information on sound propagation. It was accordingly decided to adopt a "magnitude and scatter" approach to sound propagation decrements as measured between the three stations, using measurements of atmospheric variables made at the subject site only.

Since preliminary trials showed that the aircraft which were to be utilized were detectable under certain conditions at distances in excess of 40,000 feet, it was necessary when following the above approach to monitor sound propagation over distances of the same order of magnitude. In order to accomplish this on approaches from the east, the first microphone station was located on a boat in Queens Sound Channel (Figures 11 and 16A) approximately 20,000 feet from the subject site. The second microphone station was located at the end of a 1000-foot cable from a specially instrumented mobile acoustic van (Figures 11 and 16B) at a distance of 7300 feet from the subject site. For approaches from the west, two mobile acoustic vans near microphone stations were used, located approximately 10,100 feet and 8000 feet, respectively, from the subject site.

Weather Systems and Limits

Temperature, relative humidity, wind speed and direction were measured continuously at an altitude of 15 feet near the subject site.

To provide additional information, weather balloons were deployed at approximately 1-hour intervals. Wind velocity as a function of altitude

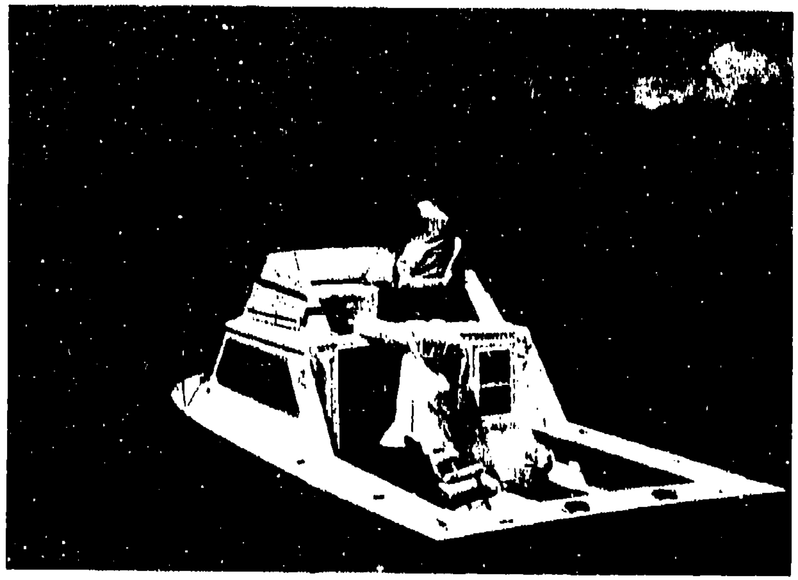

A

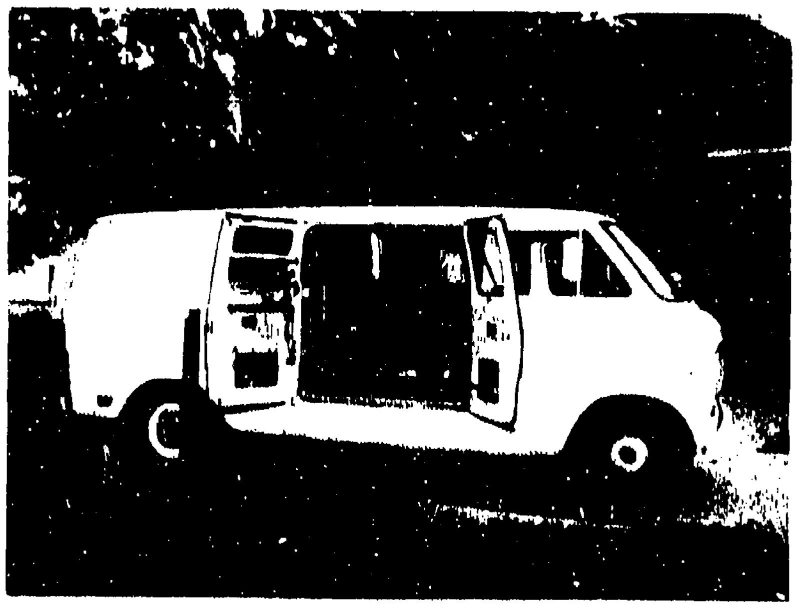

B

Figure 16. Mobile Acoustical Stations

was obtainable from each balloon, and alternate balloons gave temperature and humidity as a function of altitude.

Weather conditions outside the following limits caused tests to cease:

1. Wind Velocity > 12 knots
2. Relative Humidity > 90%
3. Relative Humidity < 30%

The first limit was imposed due to the difficulty in obtaining acoustic measurements in high wind due to microphone-generated wind noise. High and low humidities generally represent unstable weather conditions, influencing sound propagation in an unpredictable manner. To avoid such conditions, the latter two limits were imposed.

Acoustic Measurements at Subject Site

The three microphone locations at the subject site are shown in Figure 12. One was located on the same 30-foot radius as the subjects from the artificial noise generating system and pointed horizontally toward the noise generating system and approaching aircraft. The other two systems were located a distance of some 300 feet from the noise generating system and pointed toward the approaching aircraft. All microphones were encased in large wind screens (right-hand portion of Figure 14A).

Three microphone systems were used for the following reasons:

1. For measurements in a natural ambient with no artificial noise, it was preferable to use the cross spectrum of microphone (1) with either (2) or (3) from which to derive helicopter noise, because locally generated acoustic signals such as some wind noise and insect noise are incoherent over a large distance, whereas acoustic signals originating from far away should have a coherence function of near unity. Thus, for such measurements, significantly better signal/unwanted-noise ratio should result.

2. For measurements in an artificial ambient, the remote microphone signals (2 and 3) should contain a component of artificial ambient noise approximately 10-20 dB less than the subject microphone (1), thus making it easier to separate helicopter noise from the ambient acoustic field.

Summary of Test Conditions

Seventy-two flights were planned, under the following conditions:

- Two Conditions of Subject Alertness
  - Alert
  - Distracted
    - Completing Standard Psychological Questionnaires
    - Performing Tests
    - Reading Literature of Choice

- x Three Site Noise Conditions
  - Ambient
  - Ambient + 10 dB
  - Ambient + 20 dB

- x Three Helicopters
  - AH-1G# (Cobra)
  - UH-1B# (Iroquois)
  - OH-6A# (Cayuse)

- x Four Flight Conditions

		Altitude (feet)	Velocity (knots)
Open Path	AH-1G	NOE	90
		200	150
		1500	90
	UH-1B & OH-6A	200	90
		1500	90
		1500	110
Partially Wooded Path	AH-1G	200	150
	UH-1B & OH-6A	1500	90

Due to ideal weather and cooperation of all personnel concerned, 96 flights were completed, allowing additional correlations and increased confidence in the acquired data. A complete list of flights is contained in Volume II (Classified).

FIELD SYSTEM FOR ACOUSTIC DATA ACQUISITION

General Description

The field system for acoustic data acquisition consisted of highly sensitive microphone systems, time code generators, subject response switches and encoders, variable high-pass filters, signal conditioning electronics, magnetic tape recorders, and direct-write oscillographs.

Block diagrams of the system are presented in Figures 17 and 18. Major components of the system are listed in Table 1.

The acoustic measurement requirements in this program involved restrictions not normally faced. Specifically, it was necessary to provide a high-quality system capable of measuring very low noise levels.

Major System Components

Microphones

The microphones used were Bruel & Kjaer Type 4145, 1-inch diameter, free-field condenser microphones with a nominal sensitivity of 26 dB re 1 volt per N/m^2. Their frequency response in this system is $\pm$ 2 dB from 10 Hz to 18 kHz at normal incidence to the diaphragm. For this reason, the microphone axis was pointed parallel to the ground at all measurement stations.

Sound Level Meter

For initial amplification of the microphone signal, a Bruel & Kjaer Type 2203 sound level meter was used. This instrument was designed for outdoor and laboratory acoustic measurements. It fulfills all requirements of IEC 179, the International Standard for Precision Sound Level Meters, and was well suited to the requirement for a very reliable instrument with very low noise floor for acoustic measurements in the field.

The instrument is self-contained and completely portable. The microphone attaches directly to the unit. With the type 4145 microphone, the measuring range for linear measurements is 38 to 134 dB. For 1/3-octave measurements, the dynamic range is more than 22 to 134 dB overall, or 10 to 134 dB above 500 Hz.

The sound level meter provided a maximum output voltage (at full-scale deflection) of three volts rms. This was the maximum input signal to the signal conditioning amplifiers.

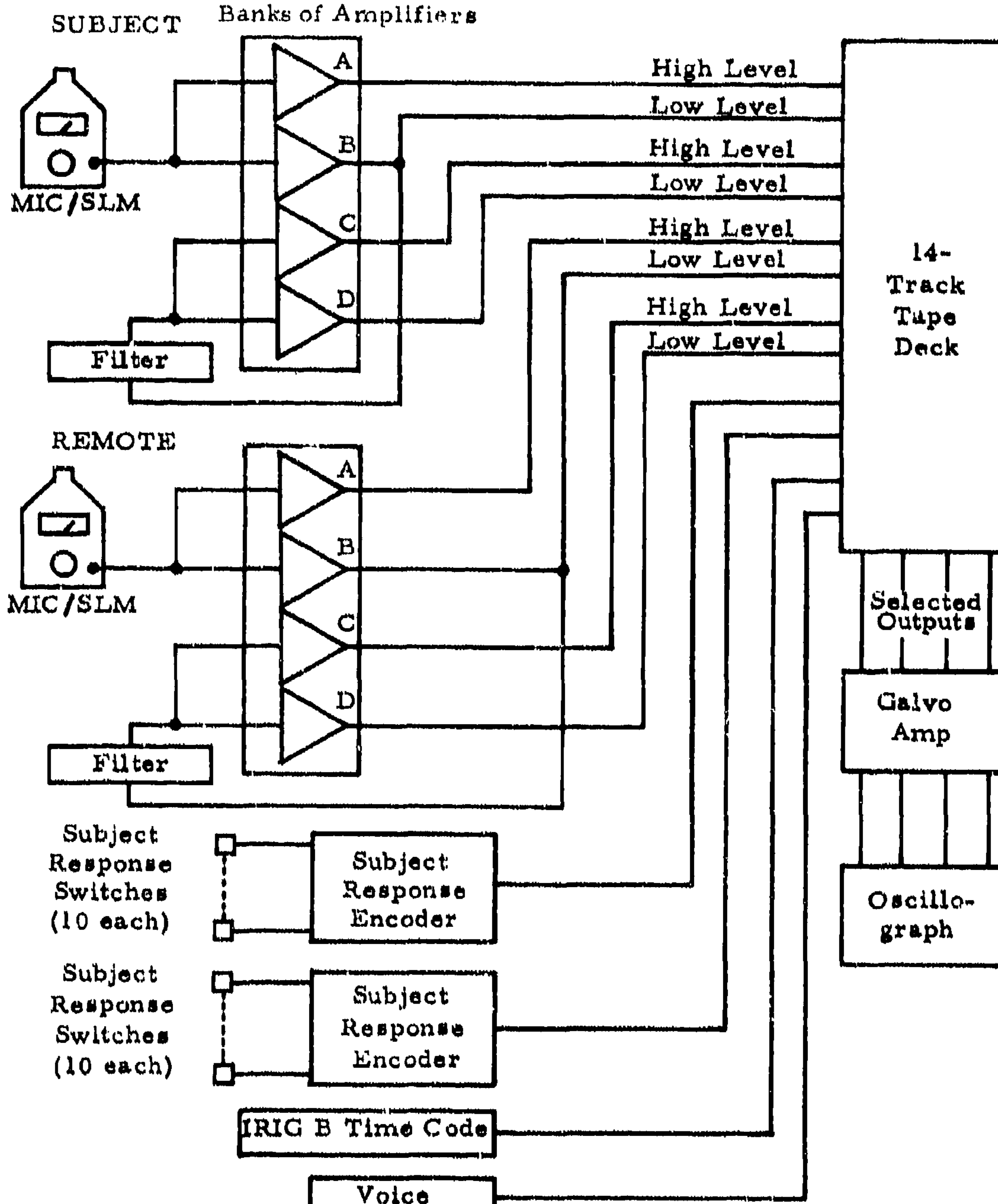

Figure 17. Block Diagram of Instrumentation at Subject Site.

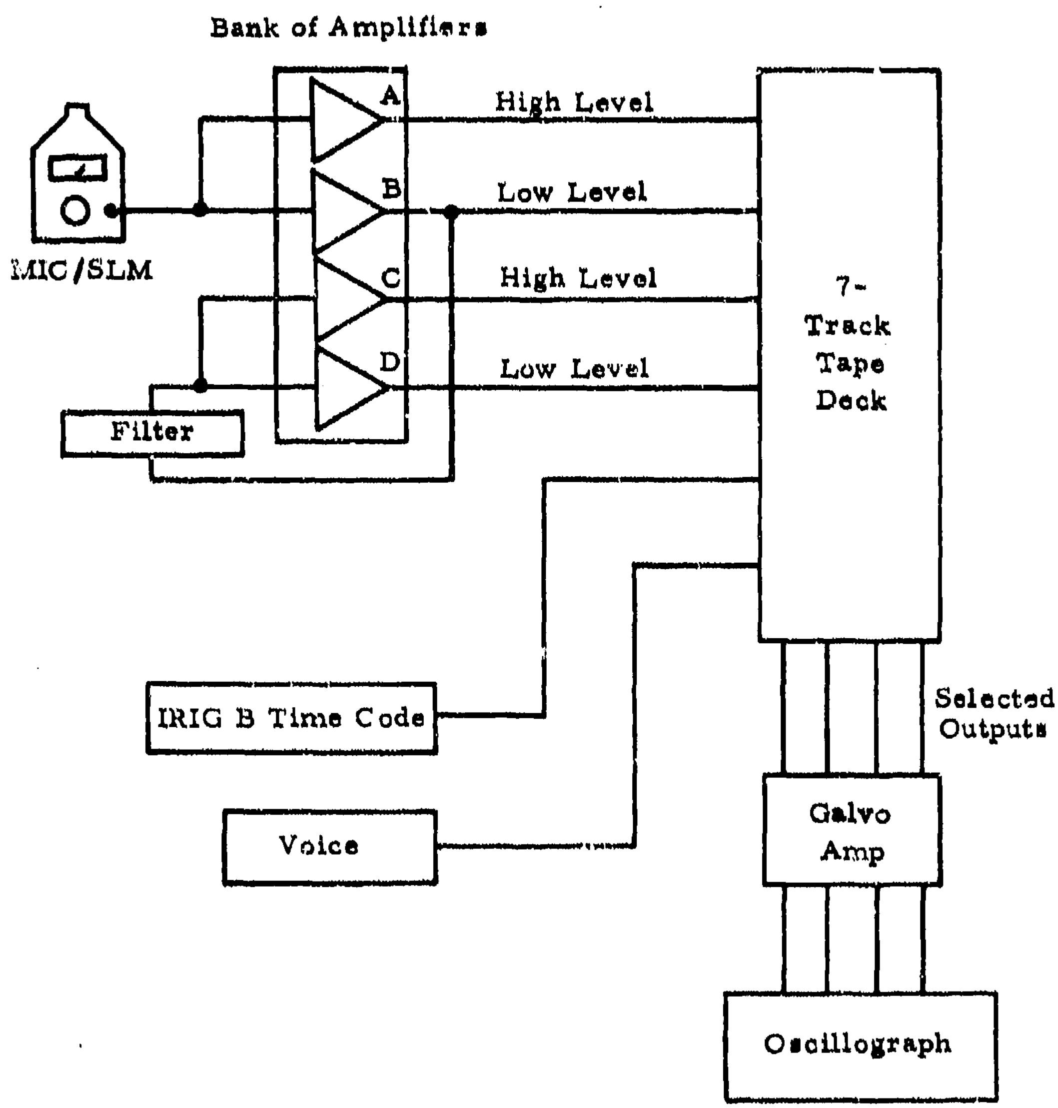

Figure 18. Block Diagram of Instrumentation at Mobile Laboratories.

TABLE 1 - FIELD MEASUREMENT SYSTEM EQUIPMENT LIST

Equipment	Quantity	Model	Manufacturer
Microphone	4	4145	Bruel & Kjaer
Sound Level Meter	4	2203	Bruel & Kjaer
Amplifier	16	ZE-0003	Bruel & Kjaer
Filter	3	3342	Krohn-Hite
Subject Response Encoder (10 channels each)	2	-	Wyle
Tape Recorder - 1 inch	1	VR-3300	CEC
Tape Recorder - ½ inch	2	VR-3300	CEC
Galvanometer Amplifier	3	1-172	CEC
Oscillograph	3	5-124	CEC
Voltmeter	1	2606	Bruel & Kjaer
Speaker	2	W-30	Electrovoice
Speaker Assembly	1	-	Allied
Amplifier	1	D-40	Crown
Amplifier	1	DL-300	Crown
Spectrum Shaper	1	123	Bruel & Kjaer
Random Noise Generator	1	650R	Allison

Signal Conditioning Amplifiers

The signal conditioning amplifier, a Bruel & Kjaer Type ZE-003, consists of a low-noise, 40-dB, four-stage transistor amplifier preceded by a 60-dB step attenuator (10 dB per step). As illustrated in Figure 17, four channels of these amplifiers were used per microphone to supply four inputs to the tape recorder consisting of two filtered and unfiltered signals, each at two sensitivities differing by 10 dB.

Variable Filter

A Krohn-Hite Model 3342 variable filter was used in the high-pass mode in order to reduce undesirable low-frequency wind or electrical noise below 50 Hz to improve the dynamic range of the recording. The instrument is battery or AC powered and provides 24 dB per octave roll-off characteristics. Two channels per unit offer a selectable gain of 0 dB or 20 dB.

Subject Response Switches and Encoders

The subject response switches consisted of hand-held, three-position momentary push-button switch assemblies. The three positions allowed the subjects to acknowledge "no detection", "think", and "sure" per the instructions given to them. Each switch energized an oscillator circuit, and each of the detents caused a different output level to be delivered by the oscillator assembly. Each encoder had ten switch inputs corresponding to ten oscillators, each generating a different, 1/3-octave center frequency sine wave. The range of these frequencies was 32 to 250 Hz.

The encoder combined the signals from all ten oscillator circuits and provided a single composite signal to the tape recorder. Upon frequency and amplitude analysis of the composite signal, the condition of each switch could be determined.

Tape Recorder

The tape recorders, CEC Model VR 3300, were standard instrumentation recorders equipped with FM record and playback electronics. Tape speed was 15 ips at the subject location and 30 ips at the two stations along the approach path. Frequency response was flat to 5 kHz at 15 ips and to 10 kHz at 30 ips.

RADAR TRACKING SYSTEM

The location of the radar station is shown in Figure 11. The device was an AN/MPS-19 S-Band unit employing a 0.8-microsecond square transmission pulse and low noise parametric receiver with image rejection filters, and an 8-foot parabolic antenna. Beacon tracking, rather than skin tracking, was used because of the low-altitude parts of the flight program. An adequate separation between aircraft was maintained to allow singular runs with no noise interference. Range precision of the system was $\pm$ 30 feet rms, and angle precision is $\pm$ 1 mil (0.0563°) rms.

Helicopter position was sampled ten times a second and acquired by the on-line computer and transcribed on magnetic tape. Subsequently, as an off-line process, this data was smoothed by digital filtration using a 4-second time constant and differentiated to yield velocity coordinates. (Note that smoothing does not impart any position error at constant velocity, but merely serves to damp the random equipment errors). Printed output at 1-second intervals of helicopter position in Polar and Cartesian coordinates, as well as the respective velocities was provided in addition to digital tapes containing the same information.

DATA ANALYSIS AND CORRELATION STUDIES

SUBJECT RESPONSE DECODING

Each subject switch controlled a unique frequency with different voltage levels corresponding to either "no response", "think you hear it", or "sure you hear it" response levels. The subject responses were decoded by replaying the combined signals through a tunable filter and noting times with corresponding levels of response for each subject.

The responses were evaluated for each subject group individually, and for both groups combined, according to each of the following methodologies:

1. One point was allowed for a "sure" response and one-half point was allowed for a "think" response, giving a maximum total for the ten subjects on each group of ten points, and for both groups combined of twenty points. This was done on the rationale that if two people thought they heard an approaching helicopter, it might be roughly equivalent to one person being sure that he identified an approaching helicopter.

2. All "think" responses were ignored and "sure" responses were summed in the same manner outlined above.

Typical examples of combined subject response patterns evaluated in this manner are plotted in Figures 19 through 22, as combined percentage of response against time. Also shown is the helicopter slant range distance, as obtained from the radar tracking data. Comments regarding extraneous stimuli (i.e., dog barking) and number of subjects noting this (e.g., 2 out of 20) are indicated in these figures.

Comparison of Figures 19 and 20 with Figures 22 and 23 shows that the percentage of subject detection may increase slowly or rapidly. Thus, the spread in distance over which the helicopter is partially detectable may be large or small. This spread does not seem to be sensibly expressible as a function of helicopter slant range but does seem to be dependent on atmospheric parameters and flight profile. For example, if the sound is undergoing substantial modulation due to nonuniform refraction and scattering, then the increase in intensity at the position of the listening subjects will not be uniform. Thus, the detection threshold of those subjects who are especially alert or who possess acute hearing may be exceeded during a large peak in the modulation early in the approach and then drop below this level and remain there until a later, larger peak in the modulation when the thresholds of a larger

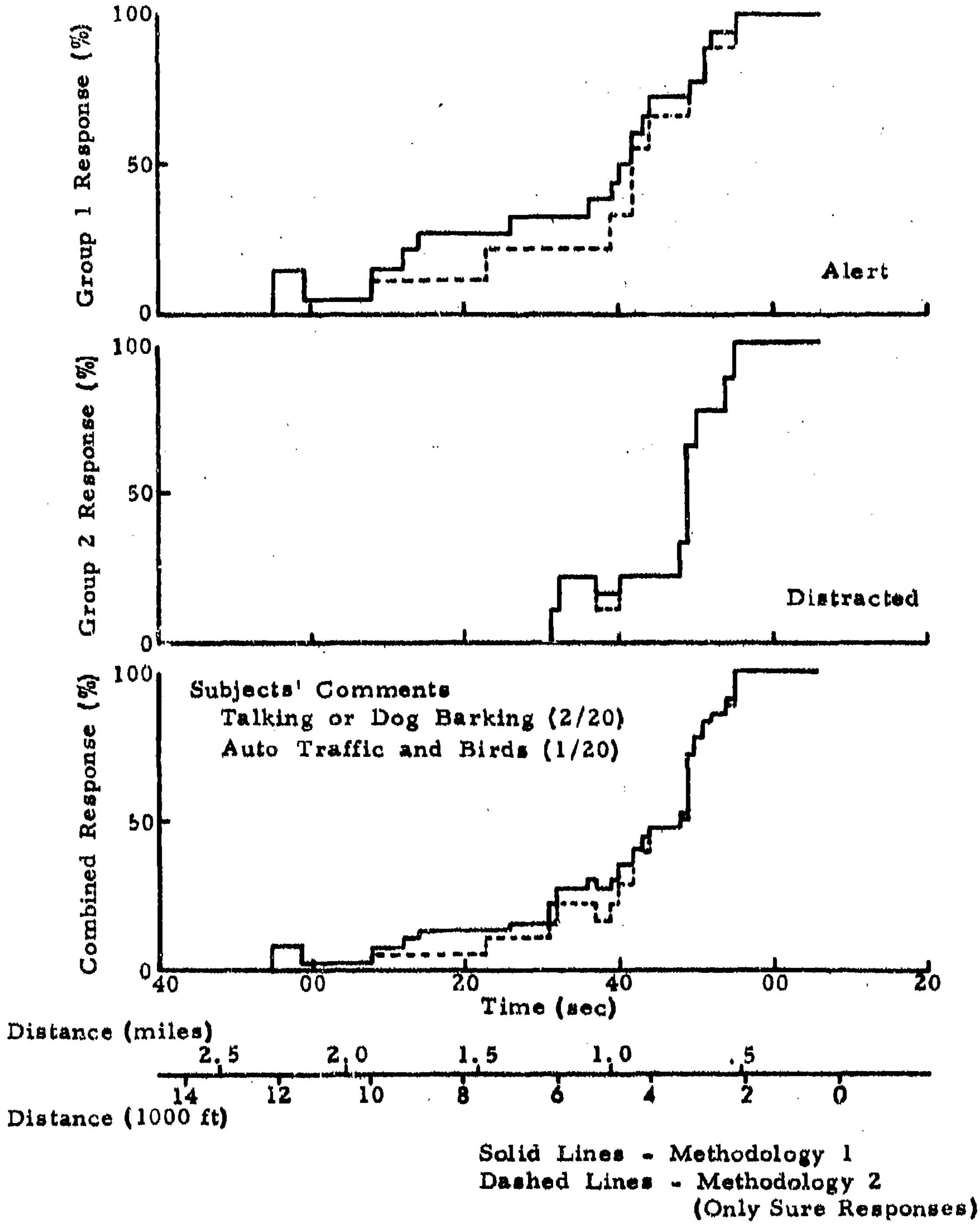

Figure 19. Subject Detection Data for Run 20.

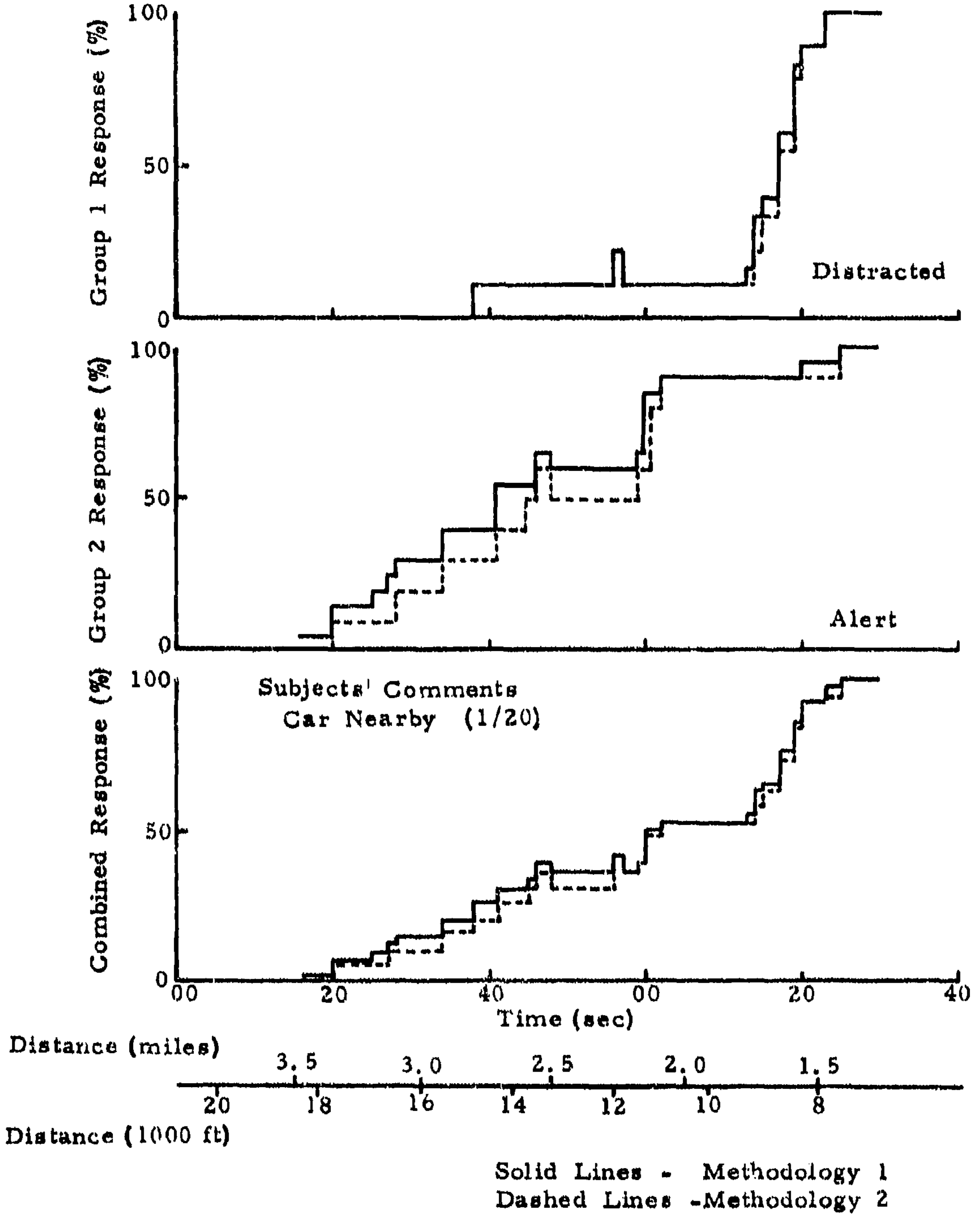

Figure 20. Subject Detection Data for Run 30.

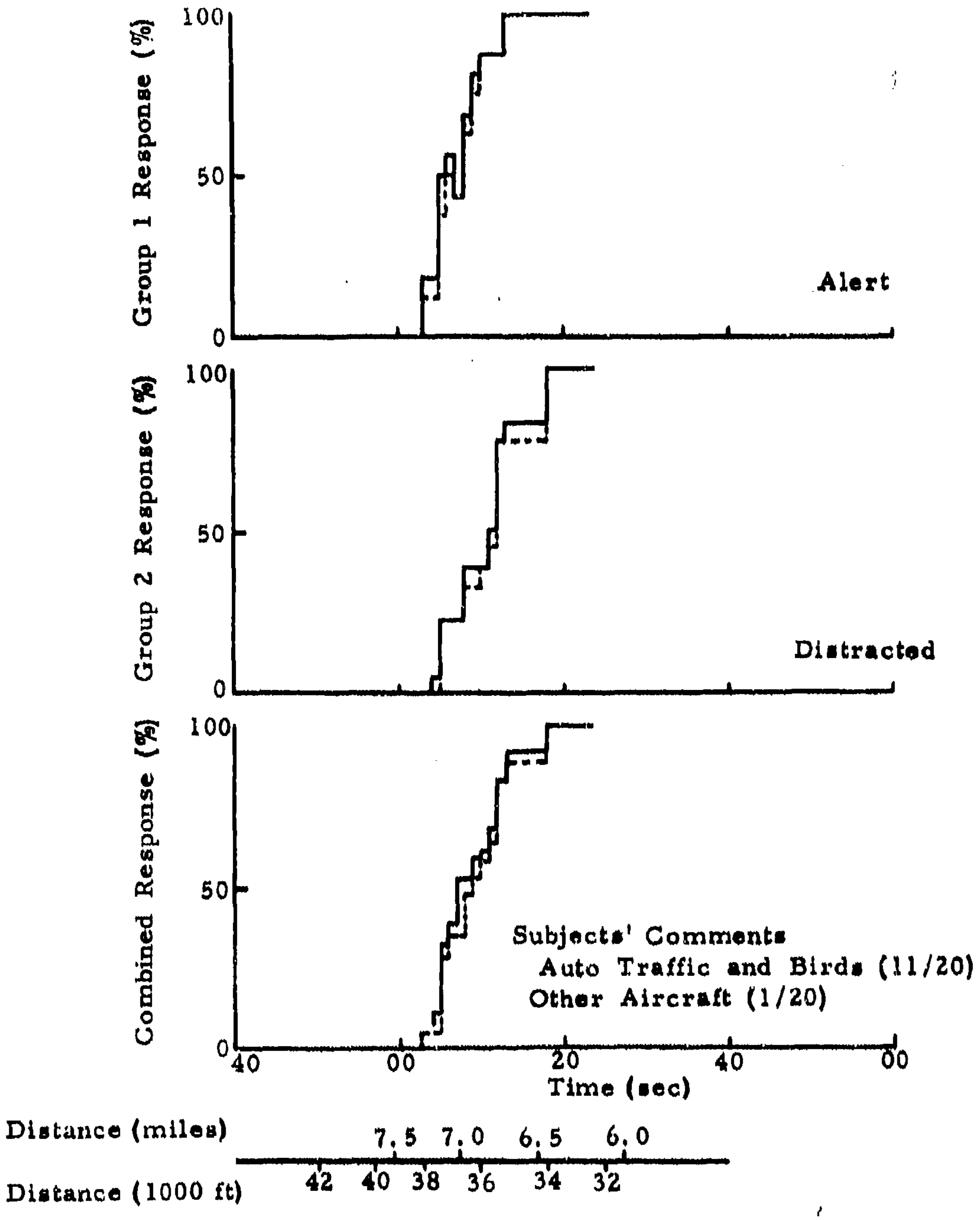

Solid Lines - Methodology 1
Dashed Lines - Methodology 2
(Only Sure Responses)

Figure 21. Subject Detection Data for Run 65A.

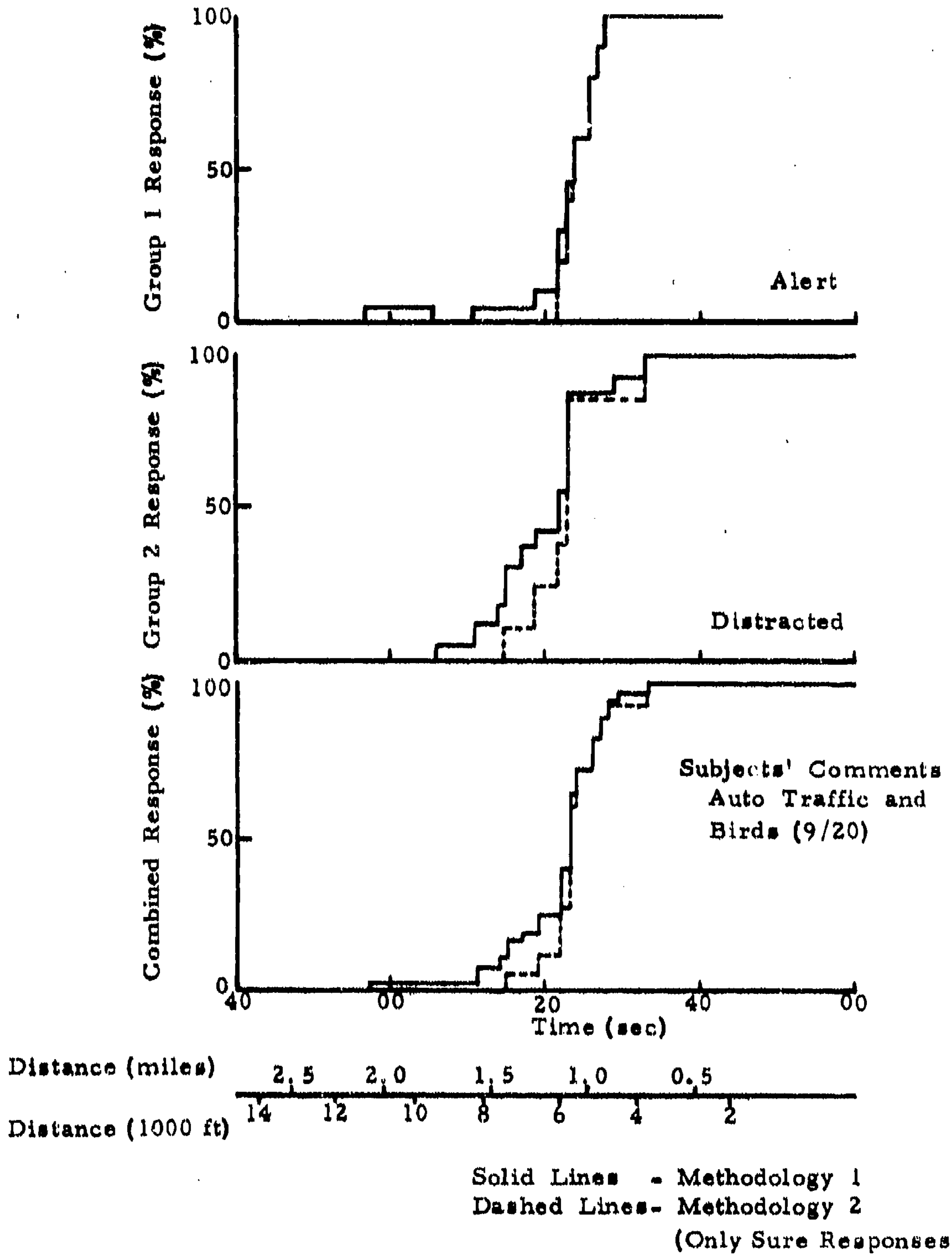

Figure 22. Subject Detection Data for Run 70.

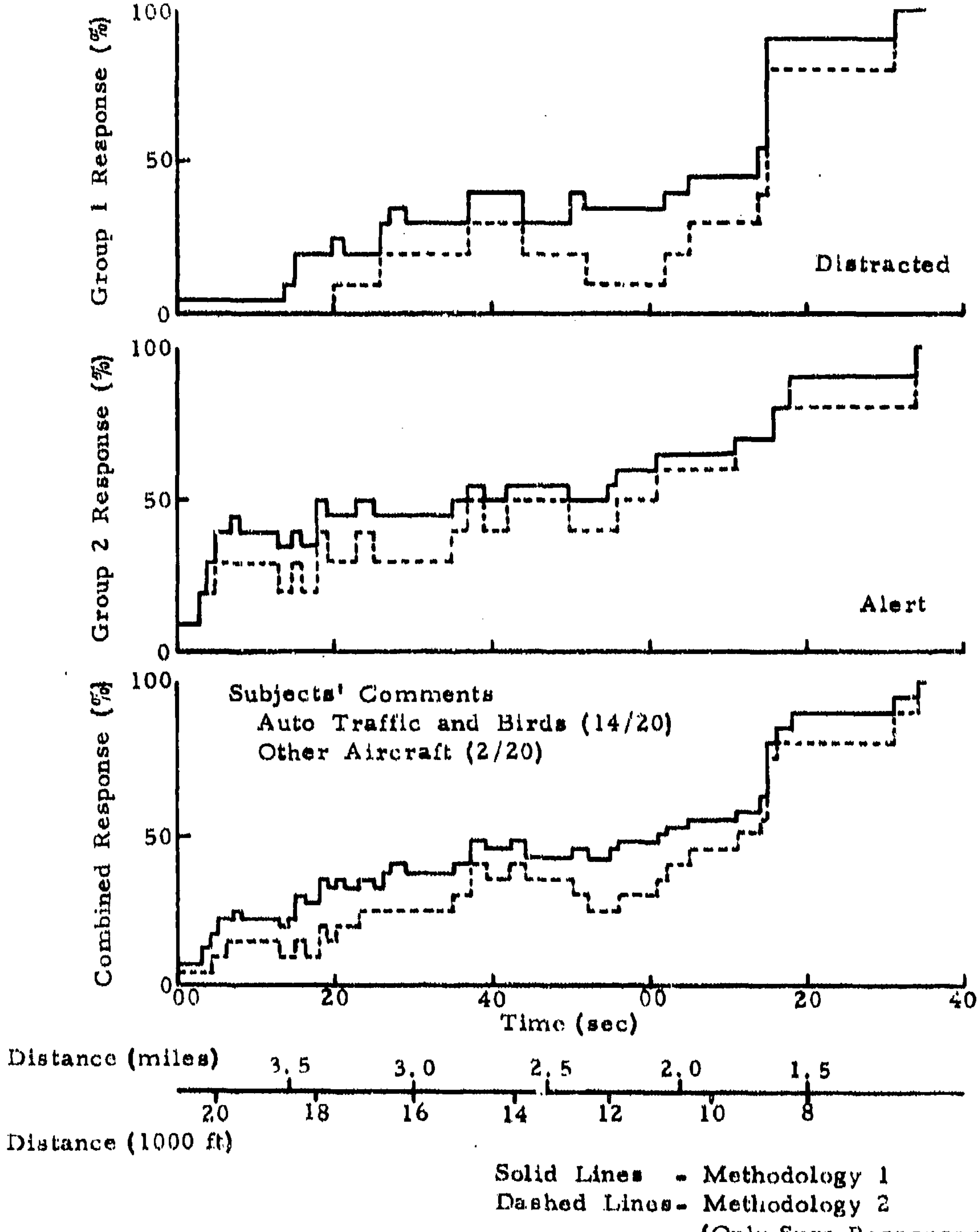

Figure 23. Subject Detection Data for Run 13.

proportion of subjects will be exceeded. This process might occur only once or several times until the thresholds of all subjects are exceeded, explaining different rates of increase in detection level.

Figures 19 through 22 show that detection responses computed from the two methodologies outlined above do not differ substantially. In Figure 23, however, during a run when another aircraft was present in the vicinity, the responses are markedly different, indicating a large proportion of "think" responses. It is also evident here that subjects changed their minds several times concerning the certainty of detection.

Detection distances for the three aircraft in the various flight profiles during different ambient noise conditions at the subject site are summarized in Volume II (Classified).

PROPAGATION ANALYSIS

Data Reduction Procedures

Acoustic data was recorded at three stations under the flight path (Figure 11) to allow interstation decrements in sound pressure level relative to the same emission time to be computed. The reason for using more than one acoustic data acquisition station is that helicopter noise is not stationary due to the unstable nature of a helicopter in flight.

Since the source itself was moving, and flight time was substantial relative to sound propagation time, a retarded time technique was necessary. Thus, with reference to Figure 24, suppose r_1, r_2, r_3, the distances of the helicopter from stations 1, 2, 3, respectively, are all known at time "t_2" when an acoustic measurement is made at station 2. These distances need to be corrected to the true distances at the time that the sound was emitted from the aircraft, namely, r'_1, r'_2, r'_3. It may be shown that

$$r'_2 = \frac{\frac{v}{c}\left(r_2^2 - h^2\right)^{\frac{1}{2}} + \left(r_2^2 - \frac{v^2}{c^2} h^2\right)^{\frac{1}{2}}}{1 - \frac{v^2}{c^2}} \qquad (1)$$

$$r'_1 = \left[\left\{ \left(r'^2_2 - h^2 \right)^{\frac{1}{2}} - s_1 \right\}^2 + h^2 \right]^{\frac{1}{2}} \tag{2}$$

$$r'_3 = \left\{ \left(s_2 + \sqrt{r'^2_2 - h^2} \right)^2 + h^2 \right\}^{\frac{1}{2}} \tag{3}$$

where c = velocity of sound
v = aircraft velocity
h = aircraft altitude
s_1 = distance between stations 1 and 2 (see Figure 11)
s_2 = distance between stations 2 and 3 (see Figure 11)

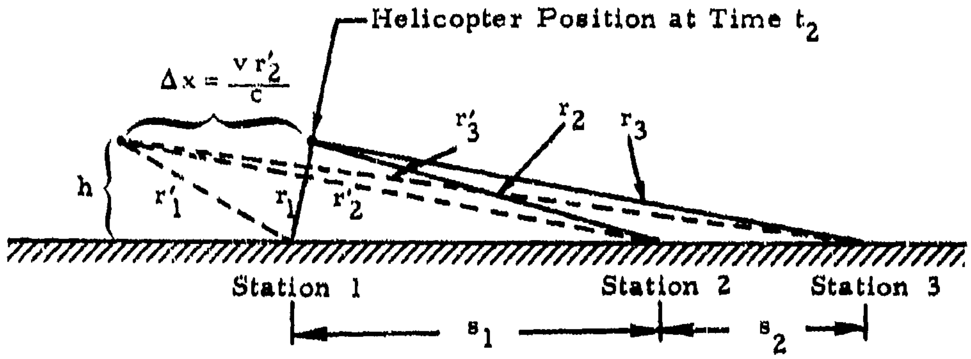

Figure 24. Time-Retarded Slant Range.

Evidently, then, the sound measured at time "t_2" at station 2 must be compared with sound measured at times "t_1" and "t_3" at stations 1 and 3 respectively, where

$$t_1 = t_2 - \frac{(r'_2 - r'_1)}{c} \tag{4}$$

$$t_3 = t_2 + \frac{(r'_3 - r'_2)}{c} \tag{5}$$

The measurement is further complicated by the necessity of making one of the following two assumptions:

1. That the natural ambient noise at each station remains constant with the approach of the helicopter. (Thus, in order to obtain a true helicopter noise signature at any time, one may simply subtract a prerecorded natural ambient signature from the combined signature recorded during the approach.)

2. That the natural ambient noise is insignificant in magnitude compared with the helicopter noise.

The former assumption has the advantage of allowing measurements down to lower helicopter noise levels and thus over farther helicopter slant ranges. It has the disadvantage that it is impossible to check the assumption. The latter assumption is more easily justified by setting a margin sufficiently large that any fluctuations in natural ambient noise are insignificant. This was the method used.

A General Radio Model 1921, real-time 1/3-octave spectral analyzer with integration time set at four seconds was used for reduction of the propagation data. The procedure used was as follows:

1. Acoustic data from station 2 was replayed through a high fidelity reproduction system so that the operator could aurally monitor the reproduction.

2. A 1/3-octave spectrum was taken at the start of each run using calibration signals recorded before and after the start of each period of testing during the field experiment to calibrate the system.

3. The tape was played on through the run until the operator could aurally detect the approaching helicopter. The time was noted and data acquisition started simultaneously on the analyzer.

4. At the end of data acquisition, the tape was stopped and a plot was made and labeled with station number, run number and time (t_2). This time was subsequently correlated with helicopter position from radar tracking data.

5. The tape deck was started again and a further spectrum acquired at a start time ten seconds after the last. This procedure was repeated until the end of the run, yielding a series of spectra at convenient intervals of ten seconds throughout the run.

The entire process above was repeated for each run.

6. Using computer printouts of radar data, distances r_1, r_2, r_3 were computed for each plot at the actual times (t_2) noted on the plots.

7. Retarded time t_1 and incremented time t_3 as well as time-retarded distances r'_1, r'_2, r'_3 were computed using the relations given earlier and the values of t_2, r_1, r_2, r_3 derived above in steps 4 and 6.

8. Tapes from station 1 were played back and 1/3-octave spectra made in a different color ink at times t_1 over the corresponding plot from station 2, as well as the start of each run.

9. Similarly, a third set of plots from station 3 at times t_3 was superimposed upon the earlier two from tapes recorded at station 3.

An example of one of the resulting series of plots is shown in Figure 25. These plots were prepared in such a manner that they could be used directly for the computation of atmospheric sound attenuation between stations.

<u>Computation of Interstation Attenuation</u>

The 1/3-octave spectral plots made in the manner described above were scrutinized and frequency areas annotated where spectral levels were a minimum of 5 dB above the ambient level recorded at the beginning of each run (yielding a maximum error of +1.2 dB with a constant ambient).

Differences between corresponding 1/3-octave spectra measured at alternate stations were computed by direct subtraction of spectral levels in dB. The effect of spherical spreading was removed by subtracting

$$\Delta_{1-2} = 20 \log \frac{r'_2}{r'_1} \tag{6}$$

$$\Delta_{2-3} = 20 \log \frac{r'_3}{r'_2} \tag{7}$$

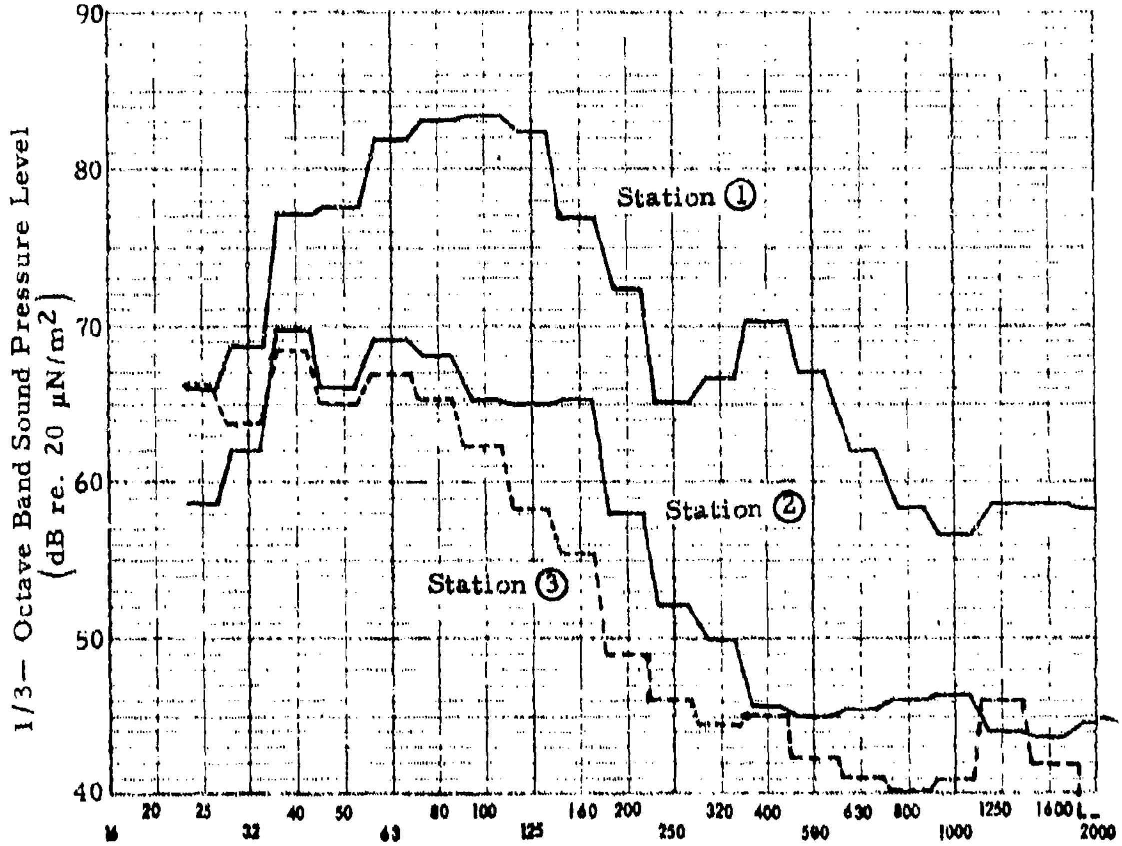

① - ②	7	6	7	11	13	15	18	17	12	14	13	17	24	22	17	12	11	15	15	13
E_1(dB/1000 ft.)	[illegible]	[illegible]	[illegible]	.6	.8	1.0	1.2	1.1	.6	.7	.6	.9	1.5	1.2	[illegible]	[illegible]	[illegible]	[illegible]	[illegible]	[illegible]
② - ③	-7	-2	1	1	2	3	3	7	10	9	6	5	0	3	4	6	5	-2	2	6
E_2(dB/1000 ft.)	[illegible]	[illegible]	[illegible]	[illegible]	[illegible]	[illegible]	[illegible]	.4	.8	.6	.2	[illegible]	[illegible]	[illegible]	[illegible]	[illegible]	[illegible]	[illegible]	[illegible]	[illegible]

$r_1' = 15430$ ft. $r_2' = 25529$ ft. $r_3' = 33529$ ft.

Spherical Spreading Losses $\Delta_{1-2} = 4.4$ dB, $\Delta_{2-3} = 2.4$ dB

Atmospheric Attenuation Losses (Reference 37):																				
(dB/1000 ft.)	.03	.03	.04	.05	.07	.08	.10	.13	.17	.21	.26	.33	.41	.52	.67	.83	1.1	1.3	1.7	2.1

E_1, E_2 = Excess Atmospheric Attenuation
(Shaded Areas Indicate Unreliable Data)

Figure 25. One-Third-Octave Spectra With Compured Values of Excess Attenuation.

from differences between stations (1 and 2) and (2 and 3) respectively. Standard values of atmospheric absorption (Reference 37) for each frequency band at measured temperature and humidity conditions (in dB per 1000 ft) were evaluated for each run, multiplied by $(r'_2 - r'_1)$ and $(r'_3 - r'_2)$, and subtracted from the remaining differences.

The resultant experimental values of excess attenuation were expressed in terms of an attenuation coefficient in dB per 1000 feet. They represented atmospheric attenuation in excess of atmospheric absorption and spherical spreading, and are presumed to be due to scattering, refraction, diffraction and ground absorption. An example of one of these spectral plots obtained from run number 75 along with an example of values of excess attenuation is contained in Figure 25.

Correlation of "Excess" Attenuation With Atmospheric Parameters

Due to the inhomogeneous nature of the lower atmosphere, the nonlinear variation of velocity and temperature with height, and the prevailing physical geometry comprising a source above a partially reflecting plane, it is not expected that a simple power law will account for the falloff of "excess" sound attenuation with distance.

Instead, as shown below, it was determined that a practical, empirical collapse of the attenuation data could be made as follows:

- For elevation angles less than 2°, a linear regression law of excess attenuation versus wind vector.
- For elevation angles between 2° and 10°, an empirical linear decrease in excess loss from the value given by the linear regression law above, to zero at 10°.

Elevation Angles Less Than 2°

In the far field, at one mile or greater from a source, and at an altitude of less than 200 feet, the angle of incidence is about 2° or less. Under these circumstances, it was found that a simple power law with distance from the source reasonably represented "excess" sound attenuation.

The most meaningful weather parameter with which to correlate "excess" attenuation was wind vector, i.e., upwind or downwind propagation. Clearly, "excess" attenuation bears a complex relationship to many other factors. However, in a combat situation, these factors are unlikely to be measurable, so evaluating the

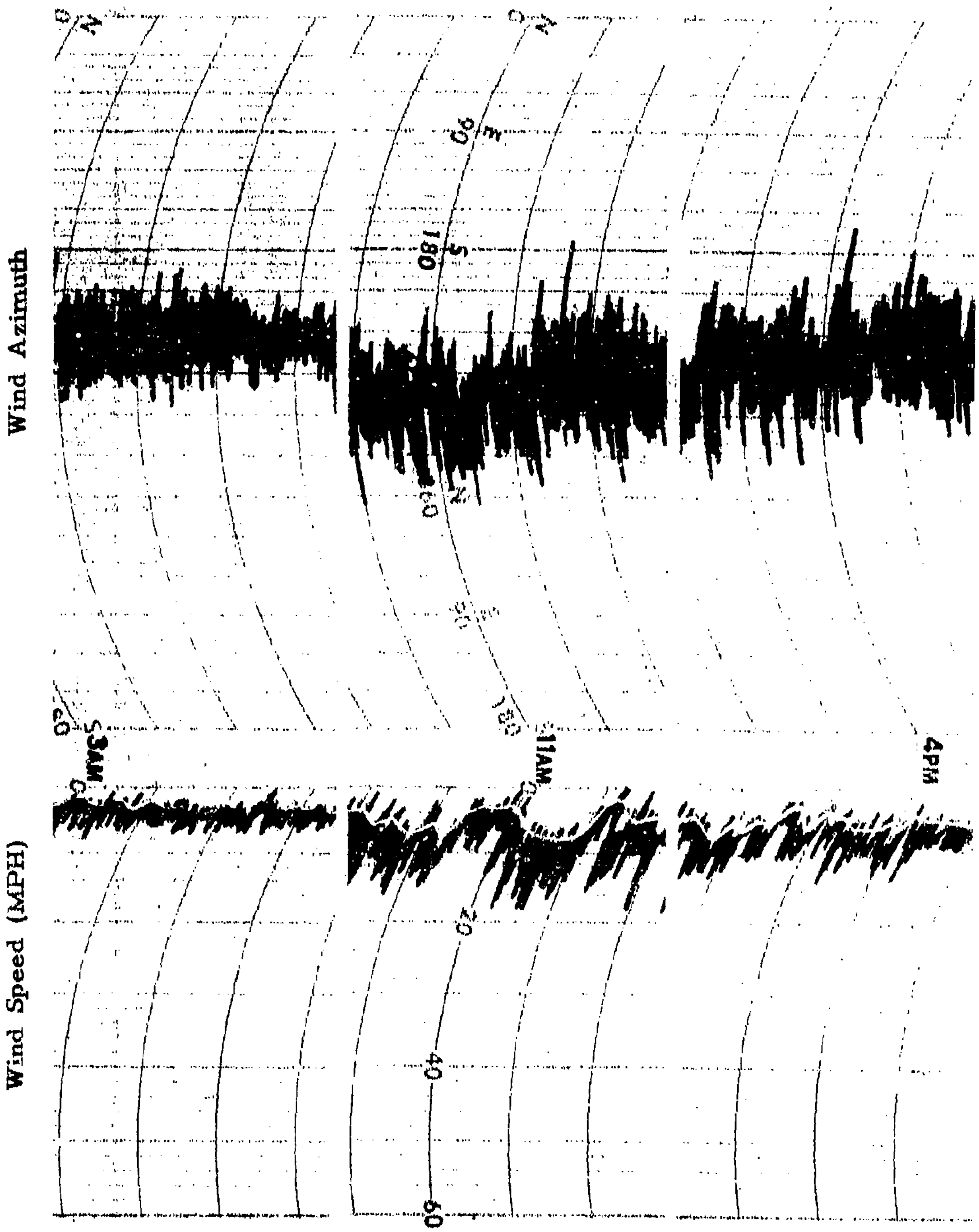

Figure 26. Typical Trace of Wind Vector Showing Extraction of Velocity at Lull.

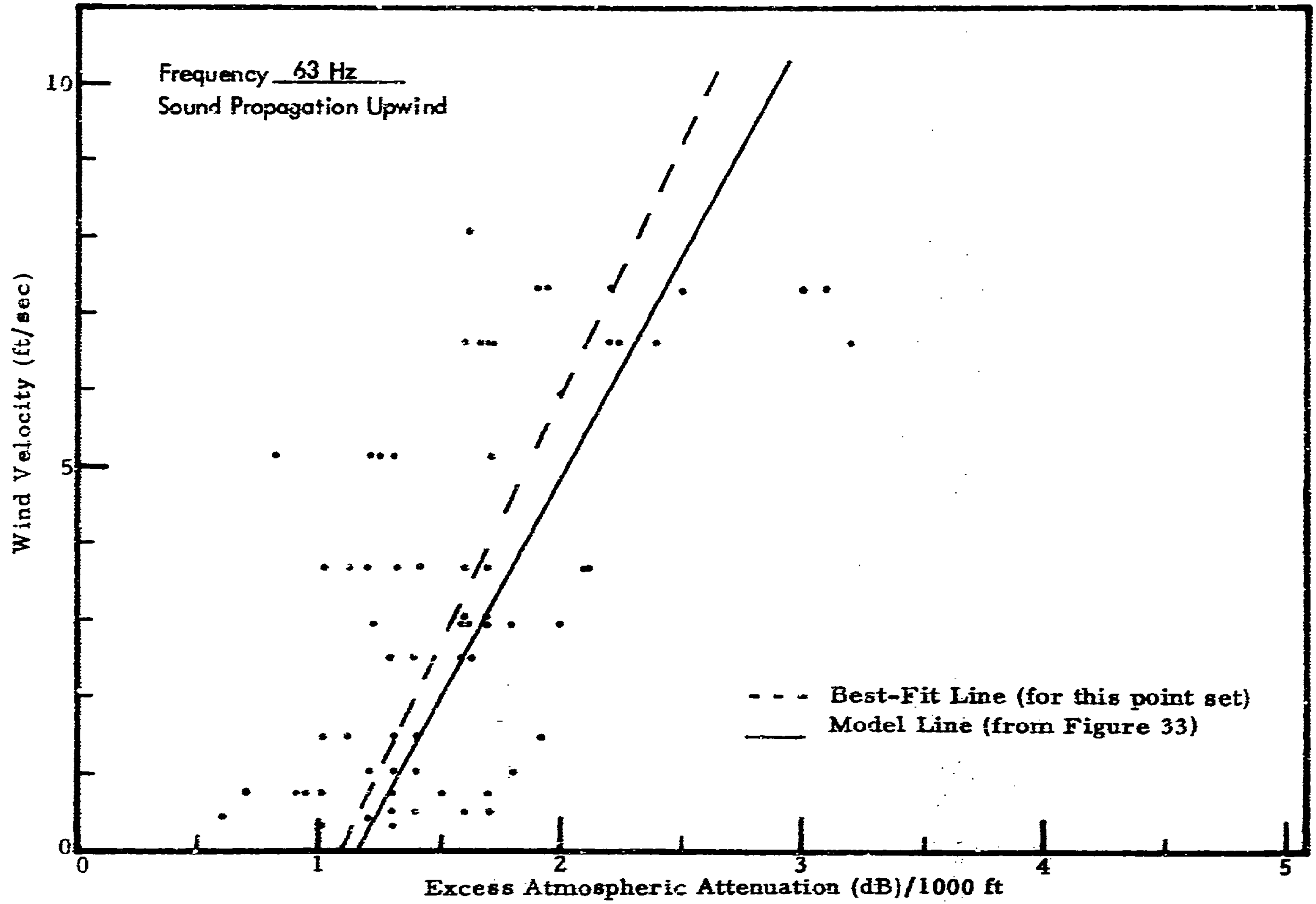

Figure 27. Effect of Wind Velocity on Excess Atmospheric Attenuation From Measured 1/3-Octave Data.

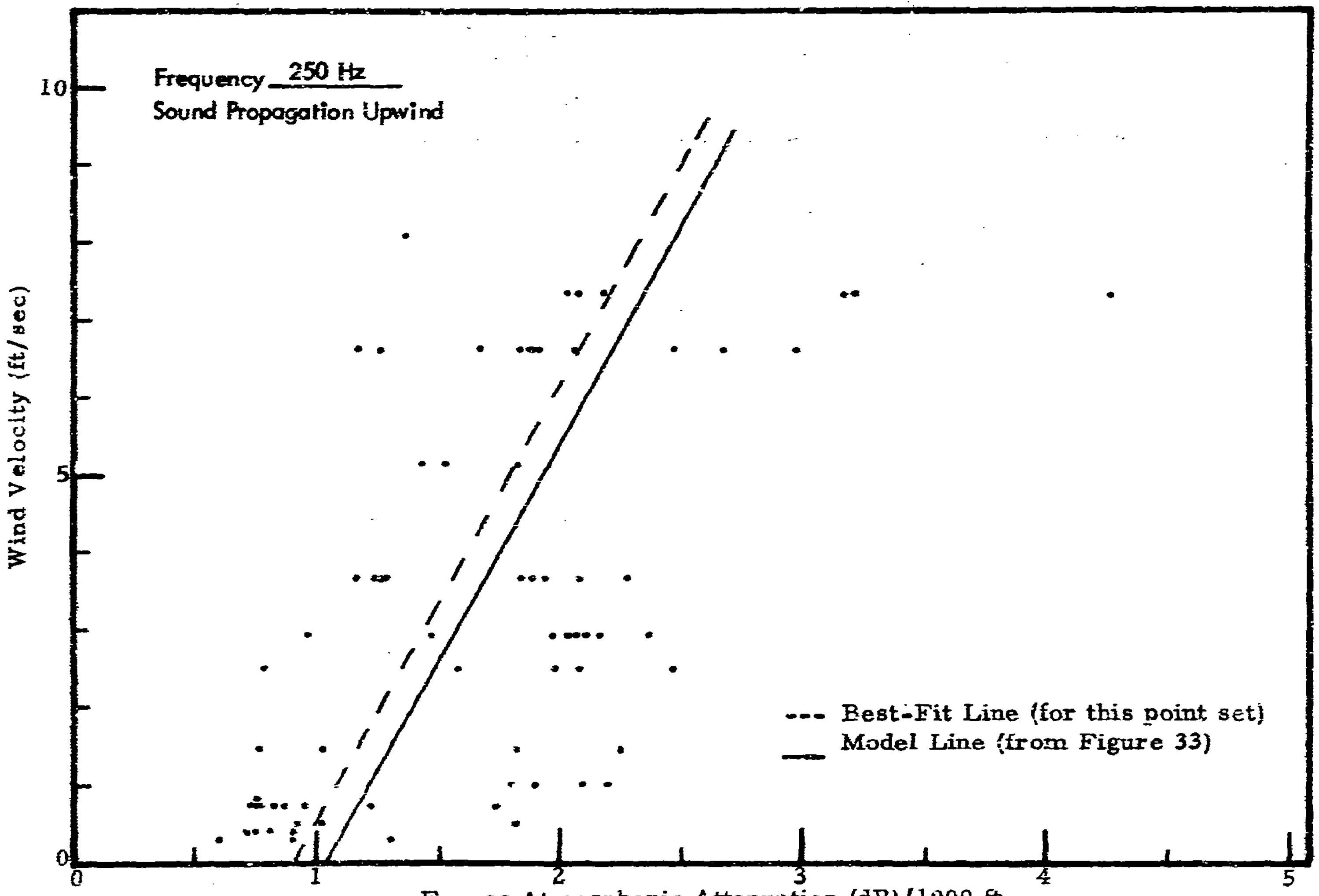

Figure 28. Effect of Wind Velocity on Excess Atmospheric Attenuation From Measured 1/3-Octave Data.

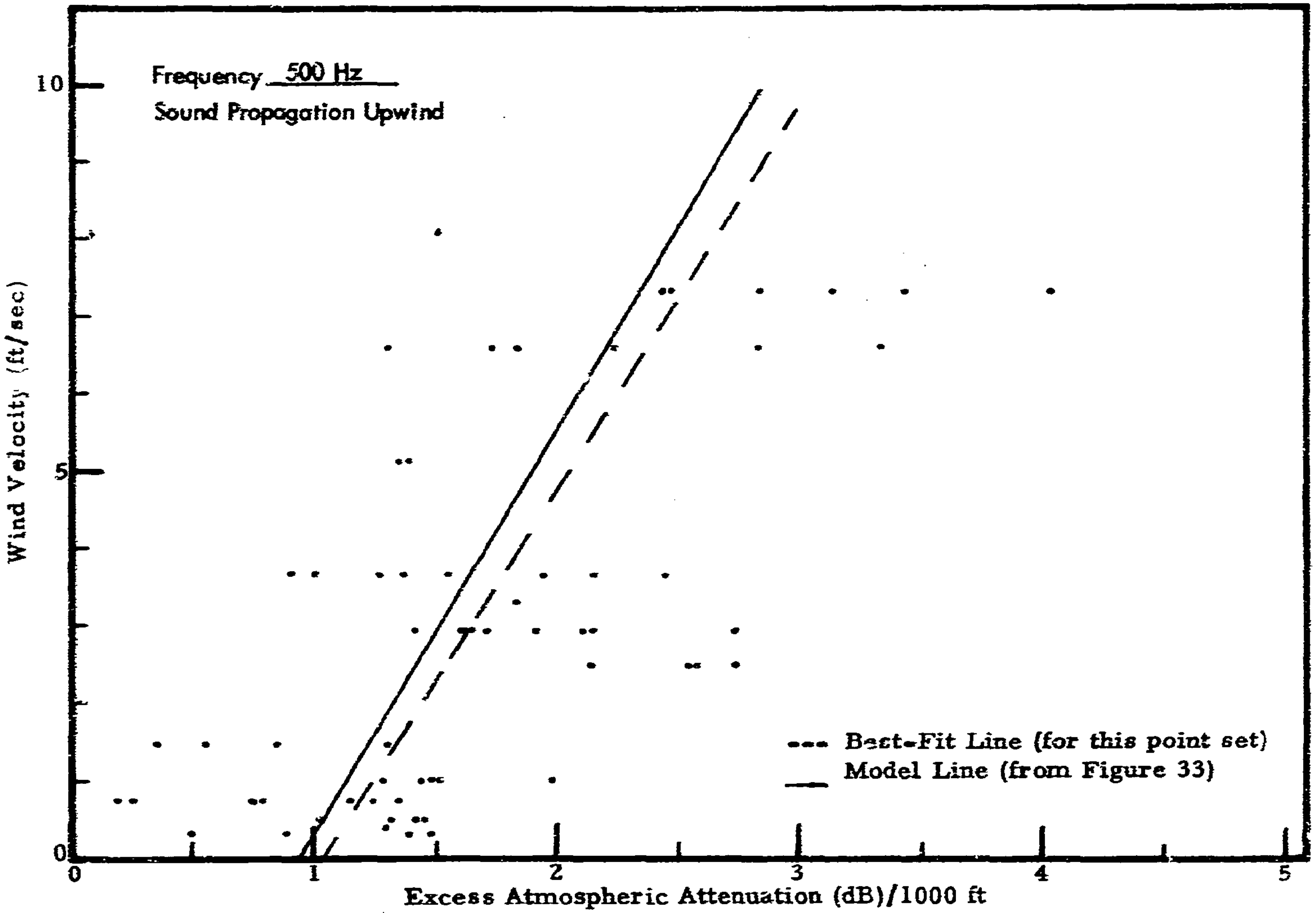

Figure 29. Effect of Wind Velocity on Excess Atmospheric Attenuation From Measured 1/3-Octave Data.

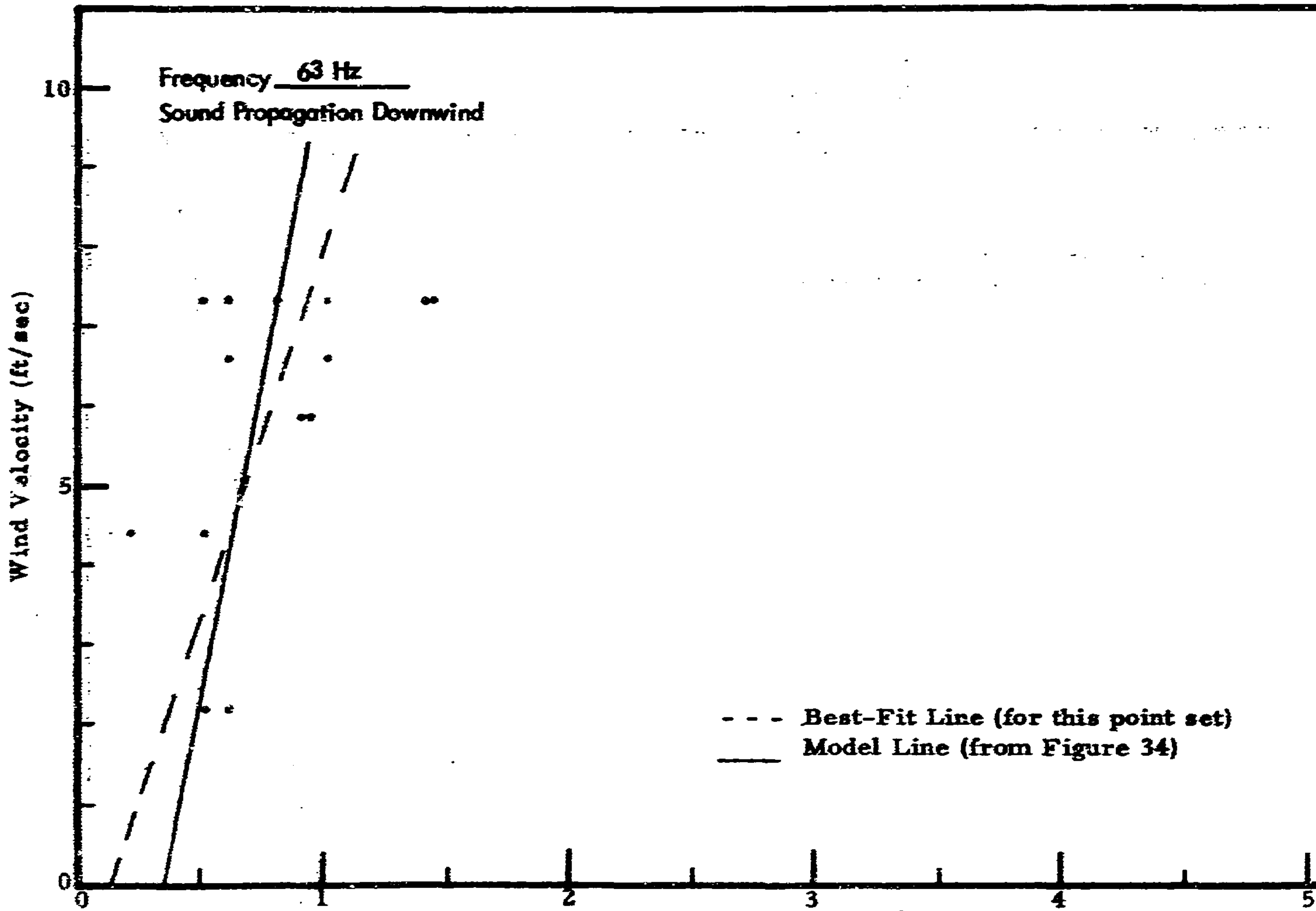

Figure 30. Effect of Wind Velocity on Excess Atmospheric Attenuation From Measured 1/3-Octave Data.

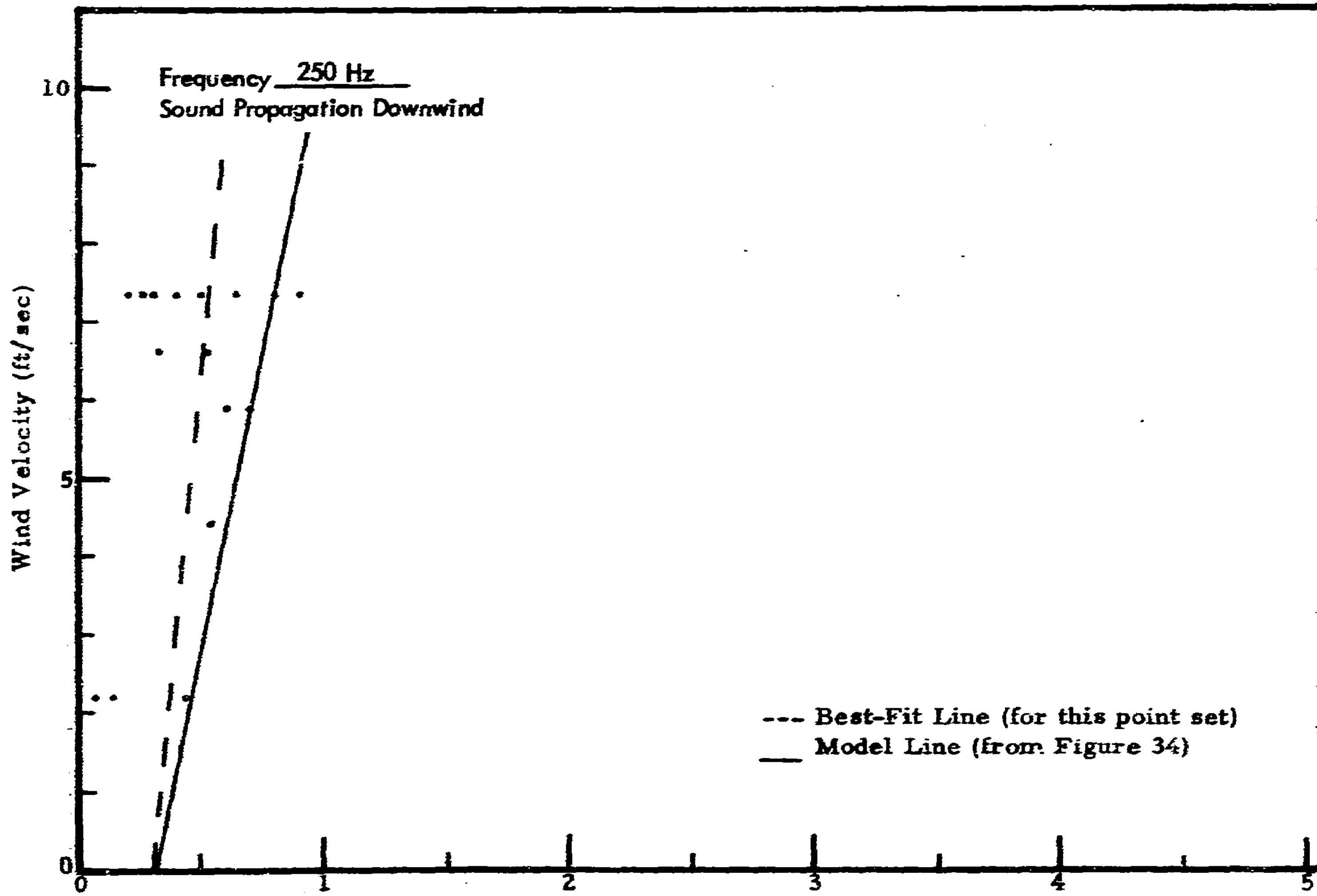

Figure 31. Effect of Wind Velocity on Excess Atmospheric Attenuation From Measured 1/3-Octave Data.

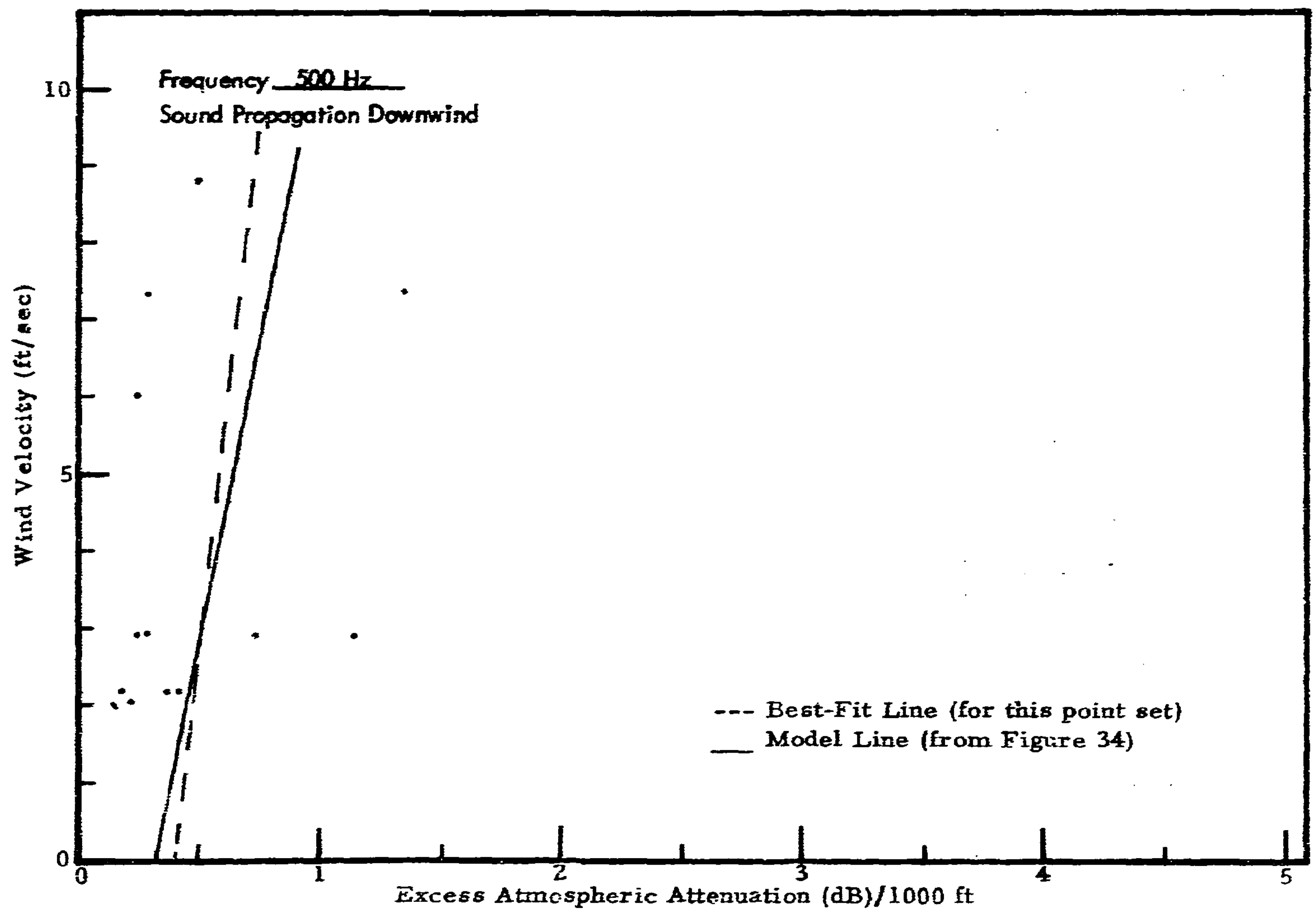

Figure 32. Effect of Wind Velocity on Excess Atmospheric Attenuation From Measured 1/3-Octave Data.

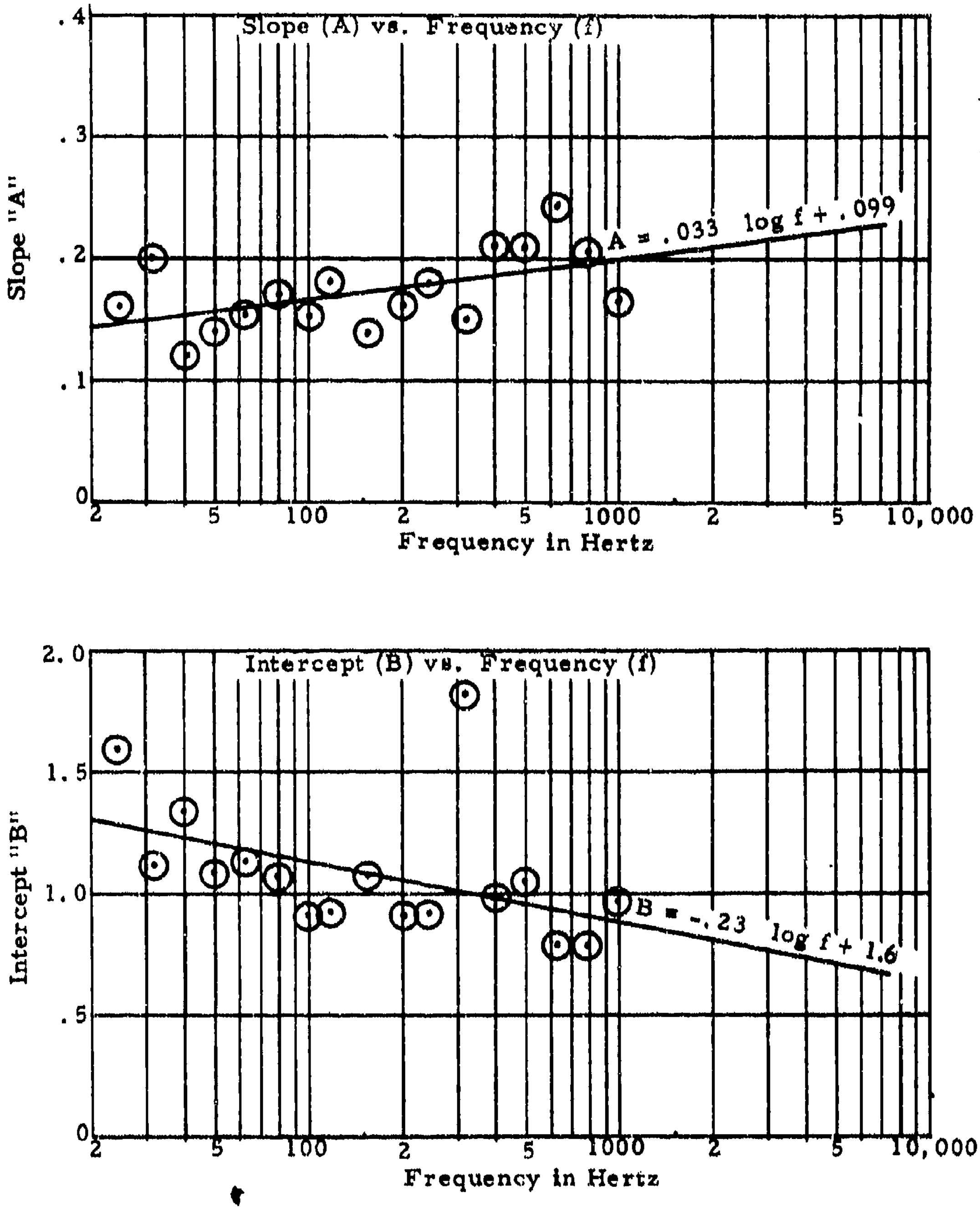

Figure 33. Results of Regression Analysis on Excess Atmospheric Absorption for Sound Propagation Upwind.

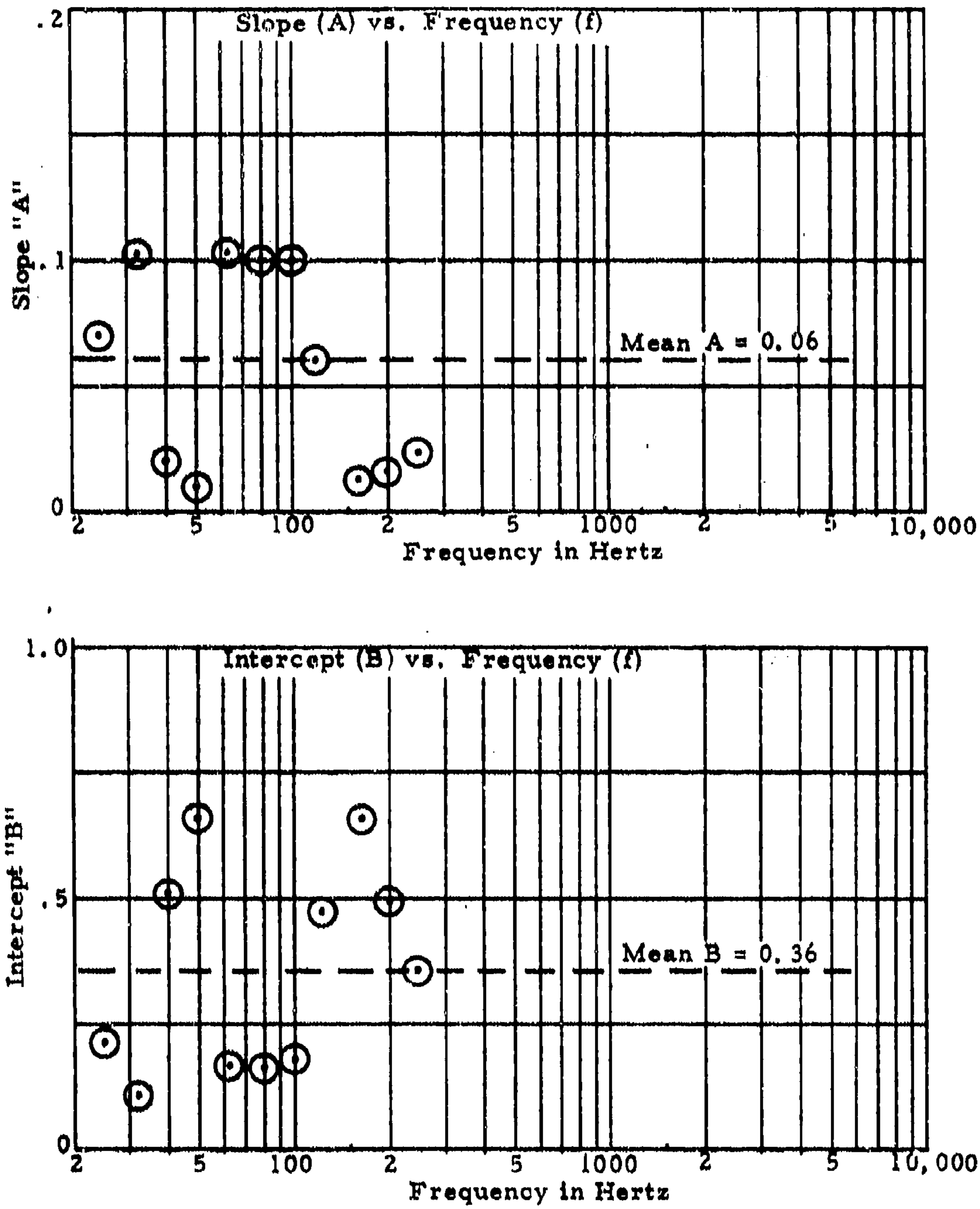

Figure 34. Results of Regression Analysis on Excess Atmospheric Absorption for Sound Propagation Downwind.

magnitude of scatter due to their influence is considered to be the only practical approach.

Wind vector was measured using a standard cup and vane anemometer. Cups mounted rigidly on the tips of a metal cross cause the entire assembly to rotate on an axis perpendicular to the plane of the cross with a velocity proportional to wind velocity. Wind direction is given by a separate vane. The dynamic response of such an anemometer provides an accuracy of about 5 percent, within a time of approximately two seconds for a change in flow velocity of eight feet per second. A typical pen recorder trace is given in Figure 26.

Even with this slow response, there was a substantial variation in the graphic records of wind velocity. Under these conditions, it is possible to extract at least three parameters to describe wind velocity: gust or peak velocity, mean velocity, and lull or minimum velocity. Better correlation was obtained between excess sound attenuation and wind velocity measured at lull than with other wind velocity parameters, so this parameter was used. It is easily obtainable from pen recorder traces as shown in Figure 26.

Values of excess atmospheric attenuation for selected 1/3-octave frequency bands are plotted against wind lull velocity in Figures 27 through 32. In some instances, as many as three points on a plot may originate from a particular run, while in some instances only one point or perhaps none at all were obtainable from a run.

Figures 27 through 29 represent sound propagation in an upwind direction for three typical 1/3-octave bands: 63 Hz, 250 Hz, and 500 Hz respectively. Figures 30 through 32 represent sound propagation in a downwind direction for the same three 1/3-octave bands. All approaches except six were made either from due upwind or downwind; thus, there was insufficient data to present for the crosswind case.

The data, of which examples were illustrated above, were subjected to a double linear regression analysis treating upwind and downwind propagation separately. The results are summarized in Figures 33 and 34, where the following linear regression parameters are given:

$$E = Au + B$$

where

E = excess atmospheric absorption in dB/1000 ft.
u = wind velocity measured at lull in ft. /sec.

and A and B are given by

$$A = .33 \log f + .099$$
$$B = -.23 \log f + 1.6$$

For sound propagation upwind and for sound propagation downwind, A and B are

$$A = .06$$
$$B = .36$$

It must be emphasized that these results are valid only for the geometry outlined earlier.

Elevation Angles Greater Than 2°

For angles of incidence larger than 2°, it may be expected that excess attenuation will be less than that derived above. It is possible to develop this quantitatively only in a limited way. The reason is that the requirement restricting comparison of sound received at different points on the ground relative to the same emission time means that angular dependence cannot be measured unless acoustic data acquisition systems are in line with the source, i.e., $\theta_1 = \theta_2 = \theta_3$ in Figure 35. However, the acoustic data acquisition systems were not in line with the source, so in order to develop a limited quantitative form for angular dependence, the following assumptions were made:

1. For values of θ of the order of 10°, no excess atmospheric attenuation was present.

2. For values of θ between 2° and 10°, no noticeable effect due to nonuniformities in helicopter radiation pattern was present.

Suppose, now, that the angle of incidence at a particular emission time is 10° as measured at station 2 during an approach at 1500 ft. altitude from the east. Applying the first of the above assumptions, it is possible to estimate noise radiated by the helicopter (at a distance close to it) from the noise record obtained from station 2. The second assumption implies that this is identical to the sound radiated in the direction of station 3. We may use this to estimate the noise at station 3, applying inverse square law and atmospheric absorption corrections as before, and compare this with the measured noise at station 3 relative to the same emission time as the

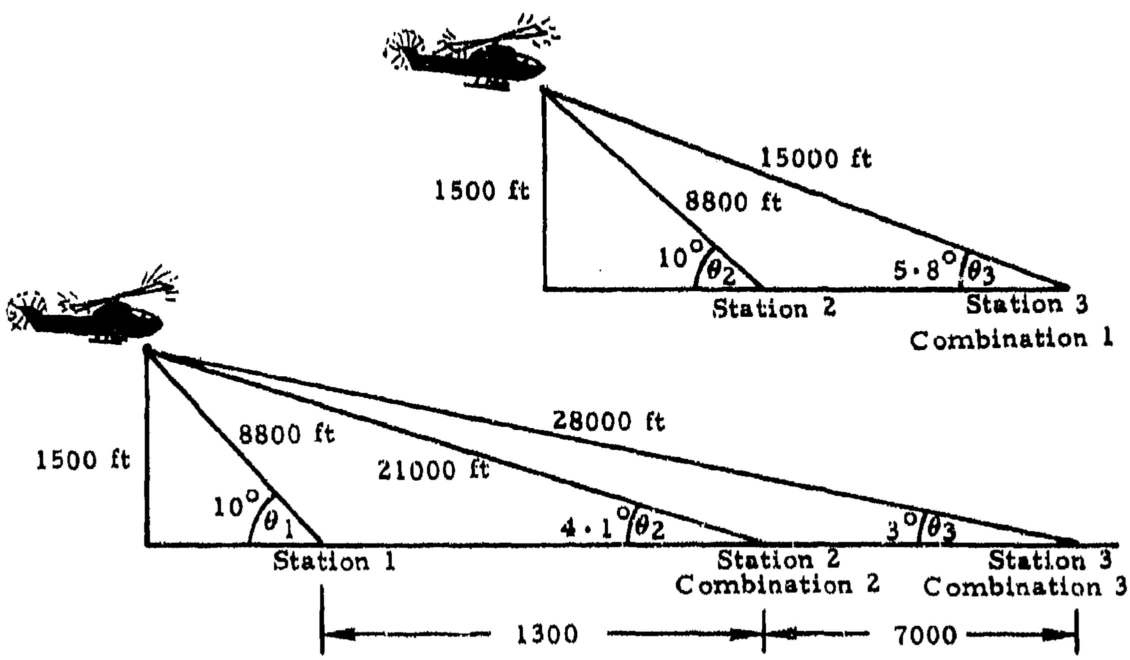

Figure 35. Combinations of Distance and Elevation Angle Between 2 and 10 Degrees.

noise record for station 2. The difference is due to excess atmospheric attenuation at an angle of 5.8° (Figure 35).

There is a limited number of cases which may be used to derive this type of data.

No flights made at 200 feet altitude or less may be used for these measurements since the assumption of uniform radiation would be violated. That is, slant ranges of approximately 1300 feet are required to fulfill the requirement of $\theta > 10°$. At a speed of 100 knots, during a period of four seconds (averaging time for 1/3-octave spectra) the angle of incidence θ changes to 18°, which violates the assumption of uniform radiation.

Flights at an altitude of 1500 feet exceed an angle of incidence of 10° at a slant range of about 8800 feet. This yields only three possible combinations of distance and angle (21,000 ft, 4.1°; 28,000 ft, 3°; and 15,000 ft, 5.8° (see Figure 35)) since values of slant range significantly smaller than 8800 feet violate the assumption of uniform radiation as before.

Values of excess atmospheric attenuation for angles of incidence between 2° and 10° are functions of at least three variables, namely, angle of incidence, slant range, and wind vector. As illustrated above, even with simplifying assumptions, only three combinations of angle and distance on any flight at 1500 feet altitude were available for obtaining excess attenuation for angles of incidence between 2° and 10°. Three points are clearly insufficient to map a nonlinear function of two variables.

An attempted solution was constructed as follows: A linear weighting factor ψ for angles between 2° and 10° was assumed, to be applied to the results of the regression analysis for angles less than 2° (Figure 36). That is, slant range dependence was assumed to be an inverse power law as before, and the results of the regression analysis for wind vector dependence were assumed to be applicable.

These assumptions were subsequently checked by comparing values of excess attenuation for five cases with values obtained at the same values of wind velocity, at angles less than 2°. The results of this comparison are shown in Figure 36, where it may be seen that the linear weighting factor provides a reasonable approximation to the limited experimental data.

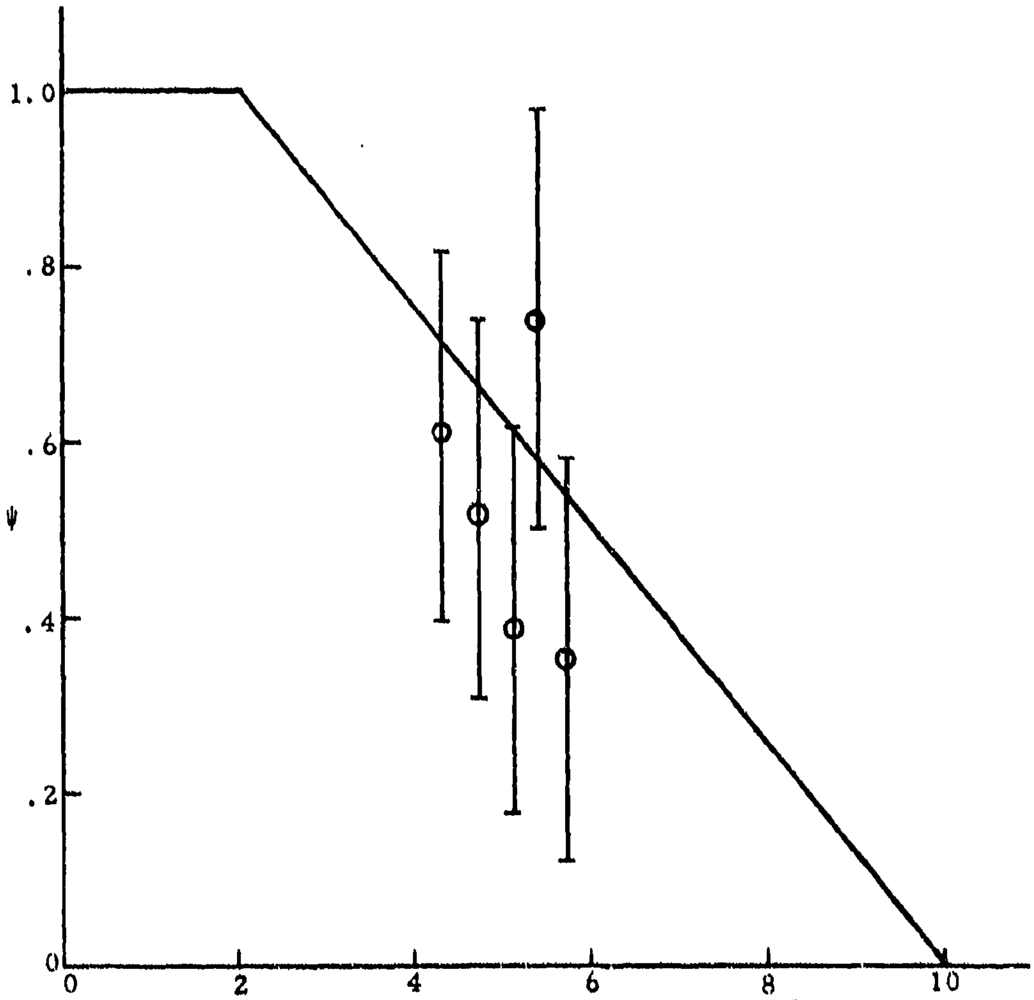

Angle of Incidence Θ = Arc Sin $\frac{h}{R}$

h = Helicopter Altitude
R = Slant Range

Figure 36. Plot of Weighting Factor ψ To Be Applied to Linearized Values of Excess Atmospheric Attenuation for $2^{\circ} < \theta < 10^{\circ}$.

DETECTABILITY ANALYSIS

Data Reduction Procedures

Acoustic measurements were made at three positions at the subject site to facilitate the separation of helicopter and ambient noise components.

Data analysis was performed initially on a Time Data, Model 1923, Fourier analyzer programmed to acquire data from the subject site microphone (microphone 1 - Figure 12) on channel "A" and one remote microphone (microphone 2 or 3 - Figure 12) on a second channel "B" in parallel. The following spectral functions were computed in realtime: (1) power spectra of "A" and "B", (2) cross spectra of "A" with "B", and (3) coherence function between "A" and "B". These were subsequently written on magnetic tape. During the transfer of the functions to magnetic tape (less than one second), acquisition of data ceased but resumed immediately after the transfer was completed. Except for this interval, data analysis was continuous.

The program used for the majority of the data reduction employed a 512-point Fourier transform with data sampled at a 4-kHz rate and with anti-aliasing filters set to cut off above 1 kHz, giving 128 spectral points between zero and 1 kHz or a spectral resolution of 7.81 Hz. Sixteen ensemble averages, i.e., two seconds, were taken to give 32 spectral degrees of freedom for the raw spectra.

Some portions of the data which did not reveal any significant response above 500 Hz were repeated, employing the same size transform as before but with data sampled at 2 kHz and antialiasing filters set to cut off above 500 Hz, giving 128 spectral points below this frequency at a spectral resolution of 3.91 Hz. The same number of ensemble averages yielding the same number of spectral degrees of freedom as before, but a 4-second averaging time, were used.

Microphone calibration data were acquired from the analog tapes for channel "A" in precisely the same manner as test data and stored as the first record on each digital magnetic tape. To ensure that cross-spectral functions between the two channels were correctly evaluated, the gain on channel "B" was adjusted so that the channel "B" calibration signal gave the same voltage level as the "A" calibration signal, so the two microphones always had effectively identical gains.

Digital tapes containing the various spectral functions were reformatted and a special-purpose subroutine was written so that they could be read easily by a FORTRAN program in a general-purpose computer.

Computation Procedures

The program for analysis of test results in the general-purpose computer was written to allow maximum flexibility. The basic procedure is as follows:

1. Extract calibration signal from first record on digital tape and find root-mean-square value.

2. Read record number, types of spectral function, and destination numbers of memory storage arrays from user card file.

3. Read specified functions for above record from digital tape; calibrate and store in memory storage arrays as specified above.

4. Repeat processes 2 and 3 until memory storage arrays are full.

5. Initiate computation by a flag in the user card file. A helicopter noise spectrum H(f) and ambient noise spectrum A(f) for a particular record number (time) are extracted in as pure a form as possible by manipulation of the spectral functions in the memory storage arrays. In each spectrum there are n values $H_k(f)$ and $A_k(f)$ where k = 1 to n.

6. Convert both helicopter noise H(f), and ambient noise A(f) power spectral densities expressed in dB/Hz to critical band levels $H^\dagger(f)$ and $A^\dagger(f)$ by evaluation of the following functions:

$$H^\dagger(f_k) = 10 \log_{10}\left[\Delta f \sum_{i=-k}^{n} 10^{\{H(f_{k+i})\}/10} \times W(Z_{k+i} - Z_k)\right] \qquad (8)$$

$$A^\dagger(f_k) = 10 \log_{10}\left[\Delta f \sum_{i=-k}^{n} 10^{\{A(f_{k+i})\}/10} \times W(Z_{k+i} - Z_k)\right] \qquad (9)$$

where k = 1 to n, and the functions $Z = Z(f_k)$ and $W = W(Z_{rel})$ represent subjective frequency (Bark) and the aural discriminatory filter shape respectively. They are defined in Figures 7 and 8. Note that in Figure 8 two possible derivations are given for Bark (Z) as a function of Hertz (f). Both derivations were used for comparison in the analysis of data.

7. Apply Ollerhead's detectability criterion to the critical band levels of helicopter and ambient noise. Values of the detectability parameter "δ_k" greater than zero at any frequency f_k should coincide with detection, where

$$\delta_k = H^{\dagger}(f_k) - 1.0 - 1.0 \log_{10} \left\{ 10^{T(f_k)/10} + 10^{(A^{\dagger}(f_k) - 5.0)/10} \right\} \quad (10)$$

and $T(f_k)$ is the pure tone threshold at frequency f_k in dB. For these calculations, values of the pure tone threshold shown in Figure 37 were used. As indicated in the figure, a sixth-order polynomial expression was used to approximate the data for T(f) from References 3 and 38.

The detectability parameter δ_k may be explained as follows. By extensive psychoacoustic testing, Ollerhead[3] showed that helicopter sounds were detected when δ_k was greater than zero or when

$$\delta_k = \left[H^{\dagger}(f_k) + M^{\dagger}(f_k) - 1.0 \right] > 0 \quad (11)$$

where $H^{\dagger}(f_k)$ is given by equation (8) and

$$M^{\dagger}(f_k) = 10 \log \left[10^{T(f_k)/10} + 10^{(A^{\dagger}(f_k) - 5)/10} \right] \quad (12)$$

is the effective level of the masking spectrum at the critical band frequency f_k. This is simply the linear summation of the mean square pure tone sound pressure at free-field threshold with the mean square critical band sound pressure of any actual ambient noise present reduced by 5 dB. Note that when the critical band level of an actual masking noise is of the order of 15 dB or more above pure tone free-field threshold levels, the influence of the latter will be negligible but that when the critical band level of the ambient noise is near pure tone threshold levels, the addition of the latter on an intensity basis

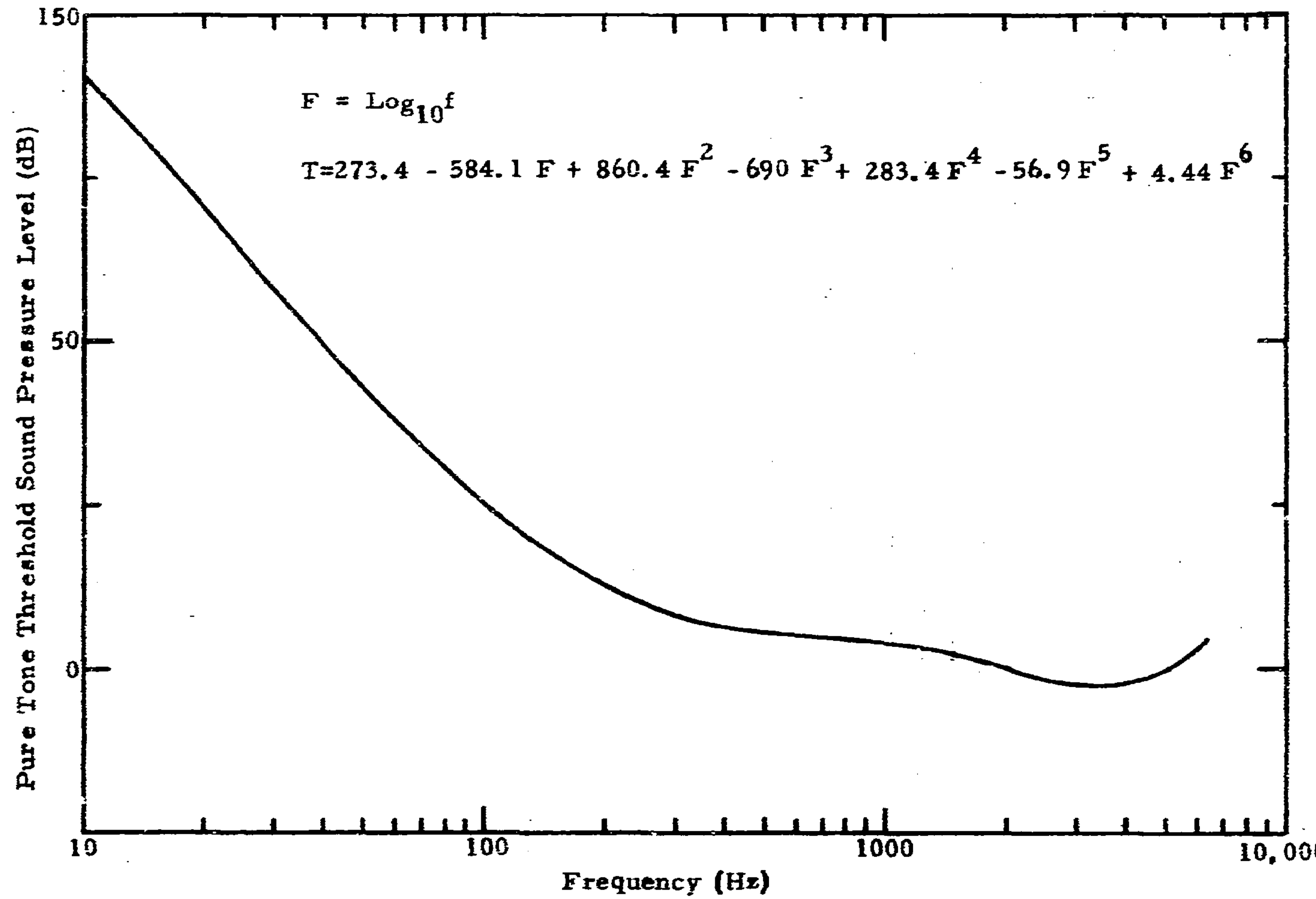

Figure 37. Pure Tone Threshold (From References 3 and 38).

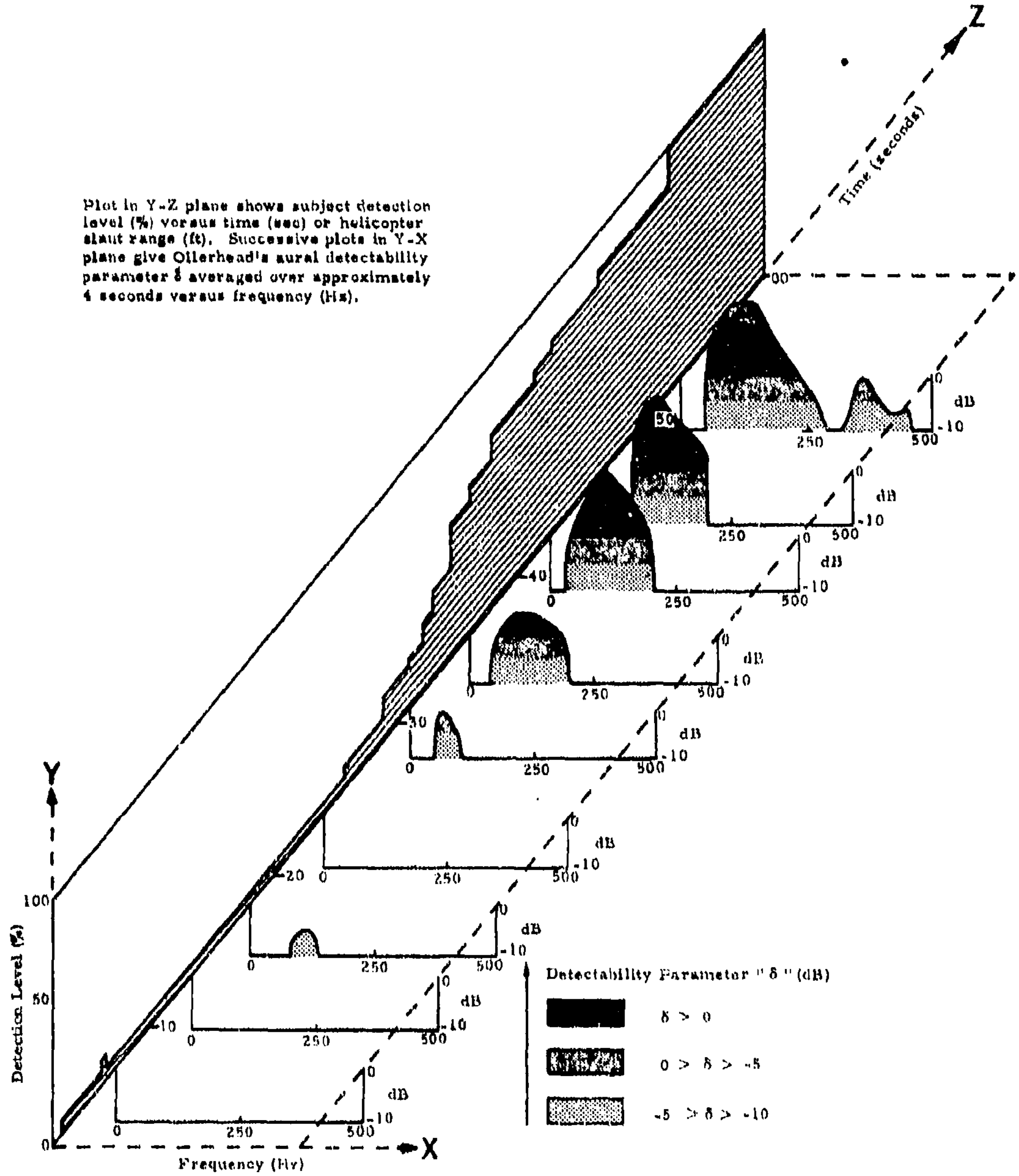

Figure 38. Summary of Measured Detection Data for Run 7 (4-Second Average).

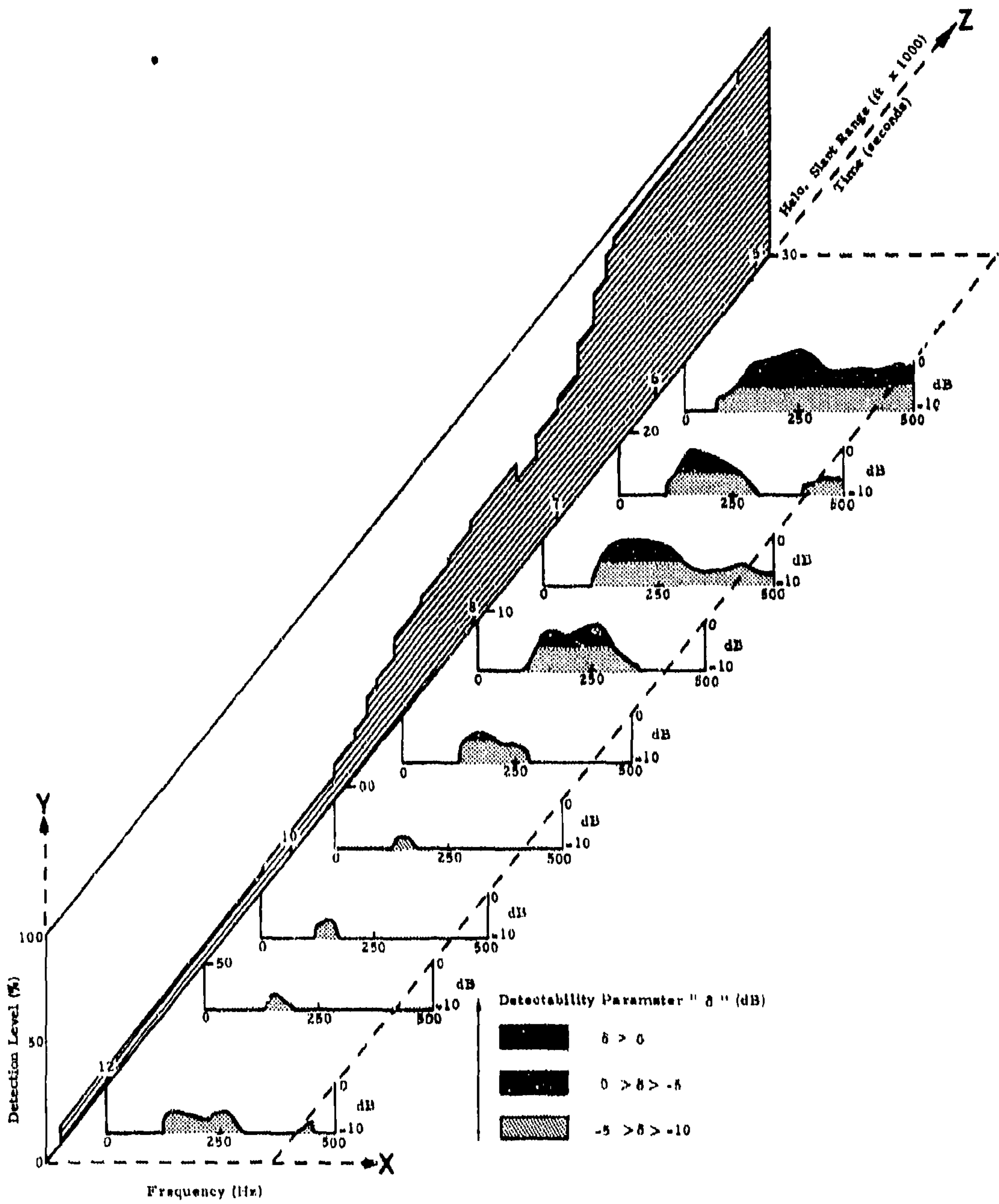

Figure 39. Summary of Measured Detection Data for Run 19 (4-Second Average).

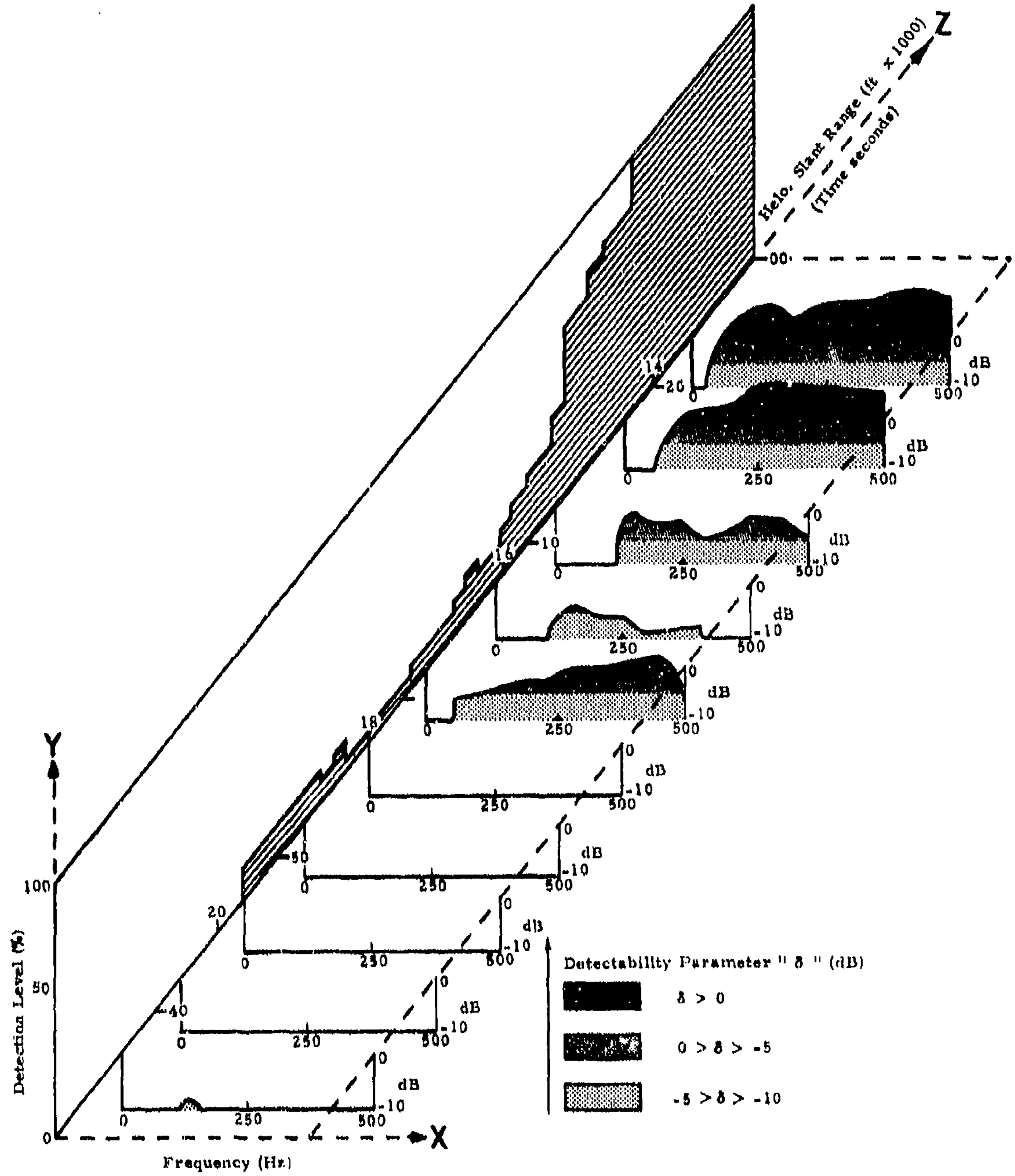

Figure 40. Summary of Measured Detection Data for Run 23 (4-Second Average).

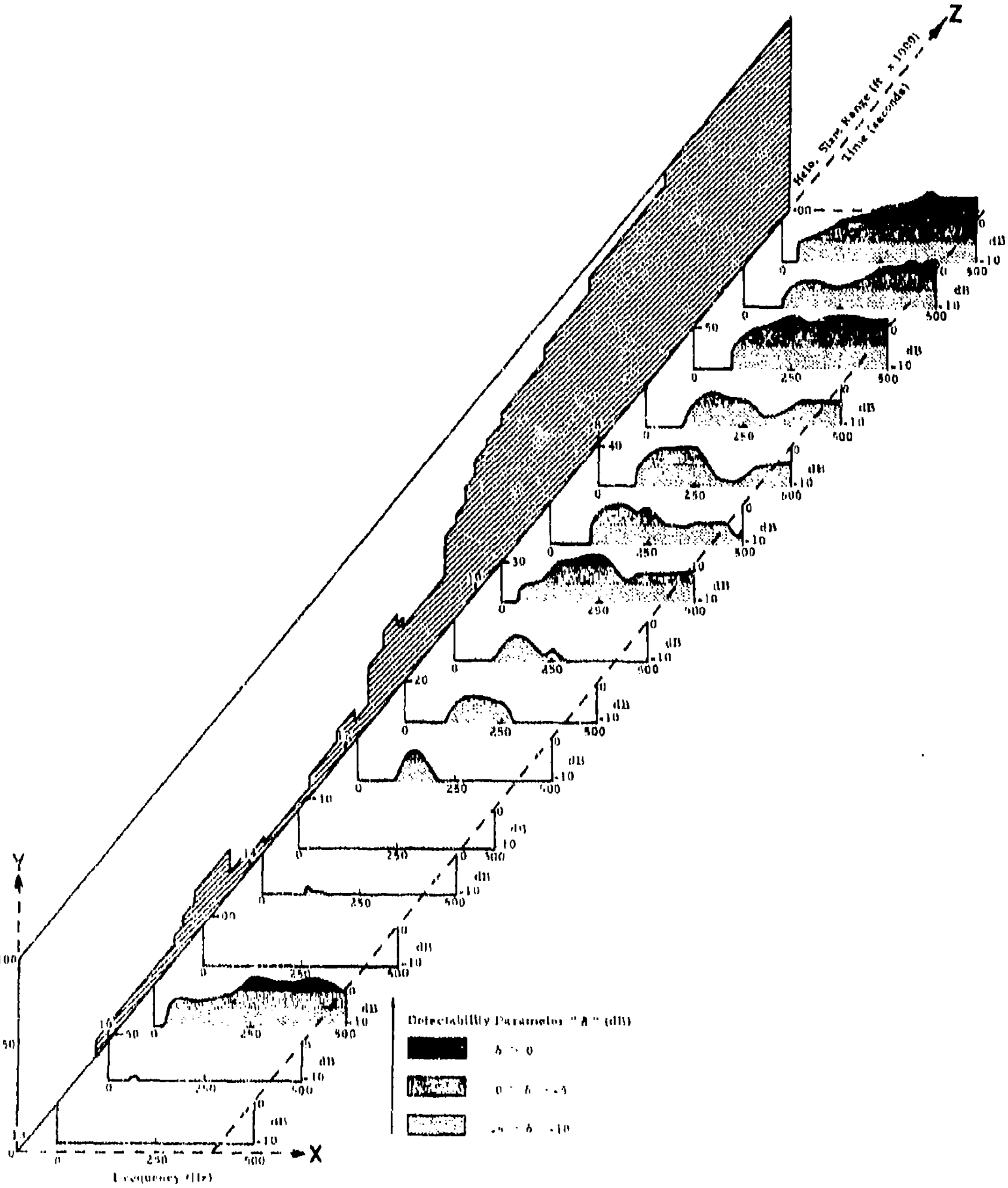

Figure 41. Summary of Measured Detection Data for Run 24 (4-Second Average).

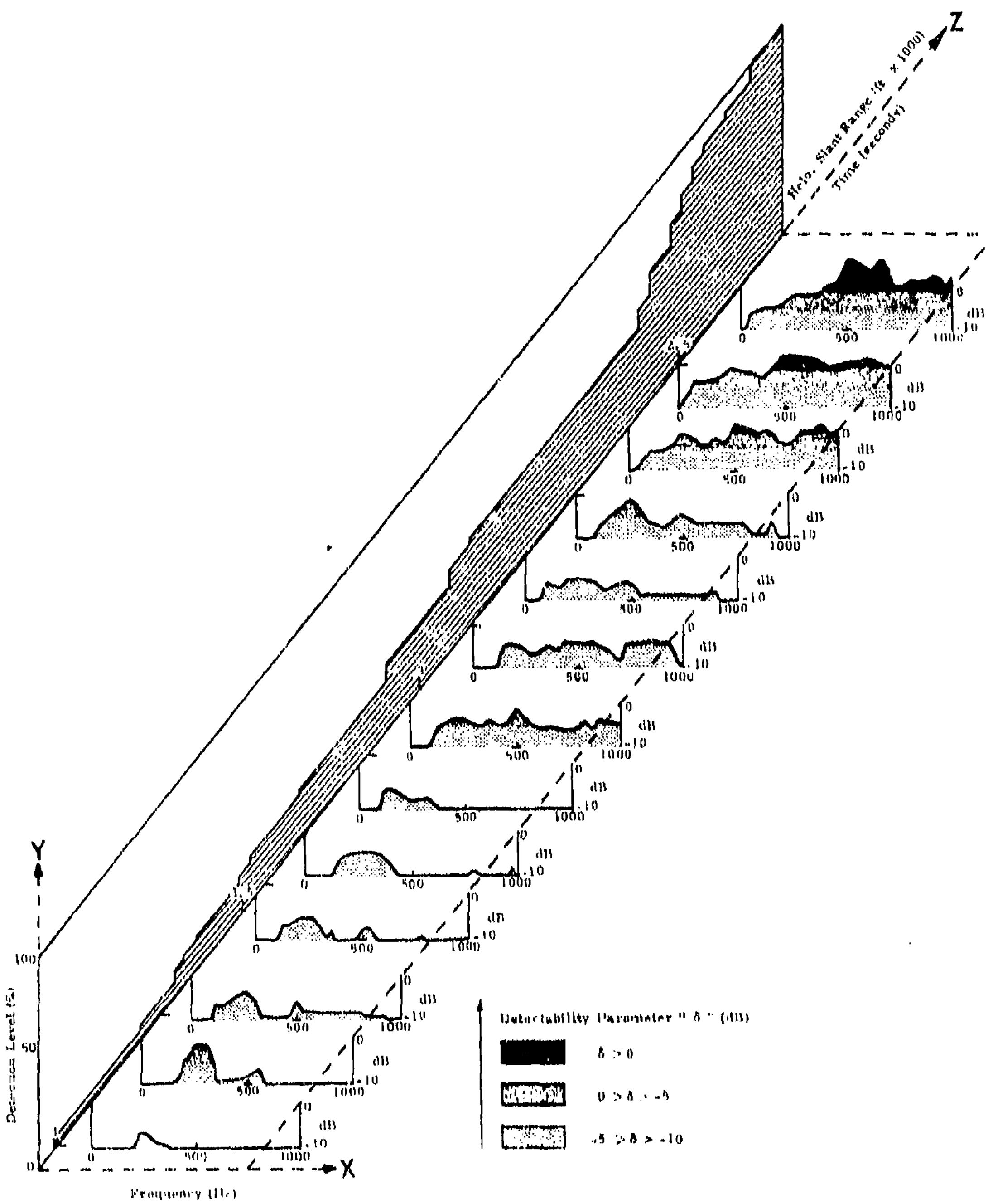

Figure 42. Summary of Measured Detection Data for Run 37 (2-Second Average).

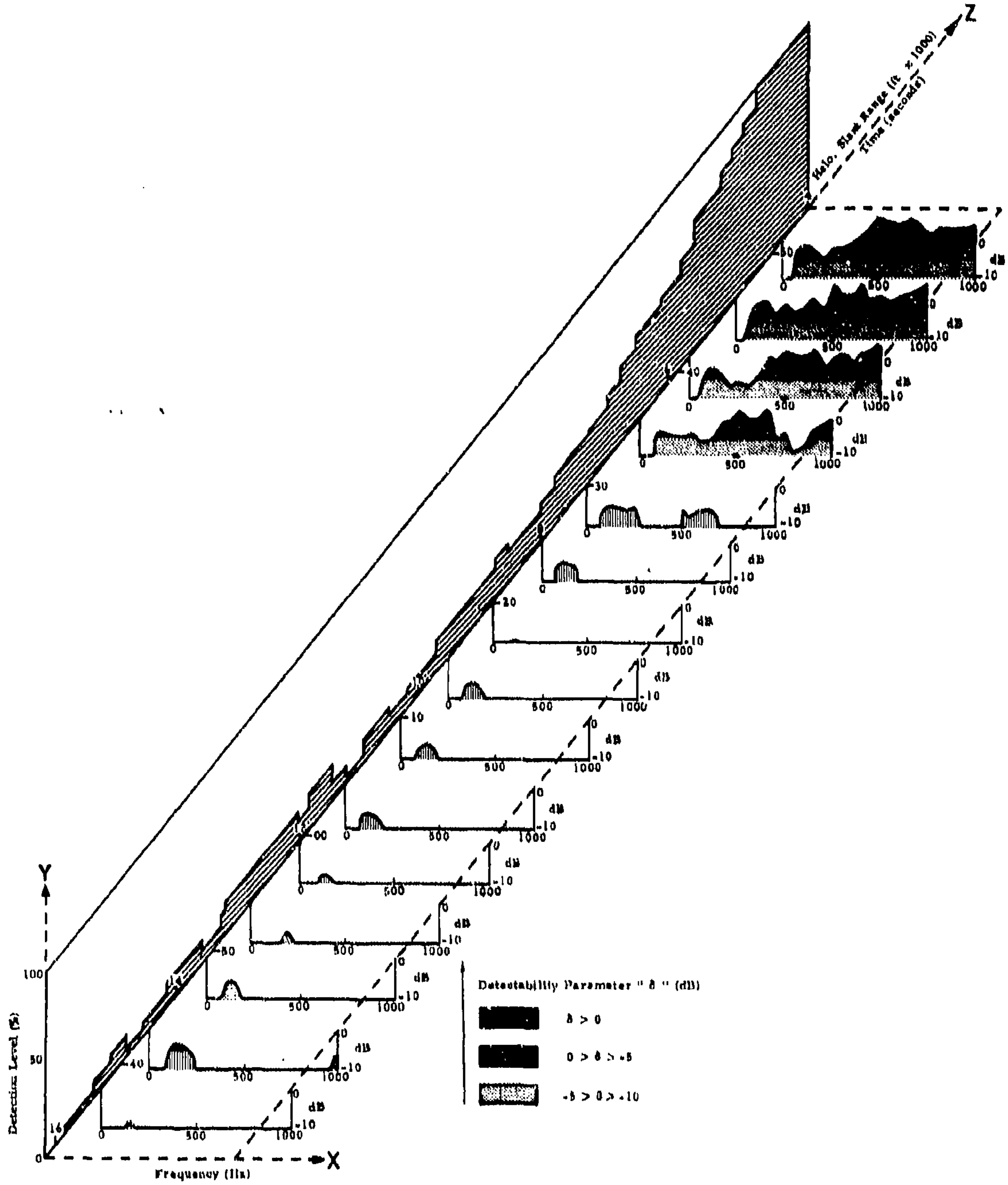

Figure 43. Summary of Measured Detection Data for Run 38 (2-Second Average).

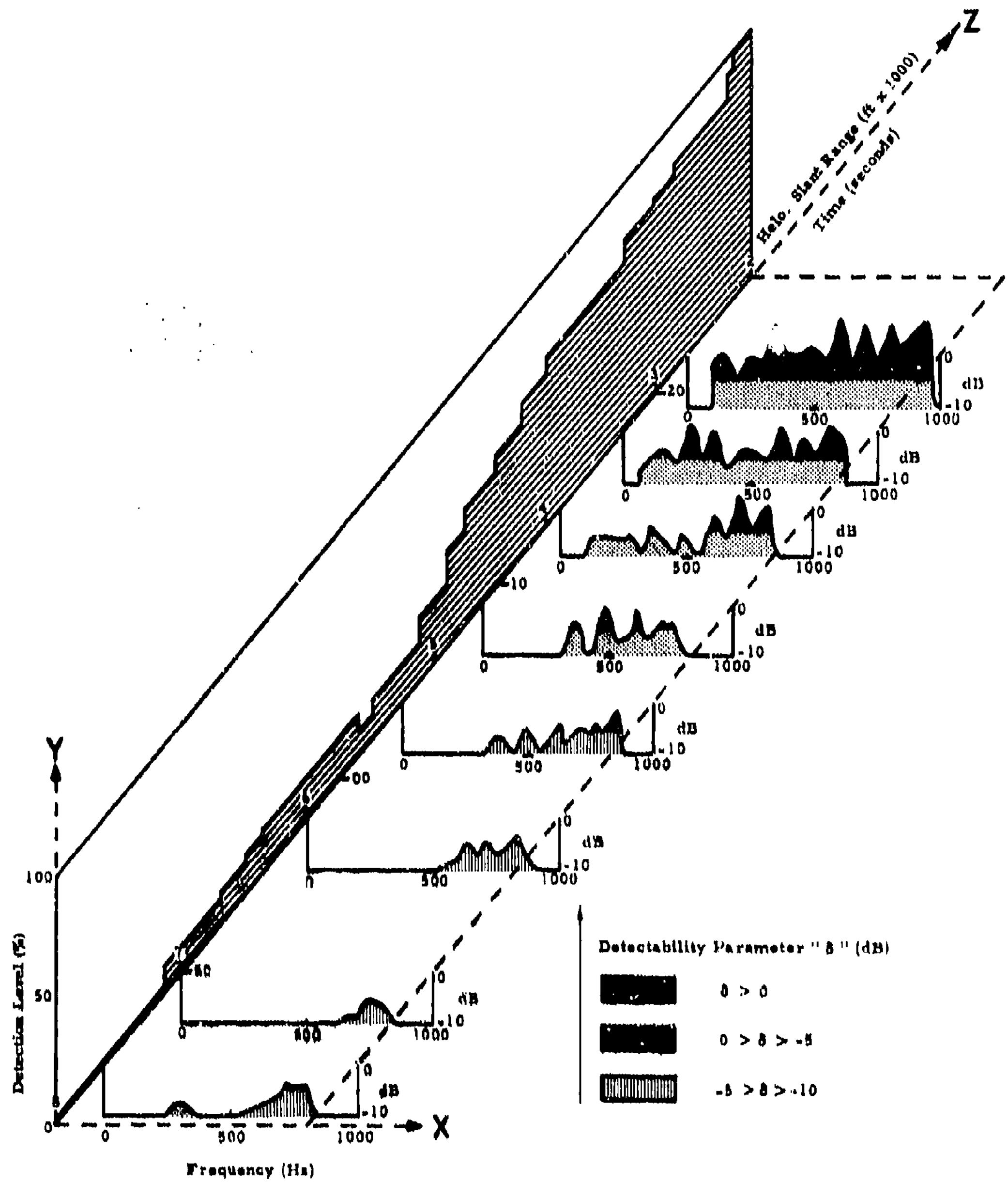

Figure 44. Summary of Measured Detection Data for Run 46 (2-Second Average).

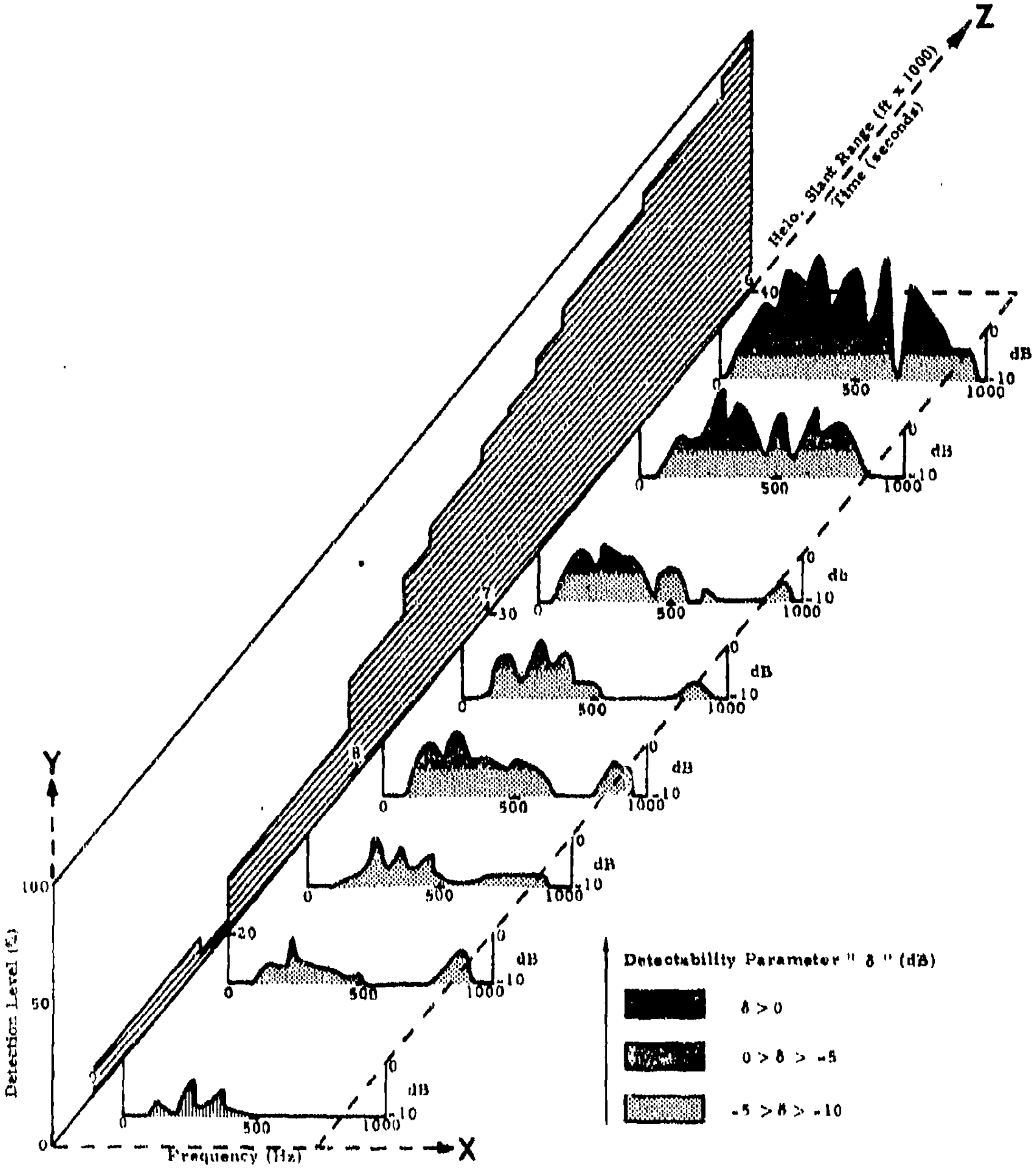

Figure 45. Summary of Measured Detection Data for Run 47 (2-Second Average).

is equivalent to assuming that pure tone threshold levels represent an internal auditory system noise floor.

The principal difficulty in exercising the above procedure occurs in Step 5, since it is not readily possible to clearly separate helicopter and ambient noise in a field experiment. Several procedures were tried, and the following two appeared optimum for the two categories of ambient noise environment:

1. Artificially generated noise at subject site:

   Power spectral densities of signals from the remote and subject microphones (microphones 2 and 1 respectively, in Figure 12) before the arrival of the helicopter were taken to represent natural ambient and total ambient, respectively. Total ambient consists of natural ambient plus artificially generated ambient. The power spectral density of the remote microphone during the helicopter's approach, minus the natural ambient derived above, was taken to represent helicopter noise. The total ambient derived above was taken to represent ambient noise.

   This method assumes that neither natural nor artificial ambients vary during the run. The process was found to yield a noise floor for computations of "δ_k" down to below -10 dB, for the combination of conditions encountered in the field test.

2. Natural ambient noise at subject site:

   The assumption was made that the natural ambient at the test site was comprised of noise originating both in the near field (e.g., insect noise and most wind noise) and in the far field (e.g., distant traffic noise). By taking the cross spectrum of the subject and remote microphones, the incoherent portion (or noise generated in the near field of each microphone) is obliterated and only the coherent portions (or noise generated in the far field) are left.

   Thus, for measurements taken before the arrival of the helicopter, the power spectrum from the subject microphone represents the ambient noise, and the cross spectrum between subject and remote microphone signals represents a residual. The cross spectrum between the two microphones during a helicopter's approach minus this residual was assumed to represent helicopter noise. This process, as with the one outlined before, assumes that neither the ambient nor the residual varies during the run. The noise floor of this process for computations of "δ_k" was similar to that found in the previous method.

Results

Three main correlations using subject detection data were made. These were in the form of:

1. Correlation of Detectability Parameter "δ" With Subject Rerponses

   To illustrate the manner in which the detectability parameter varies with subject response during a helicopter approach, eight typical cases are shown in Figures 38 through 45. Figure 38 represents a helicopter approach under natural ambient conditions, and the detectability parameter "δ" was derived using the second method outlined above. Figures 39 through 45 represent approaches under artificial ambient noise conditions with "δ" being derived using the first method outlined above.

   The plots in the Y-Z plane show measured subject detection level in percent, evaluated using the first and more comprehensive methodology described in the section "Subject Response Decoding".

   At successive time intervals, plots in the X-Y plane show values of the detectability parameter versus frequency.

   Shaded areas in each of these indicate 5-dB bands of the detectability parameter δ. Higher values of δ are associated with darker shading.

   There are several interesting points to note concerning Figures 38 through 45:

   a. There is a clear correlation between measured subject response and detectability parameter.

   b. The detectability parameter does not increase uniformly with time; for example, in Figure 41 an early rise in "δ" above zero corresponds with a rise in subject detection to 20%, but both fall substantially before rising again about 15 seconds later.

c. The region of partial detection is often spread over a substantial time, with initial detections taking place at lower frequencies and later detections corresponding to emergent peaks in "δ" at higher frequencies. For example, in Figure 42 initial detections occur at 250 Hz, while large emergent peaks at 500 Hz correspond with a sudden increase in subject detection level from 50% to 100%. A similar situation is evidenced in Figure 43.

d. Detection usually takes place over a broad frequency band (Figures 39-43) and is sometimes characterized by several discrete peaks (Figures 44 and 45).

To assess the accuracy of the detectability criterion defined above, according to the results measured in this full field test, the following procedure was adopted. Subject detection levels were broken down into five bands: 0-15%, 15-30%, 30-50%, 50-70%, and 70-100%. Peak values of the detectability parameter "δ" falling within these bands were noted and were averaged for each run. The mean values of "δ" ($\bar{\delta}$) for each run were then averaged over all runs and plotted against the average subject detection level in each of the five bands. The results are shown in Figure 46, with values of "$\bar{\delta}$" derived using Greenwood's critical band function, and in Figure 47 based on Zwicker's critical band function.

In both cases 50% detection level occurs roughly at zero "$\bar{\delta}$". Although the difference between the results using Greenwood's or Zwicker's functions is not significant, Greenwood's function yielded more low-frequency detection peaks, which was perhaps to be expected due to the narrower critical bandwidth at lower frequencies of Greenwood's data (Figure 6), resulting in less smoothing of discrete frequency helicopter rotational-noise components. Note that in Figures 46 and 47 the subject detection levels, in percent, are plotted on a probability scale; and to a first approximation, the data fell close to a straight line, suggesting a normal distribution of measured subject response versus theoretical detection level.

In summary, a principal result of this study may be drawn from the coincidence of 50% subject detection level and zero "$\bar{\delta}$". This confirms the results of Ollerhead's laboratory study that for helicopter noise, a masking level 5 dB below the ambient critical band spectrum yields a realistic model for median likelihood of detectability.

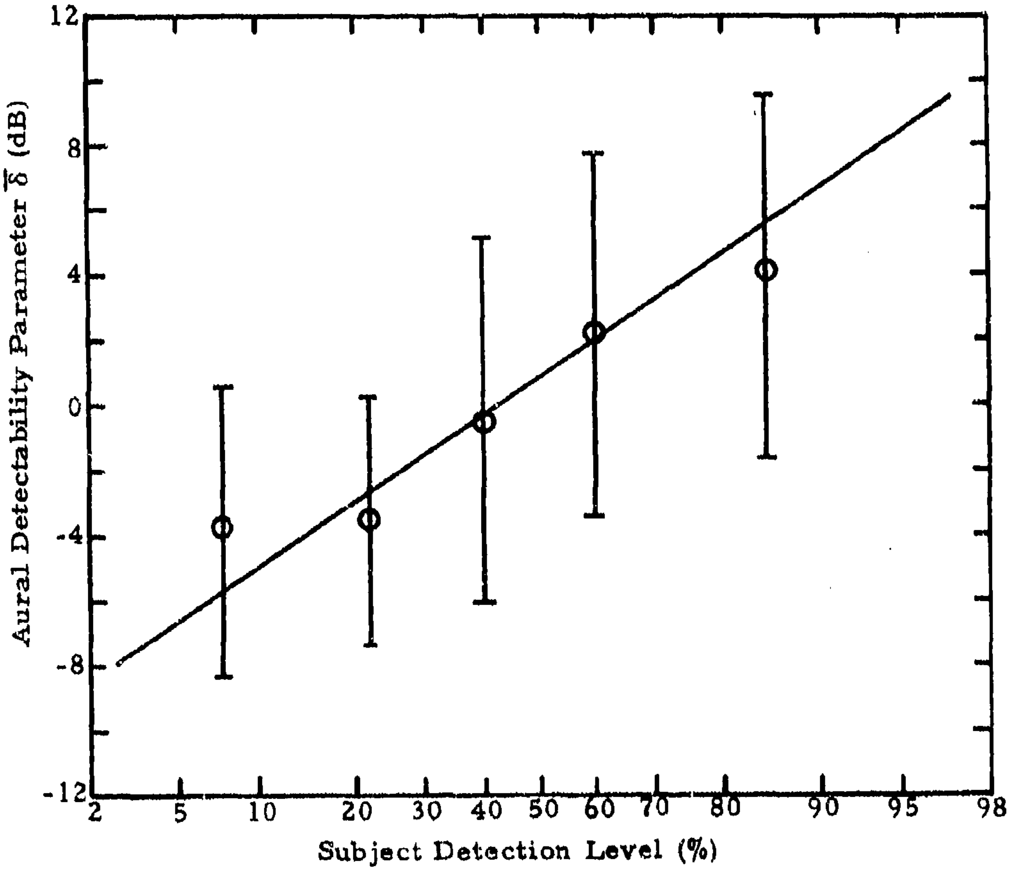

Note: Detectability parameter is derived from Greenwood's critical band function.

Figure 46. Aural Detectability Parameter Versus Measured Subject Detection Level (Case 1).

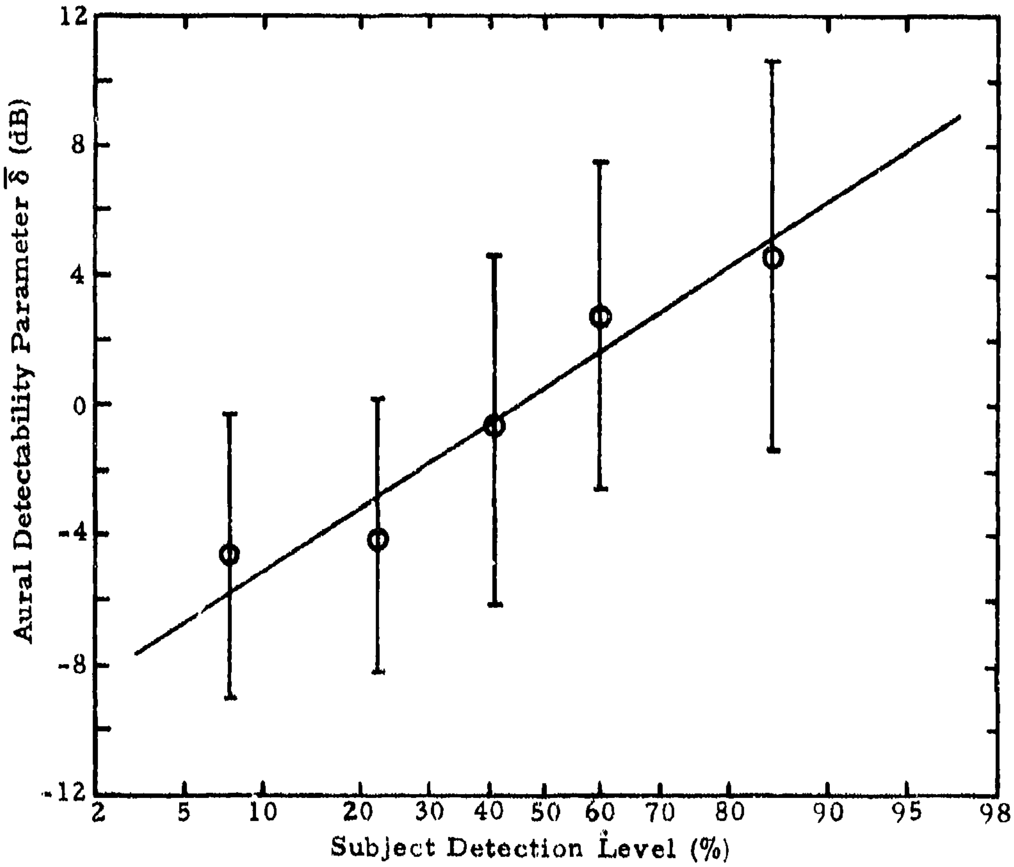

Note: Detectability parameter is derived from Zwicker's critical band function.

Figure 47. Aural Detectability Parameter Versus Measured Subject Detection Level (Case 2).

2. Effect of Altitude on Detection Distances

In order to illustrate, from a different point of view, the effect of decreased atmospheric attenuation at angles of incidence greater than 2°, the results contained in Table 2 of this volume and in Table 2 of Volume II were compiled. Here detection distances obtained from flights at less than 200 feet altitude are compared with detection distances from flights by the same aircraft at an identical velocity but at an altitude of 1500 feet. To minimize the effect of changing atmospheric parameters, whether measured or unknown, this comparison was restricted to flights close together in time. As an additional check, variations in measured atmospheric parameters between each pair of flights are listed.

Detection distances were compared for each pair of suitable flights at the following detection levels: 20%, 30%, and 50%. The mean ratio of detection distance for flights at low altitude (< 200 ft.) relative to the detection distance for flights at 1500 feet was 0.68 ± 0.22 as shown in Table 2.

That is, a helicopter approaching at an altitude of 1500 feet was detectable at approximately 1.5 (on average) times the distance of a helicopter approaching at an altitude of less than 200 feet.

3. Effect of Listener Attentiveness

The effect of listener attentiveness/distraction on relative detection distance was assessed in the following manner. As summarized in Table 3, the detection distance obtained for each flight at the 20%, 30%, and 50% detection levels for the distracted group was divided by the distance as detected by the alert group. Since each flight was repeated with only the relative conditions of attentiveness interchanged, this quotient represents an independent statistically meaningful measure of the effect of attentiveness on relative detection distance.

The mean value and standard deviation of the quotients for all cases were 0.97 ± 0.28, indicating that no significant effect of attentiveness on detection distance was observed in this study.

A cautionary note should be expressed regarding this result. No matter how diligent the effort to otherwise occupy a "distracted" subject, and no matter how highly motivated the attentive group, throughout the course of several days and

TABLE 2 - MEASURED EFFECT OF ALTITUDE ON RELATIVE DETECTION DISTANCE

% Detection Level	Altitude ≤ 200 ft Run No.	Distance (ft) D_L	Altitude ≈ 1500 ft Run No.	Distance (ft) D_H	Differences Temp. (°F)	Rel. Hum. (%)	Wind Vel. (Lull) (fps)	Elapsed Time Between Runs (min)	D_L/D_H
20	13	20060	16	20750					0.97
30	13	18480	16	19960	-3	-9	1.46	31	0.93
50	13	14520	16	19750					0.74
20	13A	12410	16	20750					0.60
30	13A	12140	16	19960	-3	-9	4.5	23	0.61
50	13A	10560	16	19750					0.54
20	17A	17950	16	20750					0.87
30	17A	13090	16	19960	0	0	6.63	6	0.66
50	17A	12670	16	19750					0.64
20	20	6600	24	14680					0.45
30	20	5810	24	11860	1	-2	0.76	27	0.49
50	20	3960	24	10610					0.37
20	26	9240	30	15360					0.60
30	26	8030	30	14260	0	-2	0.73	32	0.56
50	26	7390	30	11250					0.66
20	32	8450	36A	19430					0.43
30	32	8240	36A	19430	-2	-4	2.2	28	0.42
50	32	7390	36A	16740					0.44
20	38	13200	42	18320					0.72
30	38	7920	42	16470	0	-1	0.74	21	0.48
50	38	6490	42	15520					0.42
20	19	9240	21	16630					0.56
30	19	8870	21	16160	1	-1	-0.73	10	0.54
50	19	7340	21	13100					0.56
20	25	12140	27	17480					0.69
30	25	9780	27	15840	1	1	0.73	13	0.63
50	25	8550	27	14360					0.60
20	31	13040	33	26720					0.49
30	31	11670	33	26240	0	0	-0.73	12	0.45
50	31	11190	33	22440					0.50
20	37	19270	39	19170					1.00
30	37	17690	39	19170	2	-4	-0.8	10	0.92
50	37	13620	39	19010					0.72
20	2	21910	4	19590					1.12
30	2	21680	4	19430	0	7	0.73	9	1.11
50	2	19010	4	18320					1.04
20	8	24820	10	26930					0.92
30	8	22700	10	23020	-1	2	-2.22	15	0.99
50	8	20860	10	19170					1.09
20	59	12140	61	11350					1.06
30	59	9500	61	11040	0	-1	0	12	0.86
50	59	8920	61	11080					0.89
20	46	6450	47	8450					0.77
30	46	5020	47	7760	0	0	2.2	4	0.65
50	46	4540	47	7500					0.61
20	52	5020	53	9400					0.53
30	52	4330	53	9240	0	0	1.47	5	0.47
50	52	3590	53	8980					0.40
20	43	5810	44A	7390					0.79
30	43	5810	44A	6600	1	-1	1.5	12	0.88
50	43	5490	44A	5280					1.04
20	49	5600	50B	8870					0.63
30	49	2640	50B	7660	0	0	-3.63	36	0.35
50	49	2320	50B	6760					0.34
								Mean	0.68
								Standard Deviation	±0.22

TABLE 3 - EFFECT OF ALERTNESS ON RELATIVE DETECTION DISTANCE

Run No.	DETECTION DISTANCES(ft)						RELATIVE DISTANCE		
	Alert Group Detection Levels			Distracted Group Detection Levels			Distracted Group / Attentive Group		
	20%	30%	50%	20%	30%	50%	20%	30%	50%
2	22723	22441	19058	19651	19058	18764	.86	.85	.98
3	*	36432	35376	36432	35904	35376			
4	**	**	**	**	**	**			
5	44753	44370	44188	44935	44753	44753	1.0	1.01	1.01
6	22371	21994	20521	22558	21627	19590	1.03	.98	.95
7	*	*	*	*	*	*			
8	26400	22176	19536	23760	23232	22176			
9	43036	42295	41851	42735	42586	42446	.99	1.01	1.01
10	24224	22982	19656	24531	19221	18927	1.01	.84	1.01
11	45936	43476	42010	41824	41644	41289		.96	.98
12	21305	20781	19709	21305	18634	16831	1.00	.90	.85
13	20322	20009	17933	18413	16650	8983	.91	.83	.50
13A	12570	12396	12055	10600	10105	9747	.84	.82	.81
14	20452	20209	19232	19964	19964	19719	.98	.99	1.03
16	22176	22176	20064	18480	17952	15840			
17A	15845	13845	12365	19116	13061	12708	1.21	.94	1.03
18	21718	20984	19746	21958	21958	21718	1.01	1.05	1.10
19	8803	8046	7316	9255	9255	9103	1.05	1.15	1.24
20	8976	7392	5280	6336	3696	2640			
21	12867	12867	12435	16543	16543	16123	1.29	1.29	1.30
22	*	*	*	*	*	*			
23	18495	17289	15690	16413	16233	15520	.89	.94	.99
24	14645	12675	10560	14806	11668	11505	1.01	.92	
25	13660	13378	11704	8616	8616	7926	.63	.64	.68
26	8448	8448	7920	7920	7392	5808			
27	*	15840	15840	13728	14256	12672			
28	9385	9147	8684	7920	7392	6864			
29	21548	21548	20867	21548	20702	20529	1.00	.96	.98
30	16880	16409	14356	9157	9157	8710	.54	.56	.61
31	13379	12923	11505	12302	11349	10886	.92	.88	.95
32	8542	8235	7321	8235	8235	7321	.96	1.00	1.00
33	23765	23463	22564	33751	22865	22564	1.42	.97	1.00
34	12707	12707	11416	11416	10894	8461	.90	.86	.74
35	31043	31043	30306	24960	24960	23713	.80	.80	.78

* No Radar Track

** Other Aircraft in Vicinity

TABLE 3 (continued)

Run No.	DETECTION DISTANCES(ft)						RELATIVE DISTANCE		
	Alert Group Detection Levels			Distracted Group Detection Levels			Distracted Group / Attentive Group		
	20%	30%	50%	20%	30%	50%	20%	30%	50%
36A	22783	19302	17703	19302	16904	16427	.85	.88	.93
37	16368	13200	13200	19536	19008	17952			
38	14631	13253	6336	10277	8043	7487	70	.61	
39	19138	19138	18990	20004	19138	18834	1.05	1.00	.99
40	9663	9663	9415	9159	8912	8441	.95	.92	.90
41	30748	26030	24941	25488	24759	24759	.83	.95	.99
42	15781	15634	15490	22109	19810	15490	1.40	1.27	1.00
43	6336	5808	5280	6336	6336	5808			
44A	11158	5260	5260	7444	7339	6864	.67	1.40	
45	8401	8274	6336	8985	8540	8540	1.07	1.03	
46	6864	4752	3696	6336	4224	3696			
47	8452	8452	7750	7750	7492	7100	.92	.89	.92
48	8778	8618	8288	10085	8457	8457	1.15	.98	1.02
49	6864	6864	2493	2751	2366	1710			.69
50B	12308	11767	7392	6864	6864	6864			
51	8385	7911	6336	9862	9862	9182	1.18	1.25	
52	5520	5106	4402	8964	3430	3290	1.62	.67	.75
53	9189	8617	8471	9647	9327	9327	1.05	1.08	.10
54	15981	13047	12872	8598	8448	8127	.54	.65	.63
55	10100	8875	3696	6249	6336	4752	.62		
56	16966	16061	15376	13307	12167	11701	.78	.76	.76
58	18644	18045	17441	15675	15675	15532	.84	.87	.89
59	9121	8847	6864	13887	13737	11980	1.52	1.55	
60	5280	4752	6864	8448	8448	7392			
61	10134	9997	8768	11505	11365	11091	1.14	1.14	1.26
62	13071	13071	10664	12827	12579	11870	.98	.96	1.11
63	24603	24366	23003	25853	25340	25340	1.05	1.04	1.10
64	17512	16249	16249	14989	13720	13[illegible]04	.86	.84	.81
65	*	26275	24401	*	*	2[illegible]97			1.13
65A	37603	37603	37603	37603	36736	35886	1.00	.98	.95
66	32377	28828	26946	19440	18825	18405	.60	.65	.68
67	18287	18287	18022	32789	16959	15885	1.79	.93	.88
68	5359	5359	5667	17949	9968	9763	3.35	1.86	1.72
69	32499	32499	31149	36896	36627	31149	1.14	1.13	1.00
70	6011	6011	5614	7416	7416	6011	1.23	1.23	1.07

TABLE 3 (continued)

Run No.	DETECTION DISTANCES(ft) Alert Group Detection Levels 20%	30%	50%	Distracted Group Detection Levels 20%	30%	50%	RELATIVE DISTANCE Distracted Group / Attentive Group 20%	30%	50%
71	37456	37194	36642	37456	37194	36923	1.00	1.00	1.01
72	14256	13360	12114	13360	12529	11698		.94	.97
73	38078	37662	36390	38078	37662	36390	1.00	1.00	1.00
74	18152	16513	11749	13002	11958	11958	.72	.72	1.02
75	27173	27173	24954	23841	23305	19991	.88	.86	.80
76	18609	9537	7096	7503	6494	5281	.40	.68	.74
77	34092	28858	25559	24774	24529	21805	.73	.85	.85
78	9318	6081	5098	5494	5494	5494	.59	.91	1.08
79	35746	43143	31435	33168	32471	31262	.93	.75	.99
80	30624	30096	30096	30624	30096	24816			
81A	*	*	24381	23661	21836	20753			.85
82	23031	22847	21968	13823	13469	13296	.60	.59	.61
83	33458	33294	32581	33964	33794	33458	1.02	1.02	1.03
84	32930	32739	32556	32373	32373	32191	.98	.99	.99
85	21669	20964	19052	22729	19052	18692	1.05	.91	.98
86	15483	14596	13715	15305	15305	13715	.99	1.05	1.00
87	24409	23992	22481	27519	27096	22891	1.13	1.13	1.02
88	21623	20278	20145	30428	30166	22544	1.41	1.49	1.12
89	27133	24941	24595	29974	29645	29308	1.10	1.19	1.19
90	*	*	*	*	*	*			
91	21626	21276	21276	25789	21788	21276	1.19	1.02	1.00
92	22435	22435	22253	20115	18862	18143	.90	.84	.82
93	31680	31680	22825	19164	18794	18062			.79
95	32133	31967	29949	34342	19062	18538	1.07	.60	.62
96	22617	22436	19258	18917	18390	17877	.84	.82	.93

nearly 100 flights, it is probable that the true relative conditions of attentiveness between the groups did not differ substantially. A cursory examination of the quotients in the last columns of Table 3 does not indicate any significant trend over the course of the experiments.

MODEL FOR HELICOPTER AURAL DETECTABILITY

DESCRIPTION OF MODEL

General Outline

The computer model for helicopter aural detectability is designed essentially as described in the preceding sections of this report. It is intended to be sufficiently flexible in operation to allow the user a wide variety of possible forms of input data.

The model requires, as input, a helicopter noise spectrum, measured while the helicopter is approaching toward the acoustic data acquisition system in a flight profile as near as possible to that for which detectability contours are required. It is permissible but not good practice to predict contours at a different flight altitude but mandatory that airspeed and operating conditions be closely representative of the required approach profile. It is further recommended that the helicopter noise be significantly above the ambient noise where recordings are made, i.e., greater than 10 dB at frequencies below 2,000 Hz, and that no measurements be made at slant range distances less than 5,000 feet. These requirements ensure that a reasonably clean stationary signal, free from near-field effects, will be obtained.

The preferred method of spectral analysis for helicopter noise is to employ a constant bandwidth not exceeding 15 Hz, although the model is also designed to accept 1/3-octave levels.

The program subtracts the measured ambient noise spectrum from the measured helicopter noise spectrum and computes attenuation coefficients using measured atmospheric conditions. Measured slant range is converted to time-retarded slant range from flight profile information.

The next parameters are a set of "As Required" ambient noise spectra whose format of spectral analysis does not have to match the format of the measured spectra. In addition, a set of "As Required" atmospheric conditions should be specified whereupon the program computes attenuation coefficients for these values and proceeds to perform detectability calculations at 2,000-foot increments from 2,000 to 60,000 feet. For improved resolution at shorter distances, calculations may alternately be performed at 200-foot increments from 200 to 6,000 feet.

Three detectability calculations are performed for each value of helicopter slant range in order to account for scatter. Uncertainty bands are allowed on both excess atmospheric attenuation and audibility to give minimum, median, and maximum probable detection ranges.

The user may specify several levels of detail in intermediate outputs, but a mandatory summary table is produced at the end of each detectability calculation, giving a readily decipherable display of distance versus frequency of detection.

Form of Input Data Required

The first parameter is a level-of-detail output indicator giving the user four possible levels of output information. The input data then divides naturally into two parts: "As Measured" data and "As Required" data.

The category of measured data begins with a spectral type indicator denoting 1/3-octave levels or constant resolution power spectral analysis. Two spectra follow: a measured helicopter noise spectrum (S_1), and an ambient noise spectrum (S_2) measured in the same manner shortly before the arrival of the helicopter. In the case of 1/3-octave spectra, levels are in dB per 1/3-octave for 16 Hz through 8 kHz. In the case of constant resolution (Δf) power spectra, levels are in dB per Hz for N_1 points at intervals of Δf.

Atmospheric and flight profile parameters describing conditions under which the measured data were obtained are required in the following form:

Air Temperature	-	T_m (°F)
Absolute Humidity	-	H_m (gm/m^3)*

*Note: The Absolute Humidity may be obtained from Relative Humidity by the following relation (Reference 39):

$$H(gm/m^3) = \frac{10^{\left[23.8733 - (2939/T) - 4.922 \, Log_{10} T\right]}}{T} \cdot RH \tag{13}$$

where RH = Relative Humidity in %

T = Temperature in °K

Wind Velocity Measured at Lull	-	u_m (fps)
Wind Direction Relative to Flight Path (Note: 0° - Implies Aircraft Approach From Downwind)	-	θ_m degrees
Terrain Parameter	-	P_m (smooth surface, farmland with crops, heavily wooded)
Aircraft Altitude	-	h_m (feet)
Aircraft Velocity	-	v_m (fps)
Aircraft Slant Range at Measurement of S_1	-	r_m (feet)

In the category of "As Required" data, it is necessary to specify one or more sets of desired ambient noise spectra (S_3) which are prefaced as before with a spectral type indicator. Spectra may be input as described above in the most convenient format, which may be different from the format in which the helicopter noise spectrum was presented. Several sets of ambient noise spectra to a maximum of ten may be used.

These are followed by one or more sets of "As Required" atmospheric and flight profile data, T_r, H_r, u_r, θ_r, P_r, h_r, v_r, representing parameters as described above. A listener categorization parameter denoting either an isolated individual or a group completes the input data.

Housekeeping Procedures

It is first necessary to obtain a "correct" helicopter noise spectrum (S_1') by subtracting the ambient noise immediately before measurement:

$$S_1' = 10 \log (10^{S_1/10} - 10^{S_2/10}) \tag{14}$$

All subsequent integration and comparison procedures are performed at the same constant spectral resolution so that if 1/3-octave spectrum levels have been input, they are converted to equivalent constant bandwidth power spectra. This is carried out by a simple bandwidth correction. If ambient noise spectra of constant bandwidth different from the measured helicopter constant bandwidth spectrum are input, they then are converted using this latter spectral format as a datum, by linear interpolation.

Due to the fact that the real-time sound emission point is behind the aircraft, a time-retarded measured slant range (r'_m) is computed:

$$r'_m = \frac{\frac{v_m}{c}\left(r_m^2 - A_m^2\right)^{\frac{1}{2}} + \left(r_m^2 - \frac{v_m^2}{c^2} A_m^2\right)^{\frac{1}{2}}}{\left(1 - \frac{v_m^2}{c^2}\right)} \tag{15}$$

The propagation and detectability analyses are evaluated in two logical loops; the outer loop increments the successive sets of "As Required" ambient noise, atmospheric and flight profile parameters, while the inner loop increments "As Required" helicopter slant range distances (r_r) in steps of 2000 feet starting with a value of 2000 feet.

The first step within the inner loop is to compute the time-retarded "As Required" slant range (r'_r) using the same relation given above, substituting subscript "r" for all subscript "m"'s.

Propagation Analysis

The helicopter noise spectrum at distance r_r at the same current set of "As Required" ambient noise, atmospheric and flight profile parameters is computed for the k'th frequency (f_k) in three forms--a maximum (H_1), a median (H_2), and a minimum (H_3)--by the following relations:

$$\begin{aligned} H_1(k) = S'_1(k) + 20 \log\left(\frac{r'_m}{r'_r}\right) + \frac{r'_m}{1000}\left\{L_{1m}(k) + q_{max} L_{2m}(k)\right\} \\ - \frac{r'_r}{1000}\left\{L_{1r}(k) + q_{min} L_{2r}(k)\right\} \end{aligned} \tag{16}$$

$$H_2(k) = S'_2(k) + 20 \log \left(\frac{r'_m}{r'_r}\right) + \frac{r'_m}{1000} \left\{L_{1m}(k) + L_{2m}(k)\right\}$$

$$- \frac{r'_r}{1000} \left\{L_{1r}(k) - L_{2r}(k)\right\} \tag{17}$$

$$H_3(k) = S'_2(k) + 20 \log \left(\frac{r'_m}{R'_r}\right) + \frac{r'_m}{1000} \left\{L_{1m}(k) + q_{min} L_{2m}(k)\right\}$$

$$- \frac{r'_r}{1000} \left\{L_{1r}(k) + q_{max} L_{2r}(k)\right\} \tag{18}$$

where $L_{1m}(k)$ and $L_{1r}(k)$ represent atmospheric absorption coefficients for "As Measured" and "As Required" atmospheric parameters respectively. These are evaluated from a functional reduction of curves of standard atmospheric attenuation as given in Reference 37. $L_{2m}(k)$ and $L_{2r}(k)$ represent the empirically derived values of excess atmospheric attenuation from this study due to refraction, diffraction, scattering out of the turbulent region, and partial ground reflection for "As Measured" and "As Required" atmospheric parameters respectively. The method of evaluation is as follows. First, attenuation for the case of sound propagation upwind (E_1) is evaluated:

$$E_1 = (A_{P_m} U_m + B_{P_m})\psi \qquad \left(\frac{dB}{1000\ ft}\right)$$

where for a smooth "As Measured" terrain ($P_m = 1$, see Figure 33):

$$A_1 = .0333 \log f_k + .0994 \qquad \left(\frac{dB}{1000\ ft}\right) \Big/ \left(\frac{ft}{sec}\right)$$

$$B_1 = -.225 \log f_k + 1.58 \qquad \left(\frac{dB}{1000\ ft}\right)$$

$$\psi = 1.0 \qquad \text{for Arc Sin } \frac{h_m}{R'_m} < 2°$$

$$\psi = -.125 \text{ Arc Sin}\left(\frac{h_m}{r'_m}\right) + 1.25 \qquad \text{for } 2° < \text{Arc Sin}\frac{h_m}{r'_m} < 10°$$

$$\psi = 0 \qquad \text{for } r'_m > 10°$$

Then attenuation for the case of sound propagation downwind (E_2) is evaluated:

$$E_2 = (C_{P_m} U_m + D_{P_m})\psi \qquad \left(\frac{dB}{1000\text{ ft}}\right)$$

where for a smooth "As Measured" terrain ($P_m = 1$, See Figure 36):

$$C_1 = 0.06 \qquad \left(\frac{dB}{1000\text{ ft}}\right) \Big/ \left(\frac{ft}{sec}\right)$$

$$D_1 = 0.36 \qquad \left(\frac{dB}{1000\text{ ft}}\right)$$

A cosine interpolation is carried out for other angles of approach relative to wind:

$$L_{2m}(k) = .5 \left\{(E_1 - E_2) \text{ Cos } \theta_m + (E_1 + E_2)\right\} \left(\frac{dB}{1000\text{ ft}}\right) \qquad (19)$$

Similarly, L_{2r} is evaluated for the "As Required" case.

No adequate data is available at present for any other than smooth terrain. Thus, although the facility for propagation over other terrains is incorporated in the model, values of P_m or P_r other than unity will cause an "error halt" message to be output.

The factors q_{max} and q_{min} account for the standard deviations on measurements of excess atmospheric attenuation. They are numerically equal to approximately 1.15 and 0.85 respectively. These numerical values are slightly smaller than measured standard deviations of excess atmospheric attenuation since they have been adjusted for estimated errors arising due to experimental technique.

Detectability Analysis

Correctly formatted helicopter and ambient noise spectra, defined as power spectral densities and corrected for propagation to the current "As Required" slant range, are converted to critical band levels by evaluation of the following functions:

$$H^{\dagger}{}_j(f_k) = 10\log_{10}\left[\Delta f \sum_{i=-k}^{n} 10^{\left\{H_j(f_{k+i})\right\}/10} \times W(Z_{k+i} - Z_k)\right] \qquad (20)$$

$$A^{\dagger}(f_k) = 10\log_{10}\left[\Delta f \sum_{i=-k}^{n} 10^{\left\{A(f_{k+i})\right\}/10} \times W(Z_{k+i} - Z_k)\right] \qquad (21)$$

where the functions Z(f) and W $(Z_{rel.})$ are defined in Figures 6 and 7. In the model, these relations are expressed in the following functional forms:

$$(Z \leq 5) \qquad Z = \frac{4.268}{10^2} + \frac{4.69}{10^2} f - \frac{1.453}{10^4} f^2 + \frac{4.086}{10^7} f^3 - \frac{6.834}{10^{10}} f^4 + \frac{4.757}{10^{13}} f^5$$

$$(Z \geq 5) \qquad Z = 4.671 + \frac{1.371}{10^2} f - \frac{5.057}{10^6} f^2 + \frac{1.143}{10^9} f^3 - \frac{1.333}{10^{13}} f^4 + \frac{6.135}{10^{18}} f^5$$

where Z is subjective frequency in Bark and f is frequency in Hz, derived from Greenwood's published relation for critical bandwidth (Reference 20), and

$$(Z_{rel} \leq 0) \qquad W = 10^{6.7\left\{e^{-.1103(-1.3 Z_{rel})2.506} - 1\right\}}$$

$$(Z_{rel} \geq 0) \qquad W = 10^{6.7\left\{e^{-.144 Z_{rel}^{1.2}} - 1\right\}}$$

where W is the aural discriminatory weighting characteristic derived from Zwicker's[21] published data, in terms of relative subjective frequency in Bark. The integral of this function is nearly unity as shown in Figure 7.

Ollerhead's detectability parameter δ is then evaluated three times for the three helicopter spectra expressed in critical band levels each associated with the current "As Required" ambient noise spectrum:

$$\delta_j(f_k) = H^{\dagger}_j(f_k) - 1.0 - 10\log_{10}\left[10^{T(f_k)/10} + 10^{\left\{A^{\dagger}(f_k) - 5.0\right\}/10}\right]$$

for j = 1, 2, 3

where $T(f_k)$, the pure tone threshold in dB, at frequency f_k is given as in Figure 37 by the relations $F = \mathrm{Log}_{10} f_k$ and,

$$T = 273.4 - 584.1F + 860.4F^2 - 690.0F^3 + 283.4F^4 - 56.9F^5 + 4.44F^6$$

Evaluation of the δ_j's now depends on the listener categorization parameter. The results derived in the field test and presented in Figures 46 and 47 represent the responses of isolated individuals. Thus, for this case, it is reasonable to adopt a confidence band of plus or minus one standard deviation. That is, from Figure 46 for values of δ in the range -3 dB to +3 dB, 66.6% of a random sample of listeners would indicate positive detection. Thus, for the case of an individual listener, the maximum detection distance will be given when any $\delta_1(f_k) \geq -3$ dB, the median detection distance when any $\delta_2(f_k) \geq 0$ dB, and the minimum detection distance when any $\delta_3(f_k) \geq 3$ dB.

For a group of listeners, the situation is clearly different, due to a real range of hearing acuity. Thus, those with more acute hearing will communicate with others, and an earlier detection will be made than by an isolated individual. From Figure 46, based on the assumption that detection by the first 20% will alert the entire group, maximum detection distance will be given when any $\delta_1(f_k) \geq -4$ dB; the medium detection distance, when any $\delta_2(f_k) \geq -2$ dB.

Form of Output

Four possible levels of output detail have been allowed, yielding the following:

Level 0: The following input data will be printed for identification and verification:

All titles

"As Measured" and "As Required" atmospheric and flight profile parameters

Results of the detectability analysis will be summarized in the form shown in Table 4, where the abscissa is a distance axis in increments of 2,000 feet, and the ordinate represents frequency bands where detection occurs.

Detectability is indicated by a "D" for certain detection, with the band of likely detection given by dots with the median probable detection distance indicated by an "X".

Level 1: Output as in Level 0, plus,

Helicopter and ambient noise spectra as input for verification.

Level 2: Output as in Level 1, plus,

Reformatted spectra, critical band spectra levels, and tables of values of the detectability parameter.

Level 3: Output as in Level 2, plus,

Tables of propagation decrements for "As Measured" and "As Required" conditions, as well as a table of pure tone thresholds.

The latter two levels of output generate large quantities of line printer paper and should be used only when required.

TABLE 4 - SUMMARY OF DETECTABILITY ANALYSIS

PROBABILITY OF DETECTION FROM:

68% to 100% = D

50% to 68% = +

ABOUT 50% = X

32% to 50% = -

0 to 32% = BLANK

FREQ (Hz)	RANGE IN THOUSAND FEET											
	2	4	6	8	10	12	14	16	18	20	22	24
0- 50	D	D	D	D	X	-						
50- 100	D	D	D	D	D	+	X	-				
100- 150	D	D	D	D	D	D	X	-				
150- 250	D	D	D	D	D	D	X	-				
250- 350	D	D	D	D	D	D	+	X	-			
350- 500	D	D	D	D	D	D	+	X	-			
500- 700	D	D	D	D	D	D	+	X				
700-1000	D	D	D	D	D	D	+	X				
1000-1500	D	D	D	D	D	D	X	-				
1500-2000	D	D	D	D	D	X	-					
2000-3000												
3000-5000												

COMPARISON OF MODEL WITH EXPERIMENTAL DATA

Tests Using "Same Run" Acoustic Data

In order to carry out a preliminary assessment of the accuracy of the basic model, helicopter and ambient noise 1/3-octave spectra were obtained for each of the 96 flights. It was not always possible to obtain natural ambient noise on the acoustic measurement system before the arrival of the helicopter, so the attempt was made always to select helicopter noise spectra significantly above the ambient.

Each pair of measured spectra was then applied, together with measured atmospheric and flight profile data, to predict individual detection distances for the same flight from which the data was taken. These predictions were evaluated only for the median detection distance and were correlated with measured detection distances at the 10%, 20%, 30%, and 50% detection levels. These correlations are shown in Figures 48 through 51.

This procedure provides an accuracy check of the model under a wide variety of ambient noise, atmospheric and flight profile parameters without confusing the comparison by using the additional facility of translating from one set of atmospheric and flight profile parameters to another.

Best correlation occurs at the 20% detection level, whereas from Figure 46, an optimum correlation would be expected at the 50% level. This is probably due to error incurred initially by not subtracting natural ambient noise from measured helicopter spectra, resulting in an overestimate of helicopter noise.

The correlation between measured and predicted values shows a surprisingly small degree of scatter.

Tests Using "Same Flight Profile" Acoustic Data

A comprehensive test of the accuracy of the model was carried out by extracting helicopter acoustic data from a single flight for each of the three aircraft and associated three flight profiles and using it to evaluate theoretical detection distances for all other flights of the same aircraft at the same flight profile but under different atmospheric conditions.

For this set of calculations, a mixture of 1/3-octave and constant bandwidth spectra was used.

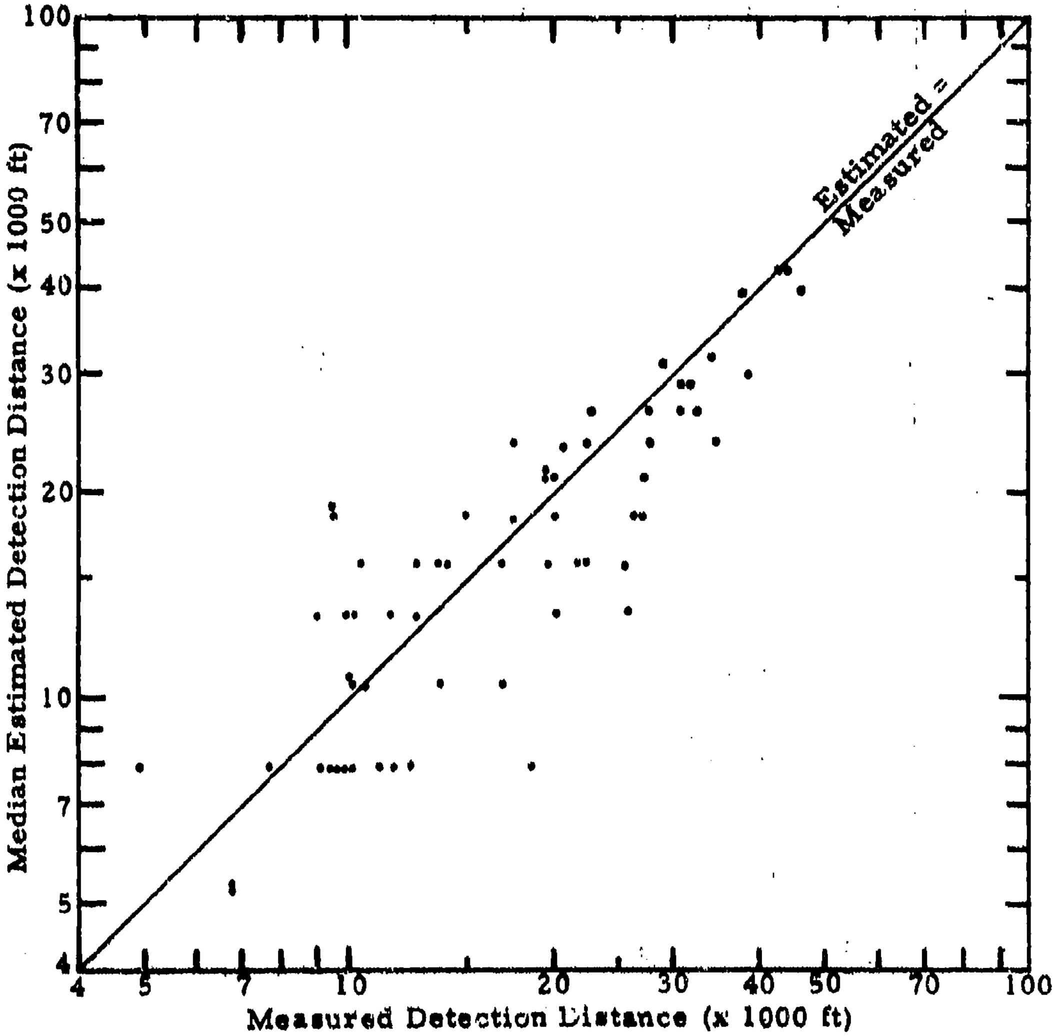

Figure 48. Comparison of Median Estimated and Measured Detection Distances for 10% Measured Detection Level (From 1/3-Octave Acoustic Spectra Measured on Same Flight).

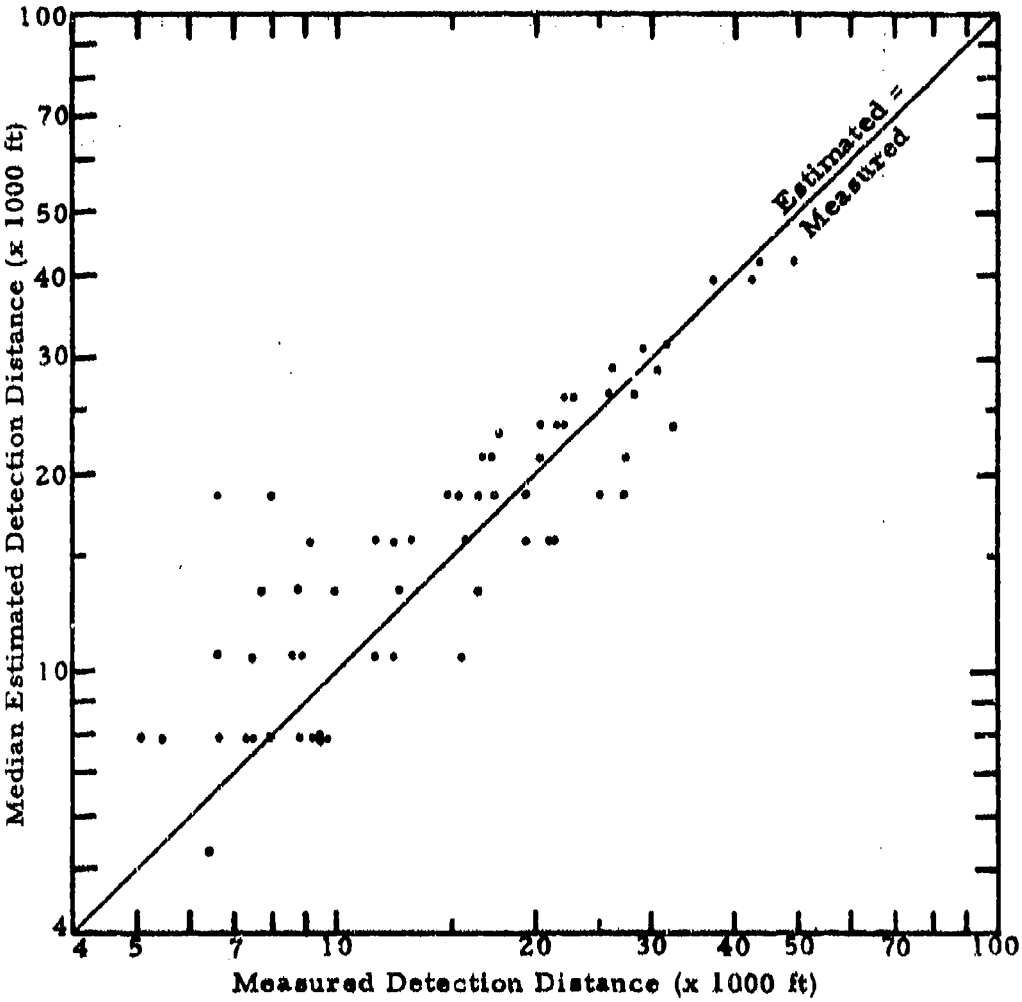

Figure 49. Comparison of Median Estimated and Measured Detection Distances for 20% Measured Detection Level (From 1/3-Octave Acoustic Spectra Measured on Same Flight).

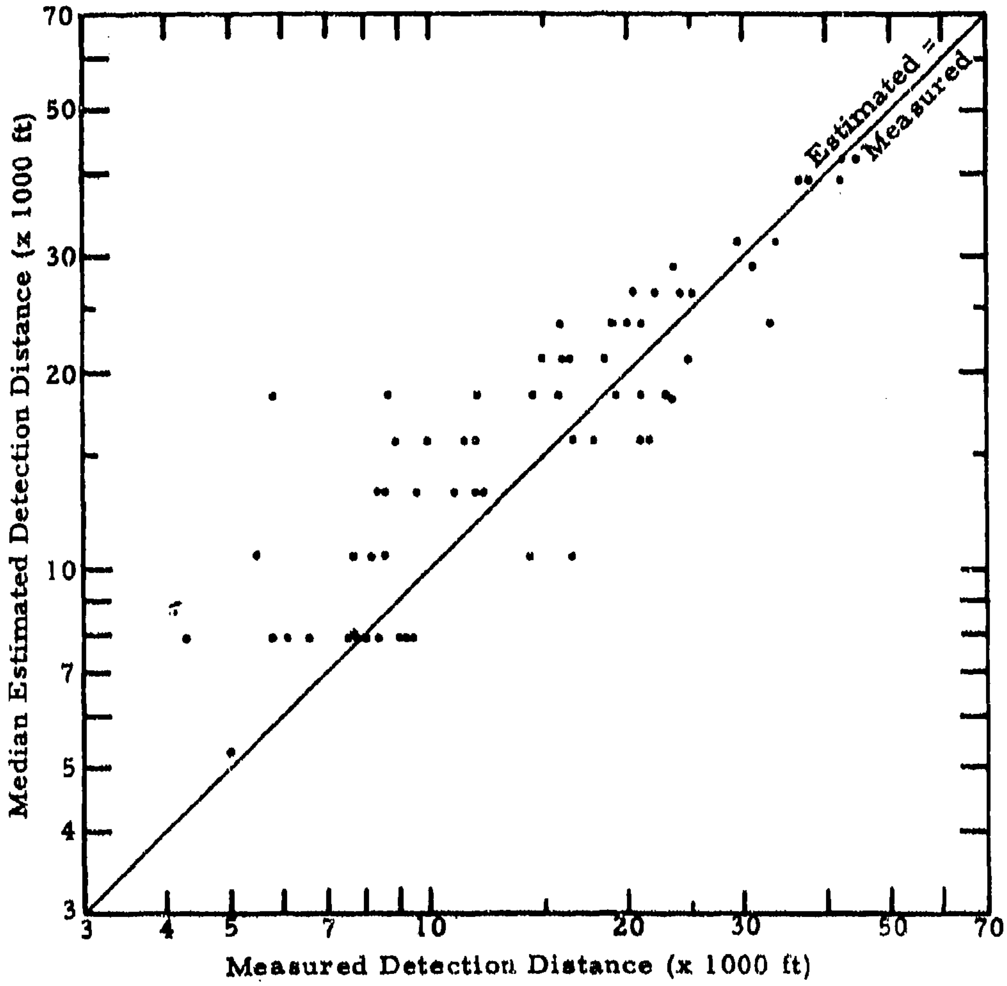

Figure 50. Comparison of Median Estimated and Measured Detection Distances for 30% Measured Detection Level (From 1/3-Octave Acoustic Spectra Measured on Same Flight).

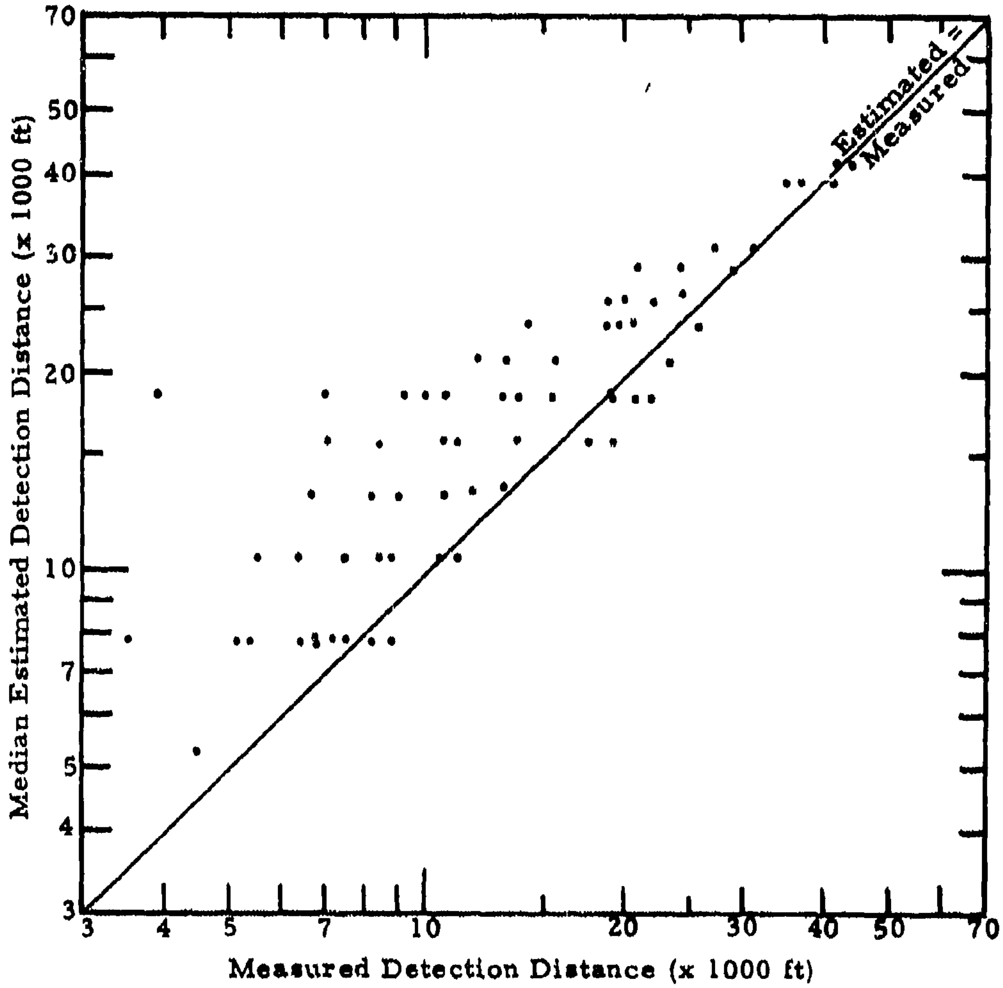

Figure 51. Comparison of Median Estimated and Measured Detection Distances for 50% Measured Detection Level (From 1/3-Octave Acoustic Spectra Measured on Same Flight).

As before, theoretical and measured detection distances were correlated, and the results are shown in Figures 52 through 55.

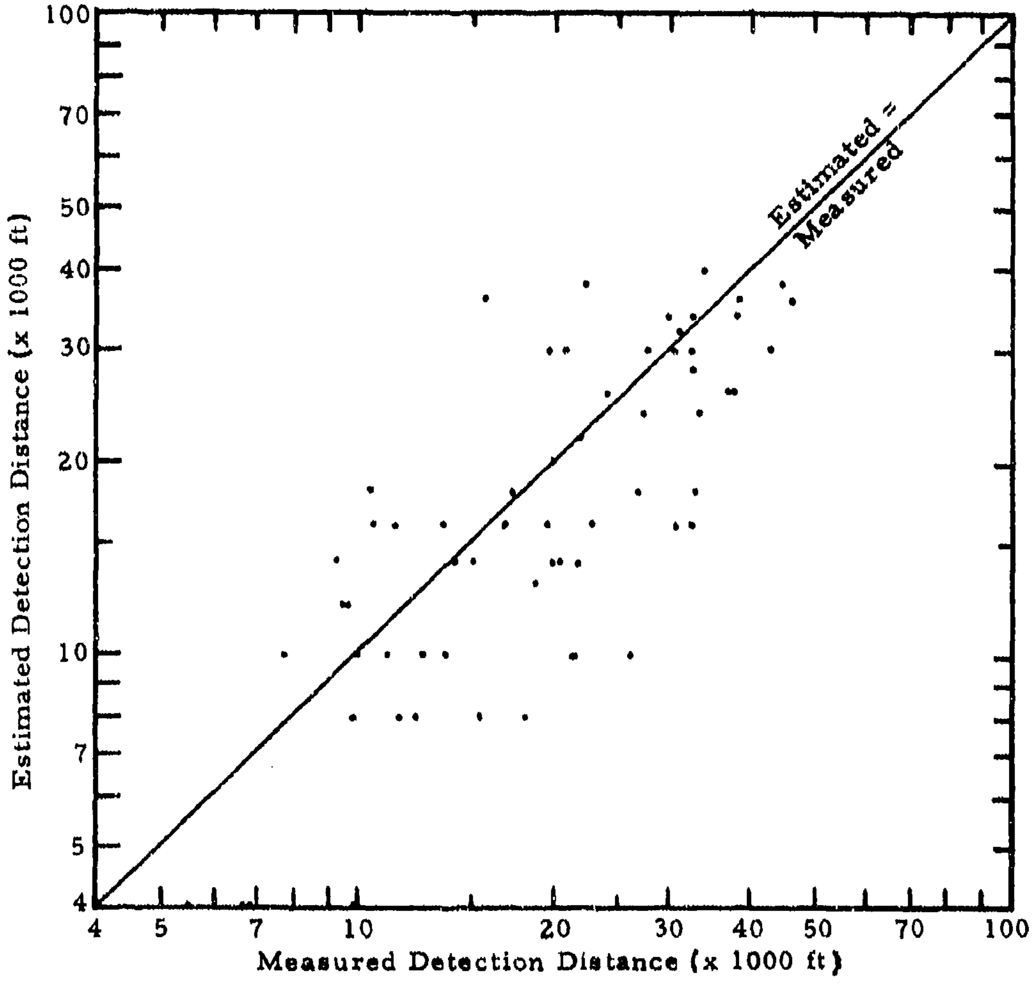

Figure 52. Comparison of Estimated and Measured Detection Distances for 10% Measured Detection Level. Estimated Distances From Acoustic Data Measured for "Same Flight Profile".

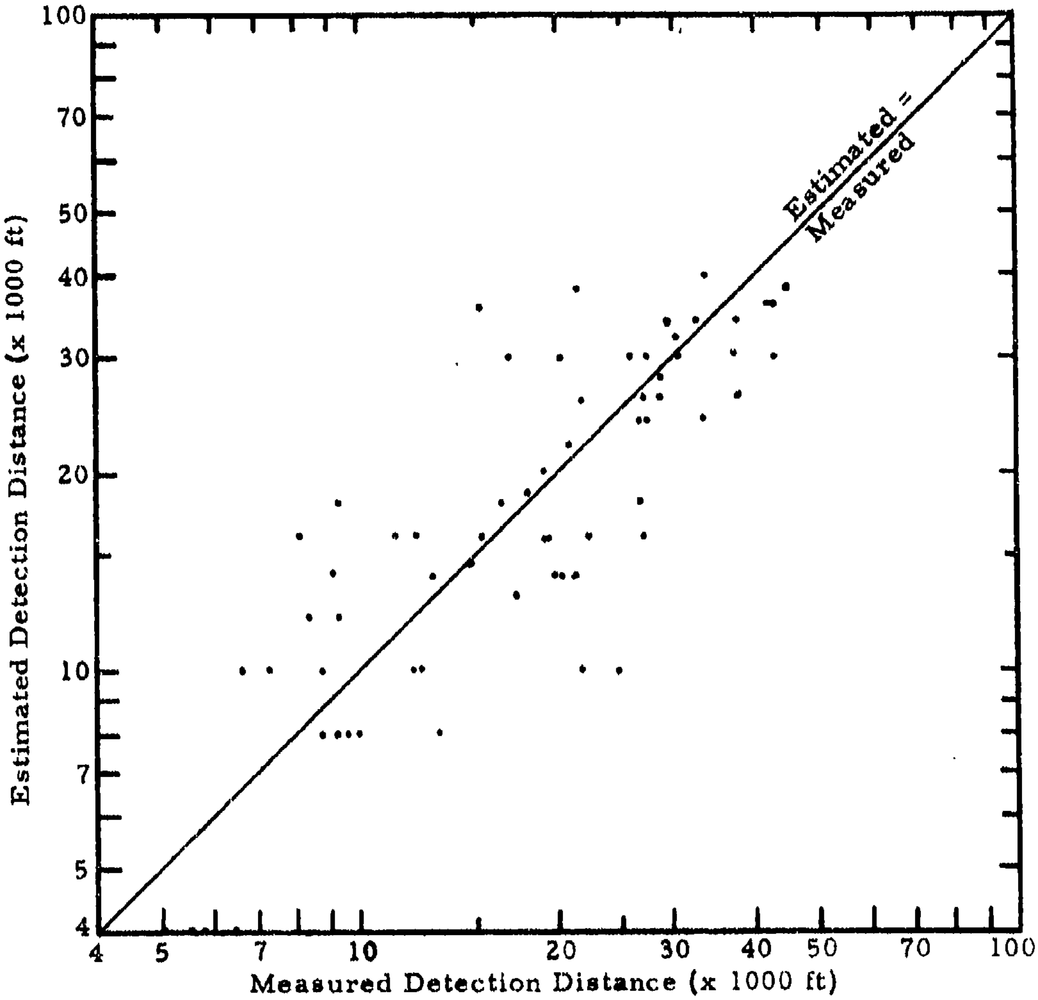

Figure 53. Comparison of Estimated and Measured Detection Distances for 20% Measured Detection Level. Estimated Distances From Acoustic Data Measured for "Same Flight Profile".

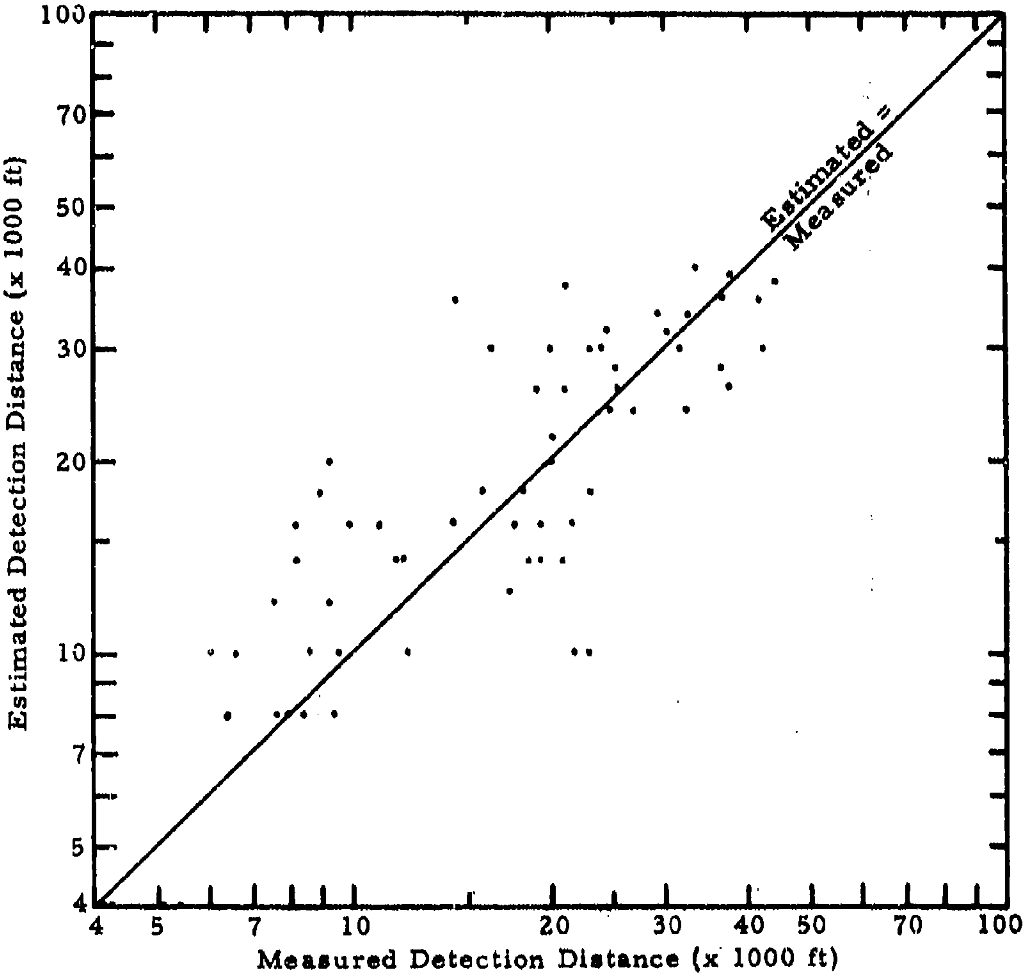

Figure 54. Comparison of Estimated and Measured Detection Distances for 30% Measured Detection Level. Estimated Distances From Acoustic Data Measured for "Same Flight Profile".

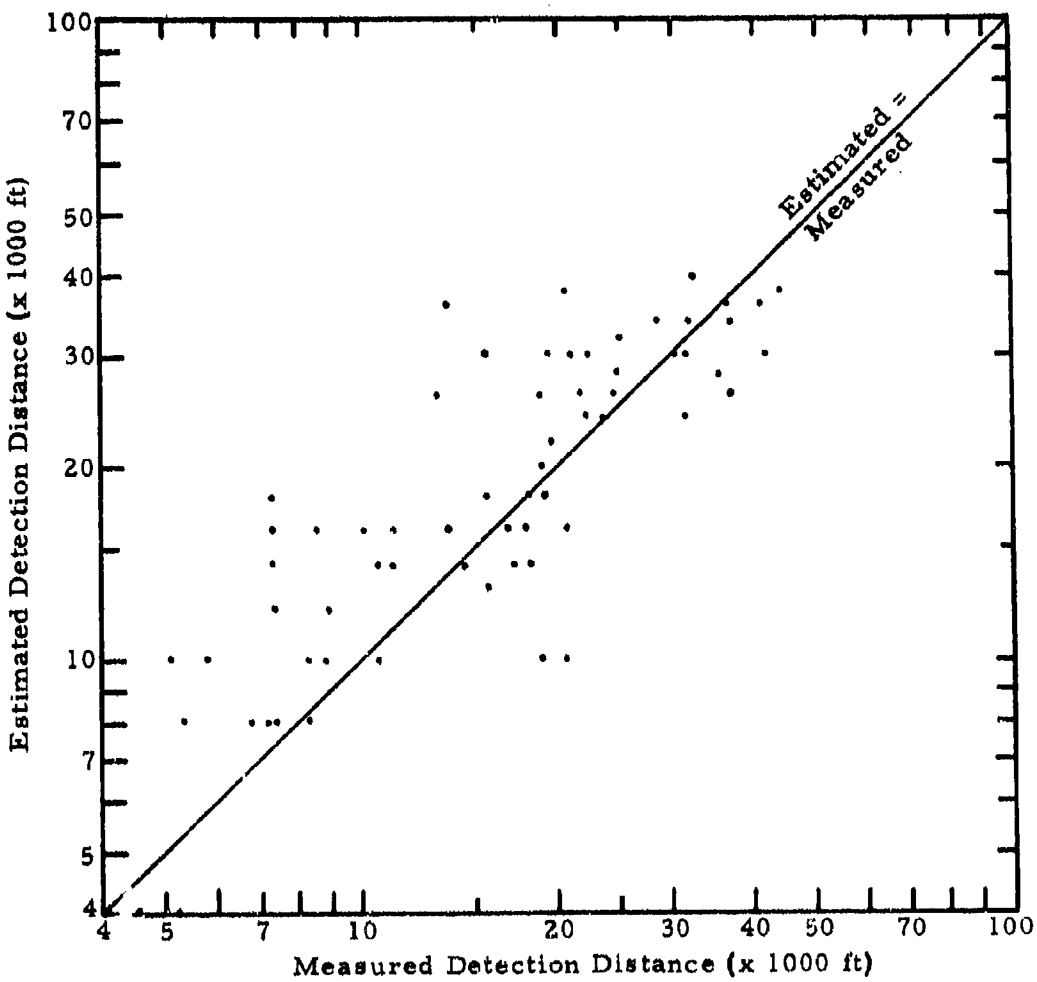

Figure 55. Comparison of Estimated and Measured Detection Distances for 50% Measured Detection Level. Estimated Distances From Acoustic Data Measured for "Same Flight Profile".

CONCLUSIONS AND RECOMMENDATIONS

The study described in this report is based on pragmatic empiricism and should be regarded as a practical engineering, rather than a scientific, study. Nevertheless, it is expected that the computer model which was developed from the results of the field experiment should provide satisfactory estimates of detection distances for helicopters not differing significantly in noise characteristics from those in the experiment, and travelling over similar terrain.

Within these qualifications there are significant improvements over the model developed by Ollerhead:

1. Addition of a statistical distribution to Ollerhead's detectability criterion.

2. Quantization of a "group" or "individual listener" parameter.

3. Introduction of a new procedure for simulating aural frequency decomposition of sound.

4. Formulation of an empirical model for atmospheric attenuation of sound in the lower atmosphere over long distances.

Additionally, the experiment confirmed Ollerhead's detectability criterion as a median value for individual response.

The following quasi-deterministic effects have been included to increase accuracy and convenience of the model:

1. Time-retarded distances.

2. Corrections from measured to required flight profile and atmospheric parameters.

3. Spectral format conversion.

The facility for incorporating data for more heavily vegetated terrains than those encountered in the experiment has been provided in the model, but no reliable data are available as yet for such conditions.

In terms of practical interpretation, the results of the experiment clearly indicated the following:

1. A helicopter approaching at high altitude ($\geq$ 1500 feet) was detected substantially (about 50%) farther away than one approaching at low altitude ($\leq$ 200 feet).

2. A helicopter approaching from downwind is substantially less detectable than one approaching from upwind even if there is low prevailing wind.

3. Helicopter noise is apparently sufficiently distinctive that unprepared or inattentive listeners appear to detect the sound, on an average, as early as alerted listeners.

4. In quiet ambient noise conditions, it is to be expected that noisier helicopters may be detected at distances in excess of eight miles.

5. The spread in distance over which the helicopter is partially detectable may be large or small. This spread does not seem to be sensibly expressible as a function of helicopter slant range but does seem to be dependent on atmospheric parameters and flight profile.

Areas for further work, in descending order of importance, include:

1. A theoretical study of sound propagation in lower atmosphere should be carried out using a realistic atmospheric model, and applying known physical principles to determine relative magnitude of the major effects.

2. An experimental study of sound propagation in lower atmosphere over a well instrumented course for several categories of terrain and meteorological conditions should follow or be associated with the theoretical study.

3. In the area of detectability, a computer simulation of human perception of complex sounds supported by small-scale laboratory experiments would not only increase the accuracy of the model, but would also create an entirely analytical tool for application to other aural detection problems.

The attempt was made in the introductory sections to illustrate the full complexity of the phenomenon of helicopter aural detectability. As was clear from even an initial consideration of the problem, there is scope for substantially more detailed study in the areas of sound propagation in the lower atmosphere and in human recognition of complex sounds.

REFERENCES

1. Hubbard, H. H., and Maglieri, D. J., AN INVESTIGATION OF SOME PHENOMENA RELATING TO AURAL DETECTION OF AIRPLANES, National Advisory Committee for Aeronautics, Technical Note NACA TN 4337, September 1958.

2. Loewy, R. G., AURAL DETECTION OF HELICOPTERS IN TACTICAL SITUATIONS, Journal of the American Helicopter Society, October 1963, pp. 36-53.

3. Ollerhead, J. B., HELICOPTER AURAL DETECTABILITY; USAAMRDL Technical Report 71-33, Eustis Directorate, U. S. Army Air Mobility Research and Development Laboratory, Fort Eustis, Virginia, July 1971 AD 730788.

4. Ungar, E. E., A GUIDE FOR PREDICTING THE AURAL DETECTABILITY OF AIRCRAFT, Air Force Flight Dynamics Laboratory, Air Force Systems Command, Wright-Patterson Air Force Base, Ohio, Technical Report AFFDL-TR-71-22, 1971.

5. Fidell, S., Pearson, K. S., and Bennett, R. L., PREDICTING AURAL DETECTABILITY OF AIRCRAFT IN NOISE BACKGROUNDS, Air Force Flight Dynamics Laboratory, Air Force Systems Command, Wright-Patterson Air Force Base, Ohio, Technical Report AFFDL-TR-72-17, 1972.

6. Hartman, L., and Sternfeld, H., AN EXPERIMENT IN AURAL DETECTION OF HELICOPTERS; USAAMRDL Technical Report 73-50, Eustis Directorate U. S. Army Air Mobility Research and Development Laboratory, Fort Eustis, Virginia, December 1973, AD 917355L.

7. Lowson, M. V., and Ollerhead, J. B., A THEORETICAL STUDY OF HELICOPTER ROTOR NOISE, Journal of Sound and Vibration, Vol. 9, No. 2, March 1969, pp. 197-222.

8. Sharland, I. J., and Leverton, J. W., PROPELLER, HELICOPTER AND HOVERCRAFT NOISE, London, John Wiley, 1968, Chapter 9.

9. Guton, L. Ya., ON THE SOUND FIELD OF A ROTATING PROPELLER, Physiks Zeitschrift der Soujetunion, Bond Heft 1, 1936, pp. 57-71.

10. Curle, S. N., GENERAL THEORY OF AERODYNAMIC SOUND, London, John Wiley, 1968, Chapter 5.

11. Lighthill, M. J., ON SOUND GENERATED AERODYNAMICALLY, I-GENERAL THEORY, Proc. Royal Society, A211, 1952, pp. 564-587.

12. Lighthill, M. J., ON SOUND GENERATED AERODYNAMICALLY, II-TURBULENCE AS A SOURCE OF SOUND, Proc. Royal Society, A222, 1954, pp. 1-32.

13. Leverton, J. W., HELICOPTER NOISE--BLADE SLAP, PART I--THEORY; National Aeronautics and Space Administration Contractor Report 1221, 1968.

14. Leverton, J. W., HELICOPTER NOISE--BLADE SLAP, PART II--EXPERIMENTAL RESULTS; National Aeronautics and Space Administration Contractor Report 1983, 1972.

15. Ffowcs-Williams, J. E., THE NOISE FROM TURBULENCE CONVECTED AT HIGH SPEED, London, Trans. Royal Society, 1963, pp. 469-503.

16. Morfey, C. L., ROTATING PRESSURE PATTERNS IN DUCTS: THEIR GENERATION AND TRANSMISSION, Journal of Sound and Vibration, Vol. 1, 1963, pp. 60-87.

17. Sharland, I. J., SOURCES OF NOISE IN AXIAL FLOW FANS, Journal of Sound and Vibration, Vol. 1, 1964, pp. 302-322.

18. Kemmers, E. P., DYNAMICS OF GEAR PAIR SYSTEMS, American Society of Mechanical Engineers, Vol. 71-DE-22, April 1971.

19. Lord Rayleigh, THEORY OF SOUND, Vol. 2, Dover Reprint, 1965.

20. Evans, L. B., Bass, H. E., and Sutherland, L. C., ATMOSPHERIC ABSORPTION OF SOUND: THEORETICAL PREDICTIONS, Journal of Acoustical Society of America, Vol. 51, No. 5, pp. 1565-1575, May 1972.

21. Morse, P. M., and Ingard, K. J., THEORETICAL ACOUSTICS, McGraw-Hill Book Company, 1968.

22. Sabine, H. J., SOUND PROPAGATION NEAR EARTH SURFACE AS INFLUENCED BY WEATHER CONDITIONS; WADC Technical Report TR-57-353, Four Volumes, Wright Air Development Center, Dayton, Ohio, 1957-1961.

23. Pridmore Brown, D. C., and Ingard, Uno, TENTATIVE METHOD FOR CALCULATION OF THE SOUND FIELD ABOUT A SOURCE OVER GROUND CONSIDERING DIFFRACTION AND SCATTERING INTO SHADOW ZONES, NACA Technical Note 3779, National Advisory Committee for Aeronautics, Washington, September 1956.

24. Tobias, Jerry V., (Editor), FOUNDATIONS OF MODERN AUDITORY THEORY, Vol. 1, Academic Press, 1970.

25. Tobias, Jerry V., (Editor), FOUNDATIONS OF MODERN AUDITORY THEORY, Vol. 2, Academic Press, 1972.

26. Zwicker, E., Flottorp, G., and Stevens, S. S., CRITICAL BANDWIDTH IN LOUDNESS SUMMATION, Journal of Acoustical Society of America, Vol. 29, No. 5, May 1957.

27. Greenwood, D. D., AUDITORY MASKING AND THE CRITICAL BAND, Journal of Acoustical Society of America, Vol. 33, No. 6, April 1961.

28. Greenwood, D. D., CRITICAL BANDWIDTH AND THE FREQUENCY COORDINATES OF THE BASILAR MEMBRANE, Journal of Acoustical Society of America, Vol. 33, No. 10, October 1961.

29. Fletcher, H., AUDITORY PATTERNS, Review of Modern Physics, Vol. 12, January 1940, pp. 47-65.

30. Swets, J. A., Green, D. M., and Tanner, W. P., ON THE WIDTH OF THE CRITICAL BANDS, Journal of the Acoustical Society of America, Vol. 34, January 1962, pp. 108-113.

31. DeBoer, E., NOTE ON THE CRITICAL BANDWIDTH, Journal of Acoustical Society of America, Vol. 34, No. 7, July 1962.

32. Zwicker, E., and Feldtkeller, R., DAS OHR ALS NACHRICHTENEMPFANGER, Stuttgart, S. Hirzel Verlag, 1967.

33. Zwicker, E., and Fastl, H., ON THE DEVELOPMENT OF THE CRITICAL BAND, Journal of Acoustical Society of America, Vol. 52, No. 2, August 1972.

34. Swets, J. A., ed., SIGNAL DETECTION AND RECOGNITION BY HUMAN OBSERVERS, John Wiley and Sons, Inc., 1964.

35. Green, D. M., and Swets, J. A., SIGNAL DETECTION THEORY AND PSYCHOPHYSICS, John Wiley and Sons, Inc., 1966.

36. Wyle Laboratories Research Staff, NOISE FROM TRANSPORTATION SYSTEMS, RECREATION VEHICLES AND DEVICES POWERED BY SMALL INTERNAL COMBUSTION ENGINES, Report No. WR 71-18, Wyle Laboratories, California Research Staff, 128 Maryland Street, El Segundo, California 90245, November 1971.

37. STANDARD VALUES OF ATMOSPHERIC ABSORPTION AS A FUNCTION OF TEMPERATURE AND HUMIDITY FOR USE IN EVALUATING AIRCRAFT FLYOVER NOISE, Society of Automotive Engineers; Aerospace Recommended Practice 866, August 1964.

38. Whittle, L. S., Collins, S. J., and Robinson, D. W., THE AUDIBILITY OF LOW FREQUENCY SOUNDS, Journal of Sound and Vibration, Vol. 21, No. 4, pp. 431-448, 1972.

39. Sutherland, L. C., SUPPORTING BACKGROUND DOCUMENT FOR DRAFT STANDARD ON ATMOSPHERIC ABSORPTION LOSSES IN STILL, HOMOGENEOUS AIR, Submitted to S1-S7 Working Group on Air Absorption, Acoustical Society of America, Wyle Laboratories Report WCR 74-11, May 1974.

LIST OF SYMBOLS AND ABBREVIATIONS

A (f)	ambient noise spectrum
$A^{\dagger}$ (f)	ambient noise spectrum - critical band levels
c	velocity of sound, fps
dB	decibel
E	excess atmospheric attenuation
f	frequency
h	height, altitude, ft
H (f)	helicopter noise spectrum
$H^{\dagger}$ (f)	helicopter noise spectrum - critical band levels
H_m, H_r	humidity (measured, required), gm/m^3
i, j, k	indices
ips	inches per second
L_1	atmospheric attenuation coefficient for molecular absorption, and heat conduction losses
L_2	atmospheric attenuation coefficient due to refraction, diffraction, scattering, and ground absorption
mic	microphone
n	index
NOE	nap of the earth (variable altitude flight close to earth's surface as obstacles permit)
P	sound pressure amplitude
P_m, P_r	terrain parameter (measured, required)

PSD	power spectral density
q_{max}, q_{min}	factors on excess atmospheric attenuation
RH	relative humidity, percent
r	radial distance from source, slant range, ft
r_m, r_r	slant range (measured, required), ft
r'	time-retarded distance from source
S_1, S_2, S_3	spectra for input to aural detectability model
SLM	sound level meter
SPL	sound pressure level
t	time, sec
T	integration time, sec
T_m, T_r	temperature (measured, required), °F
T (f)	pure tone threshold
u, u_m, u_r	wind velocity, (measured, required), fps
U	free stream wind velocity, fps
v, v_m, v_r	aircraft velocity, (measured, required), fps
W	aural discriminatory characteristic
x	Cartesian coordinates
y	Cartesian coordinates
Z	subjective frequency parameter (Bark)
δ	Ollerhead's detectability parameter
δ^*	boundary layer displacement thickness, ft
Δ	spherical spreading loss

Δf	spectral resolution, filter bandwidth, Hz
θ	angle of incidence, deg
σ	standard deviation
ψ	weighting factor applied to linearized excess attenuation

474-75